ISSN 2349-8870
Volume 10, Issue 4.

EJBPS

European Journal of Biomedical and Pharmaceutical Sciences

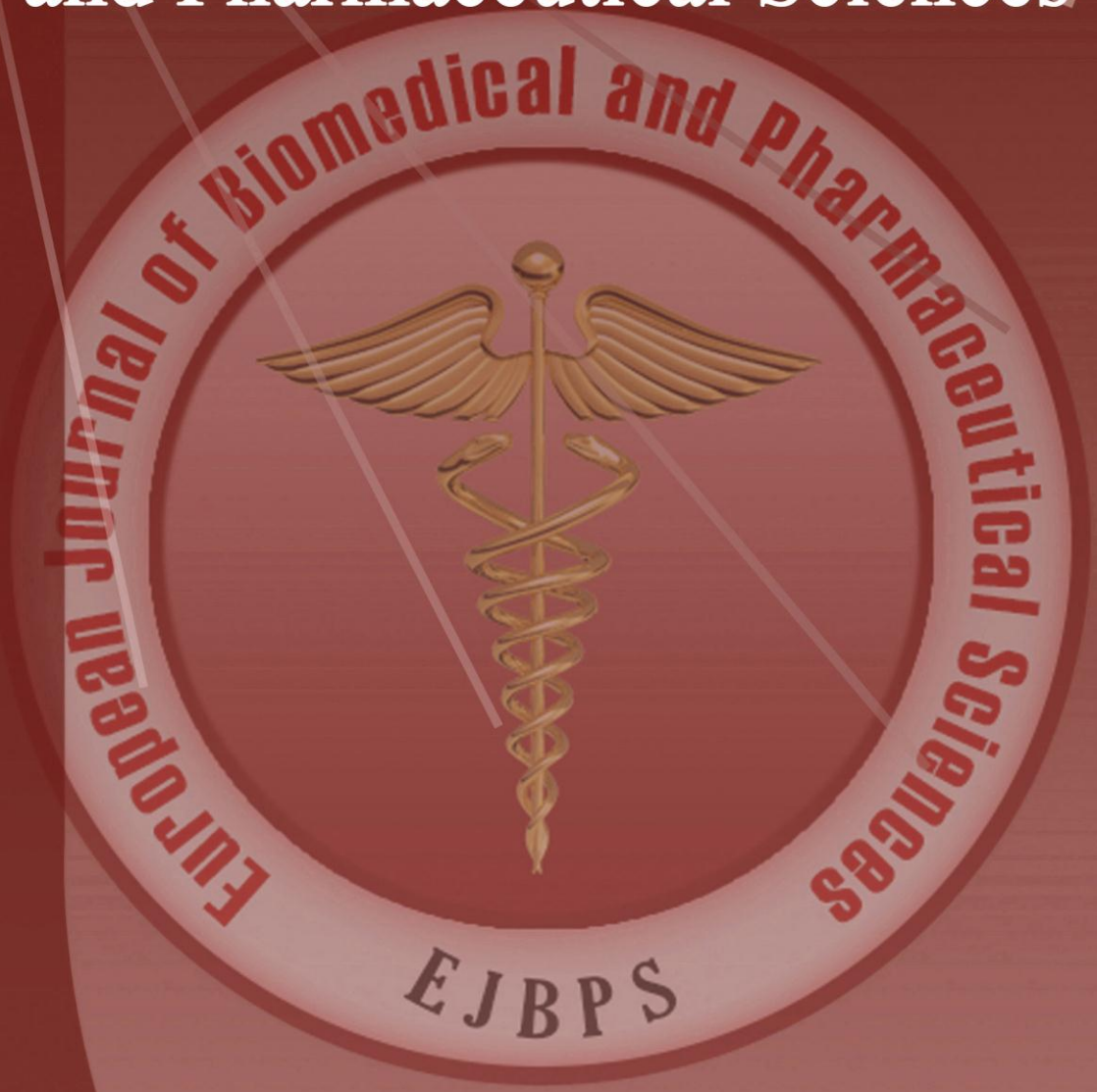

Published By
Society for Advance Healthcare Research
Bhopal, India.

RECENT DEVELOPMENTS AND NEW FRONTIERS IN COMPLEX COACERVATE-BASED MATERIALS FOR BIOMEDICINE

***Author**
Dr. Partha Sarathi Roy*

M.Tech. PhD, Post Doctorate (USA),

Professor of Medicinal Chemistry, Bharat Institute of Technology, Hyderabad.

Published By:
EJBPS
2023

RECENT DEVELOPMENTS AND NEW FRONTIERS IN COMPLEX COACERVATE-BASED MATERIALS FOR BIOMEDICINE

PREFACE

Complex coacervation [formation of a dense macroion-rich phase (the coacervate) in equilibrium with a dilute macroion-poor phase (continuous phase or supernatant)] is a particular case of associative phase separation that occurs when oppositely charged macroions (or polyelectrolytes) are mixed. Since the pioneering work of Bungenberg de Jong and co-workers on gelatin–acacia gum complex coacervation in the 1920–40s, coacervates have received increasing research interest because a variety of mature and emerging technologies depend critically on the association of oppositely charged polymers or particles. Such association could involve charge complexation in solution. Unfortunately the theoretical underpinnings of complex coacervation are widely misunderstood and conceptual mistakes have propagated in the literature. As coacervate complex formation is a well-known and widely used, but little understood, phenomenon in physical polymer science, this paper represents an attempt to give a concise and comprehensive overview on the main research streams followed in this field regarding the parameters influencing the formation of complex coacervates encompassing various technological aspects enabling the investigation of complexes coacervates in industrial applications. Finally, a critical evaluation of perspectives and future challenges related to the further advancement and development of next generation materials are proposed and insights into the outlook of the field are explored.

Dr. Partha Sarathi Roy

RECENT DEVELOPMENTS AND NEW FRONTIERS IN COMPLEX COACERVATE-BASED MATERIALS FOR BIOMEDICINE

Dr. Partha Sarathi Roy*

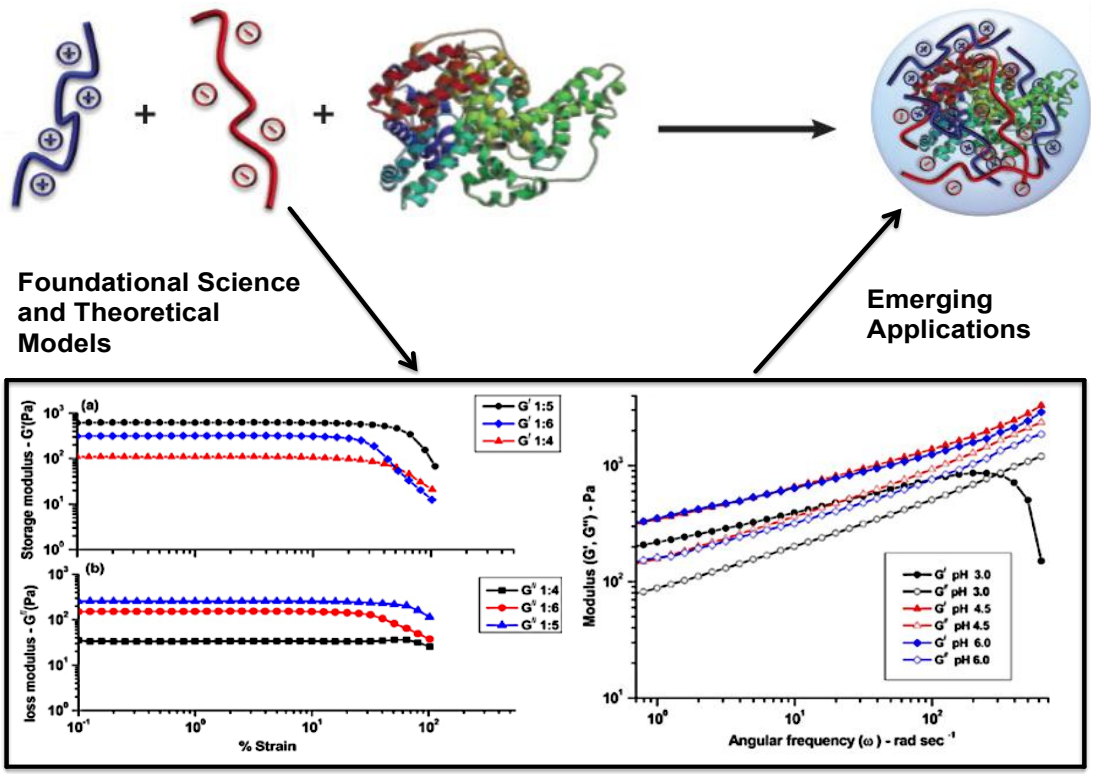

1. INTRODUCTION

Charged soft matter is ubiquitous in both the synthetic and natural worlds, where the presence of electrostatic interactions serves as a way to imbue systems with the ability to respond to stimuli and enrich the possibilities for self-assembly. In fact, charge-driven assemblies have been historically invoked in origin of life theories. In this review, we consider a class of charged materials —complex coacervates—that has emerged over the past few decades as particularly versatile. A SCOPUS exploration for "complex coacervation" divulged 140 papers before 2000 that jumped to 661 papers between 2000 and 2015, showcasing the renewed interest in this area. Biopolymer mixtures in aqueous solution are generally characterized by a thermodynamic instability that results macroscopically in a phase separation. The term coacervation derives from the Latin verb ''coacervare'', meaning ''to crowd together, to pile up''. In 1929, de Jong reported the separation of gum arabic (a carbohydrate polyanion) and gelatin (a polycation below pH 4.8) solutions into polymer-rich and -poor liquid phases upon mixing, a phenomenon they named "complex coacervation".[1] Complex coacervation (i.e., a spontaneous liquid/liquid phase separation) is a particular case of associative phase separation, that occurs when oppositely charged macroions (or polyelectrolytes) are mixed. The process of coacervation leads to the formation of a dense macroion-rich phase (the coacervate) in equilibrium with a dilute macroion-poor phase (continuous phase or supernatant).[2-4] The widespread relevance of coacervates has led to a recent surge of research over the past decade, which has led to new fundamental scientific concepts, next-generation functional (bio) materials, and has set the stage for a new wave of modern materials that is pushing the boundaries of polymer physics and chemistry.

The literature on complex coacervation is daunting because of its size, breadth of discipline (spanning physical chemistry, bio-chemistry, colloid science, chemical, biological, biomedical, and materials engineering, among others), and engagement of both natural and synthetic polymers in a myriad of combinations with other charged and uncharged components. While not aiming at an exhaustive coverage of the field, in this review, we restrict our discussion in describing and contextualizing the recent advances in the science and engineering of polymer-polymer complex coacervates, outlining (i) the need for this flurry of research, (ii) what

the soft matter community has accomplished, and (iii) some of the exciting directions enabled by this research. A critical evaluation of challenges affecting the development of next generation materials is also discussed, and insights into the outlook of the field are explored.

2. WHAT ARE COMPLEX COACERVATES?

The word "coacervation" was introduced by the pioneering work of Bungenberg de Jong and Kruyt[1] and derives from the Latin "acervus", which means aggregation (a heap), and the prefix "co" (together) to signify the preceding union of the colloidal particles. This process was initially reported by Tiebackx in 1911 without using the word;[5] he found that the addition of an acid to a mixed solution of Arabic gum and gelatin results in phase separation. It was almost two decades later that the term "coacervation" was coined by Bungenberg de Jong and Kruyt, who studied the phase behavior of several binary mixtures by optical microscopy. IUPAC defines coacervation as the separation into two liquid phases in colloidal systems (the phase more concentrated in colloid component is the coacervate, and the other phase is the equilibrium solution).[6] H. G. Bungenberg de Jong, one of the early leaders in colloid chemistry at Utrecht University in The Netherlands, defined and described the phenomenology of complex coacervation in several superb chapters in a book, Colloid Science II, edited by H.R. Kruyt,[7] written over several years and finally published in 1949. According to Bungenberg de Jong and Kruyt[7,8] (Figure 1) two types of coacervation are observed: (i) simple and (ii) complex. In simple coacervation, phase separation is induced by the addition of incompatible, and poor solvents (like acetone, alcohols etc.) to the aqueous polymer solution, while complex coacervation is commonly described as a phase separation of polymer-poor supernatant phase and a dense, polymer-rich coacervate phase which results from the association / electrostatic interactions[9] between oppositely charged macro-ions when such associates approach electroneutrality.[10-13]

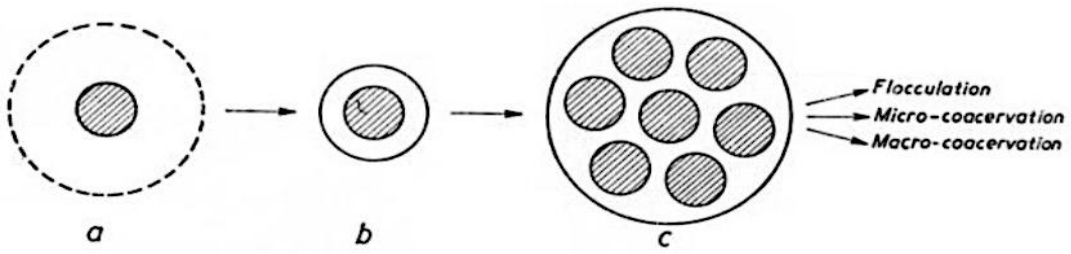

Figure 1: Schematic representation of the mechanism of phase separation by coacervation. (a) particle with a "diffuse solvate mantle" (dotted periphery), (b) particle with a "concrete solvate mantle", (c) fusion of the particles to a coacervate with their "concrete solvate mantle". This figure was reproduced from ref. 7. Copyright 1949, Elsevier.

The principal requirements for such behavior appear to be the formation of soluble complexes with near-neutral charge and noncomplementarity between macroions, including gelatins of different isoelectric points,[14-16] proteins with either synthetic[17-18] or natural polyelectrolytes (PEs),[19-20] PEs with dendrimers[21] and PEs with oppositely charged surfactant micelles.[22] If ion- pairing is too efficient, precipitation will occur. An advantage of the system consisting of PEs with oppositely charged surfactant micelles is that micelle surface charge density (σ, C nm-2) can be varied continuously in a given sample via Ph[23] or mixed surfactant stoichiometry.[24,25] Tuning σ allows construction of phase boundaries, which describe the formation of soluble complexes and coacervates at values of σ that depend on key electrostatic variables, that is, ionic strength, I, and polyelectrolyte linear charge density, ξ. The observed interdependence of σ_C, I, and ξ facilitate comparison of experiment with theories of polyelectrolyte-colloid interaction[26,27] and intermacroion condensation.[28,29]

Coacervation is considered to be an eco-friendly process as it usually takes place in water and under relatively mild conditions of pH and temperature. Additionally, it is also a cost-effective technique since neither a special device nor extensive production steps are required. The obtained structures induced by demixing are considered to be among the more intriguing systems in colloid chemistry.[30-32]

Theoretical treatment of complex coacervation of solutions of biocolloids and of synthetic polyelectrolytes followed shortly[33] after Bungenberg de Jong's pioneering studies.[8] These early approaches and extensions coupled Flory-Huggins theory with an additive Debye-Huckel electrostatic term, implicitly assuming

that the macroions could be treated as well-separated, high- valence, pointlike particles. Such an assumption is clearly invalid in the coacervate phase, which is locally of high polymer concentration beyond c^*. The earliest theories of complex coacervation, notably that due to Voorn and Overbeek,[33-35] attempted to augment the veritable Flory-Huggins description of polymer solution thermodynamics with a term to account for the screened electrostatic interactions among polyions, and following theoretical models were developed by Veis *et al*.,[36] Nakajima and Sato,[37] and Tainaka.[38] The Veis-Aranyi theory[39] described the complex coacervation in gelatin systems as a two-step phase separation. Charged molecules interact first through electrostatic interactions and then aggregate. The neo- formed aggregates (identified later as soluble intrapolymeric complexes) slowly rearrange in time to form droplets called coacervate. This theory was subsequently confirmed and completed by an intermediate step. The primary soluble complexes interact to form electrostatically neutral interpolymeric complexes. These insoluble complexes ultimately form coacervates, which coarsen with time and sediment to form the so-called coacervated phase.

A more modern approach, based on the random phase approximation (RPA), accounts for the extended nature of polyelectrolytes and the coupling between conformational and electrostatic degrees of freedom in a mixed polyelectrolyte solution.[40-42] These theories are, however, restricted to weakly charged polyelectrolytes at modest salt concentrations where local details of ion size and hydration are relatively unimportant. Similar approaches have been used to study pH effects on charged colloids.[43] Most recently, "field- theoretic" simulations have been used to examine the conditions under which oppositely charged polymers produce complex coacervates.[44,45]

3. COMPLEX COACERVATION AT THE ORIGIN OF LIFE: COMPLEX COACERVATE AS PROTOCELLS & MEMBRANELESS ORGANELLES

The importance of their exotic character attracted scientists even beyond the field of colloidal chemistry like A.I. Oparin, a Russian biologist, who cited de Jong's work, mentioned the similarity to proto-cells and coacervates, proposed that life on Earth first formed in coacervate droplets,[46] and some recent studies are heading towards the same direction.[47-51] He summarized his ideas in a famous book entitled *The Origin of Life*. The central argument of this book was that life might have originated inside coacervates containing myriad different organic molecules. Oparin observed that coacervates, intended as small droplets of high concentrations of organic molecules, often form autonomously even in dilute solutions. He therefore suggested that coacervation could have been the mechanism through which a fluid phase would separate in the 'primordial soup'. Over the next few decades, Oparin and co-workers demonstrated chemical enrichment within the droplets, in-situ enzymatic reactions, and droplet growth and fission reminiscent of cellular life.[52] This 'metabolism-first' approach, however, provided no clear connection to genetic evolution and information propagation via nucleic acids that would have been a key step at the onset of life. Their experiments also presumed the existence of large macromolecules and polymers that are unlikely to have existed in a prebiotic environment.

In order for coacervates to be viable protocells, with the ability to sustain both chemical and genetic evolution, they must be able to form from small molecular weight molecules, particularly nucleotides and their activated derivatives. This was first demonstrated in 2011 by Koga *et al*.,[47] who showed that coacervate microdroplets could be formed from nucleoside triphosphates (ATP), diphosphates (ADP, FAD, NAD), and monophosphates (AMP) when mixed with short (2–10 amino acid (aa)) lysine polypeptides (OLys) that might plausibly be produced by prebiotic processes.[53-54] This study showed that phase separation of small molecular weight ions has many similarities to complexation of larger polyelectrolytes. The dependence on electrostatic interactions, for example, is shown by the increase of the critical concentration required for coacervation (CCC) with decreasing negative charge from ATP>ADP>AMP. In addition, they found that increasing the molecular weight of Poly(diallyldimethylammonium)(Poly(DADMAC)) from 150 to 275 kDa increased charge neutralization(with ATP) from 70 to 90%, These results suggest that increased hydrophobicity, decreased solubility and increased orientational freedom from longer polymer chains all contribute to increasing charge neutralization at the CCC.

Analogous to membraneless organelles, complex coacervates are water droplets dispersed in water and formed by spontaneous liquid–liquid phase separation (LLPS) of an aqueous solution of two oppositely charged polyelectrolytes to form a dense polyelectrolyte-rich phase (coacervate) and a more dilute solution (Figure 2).[55-57]

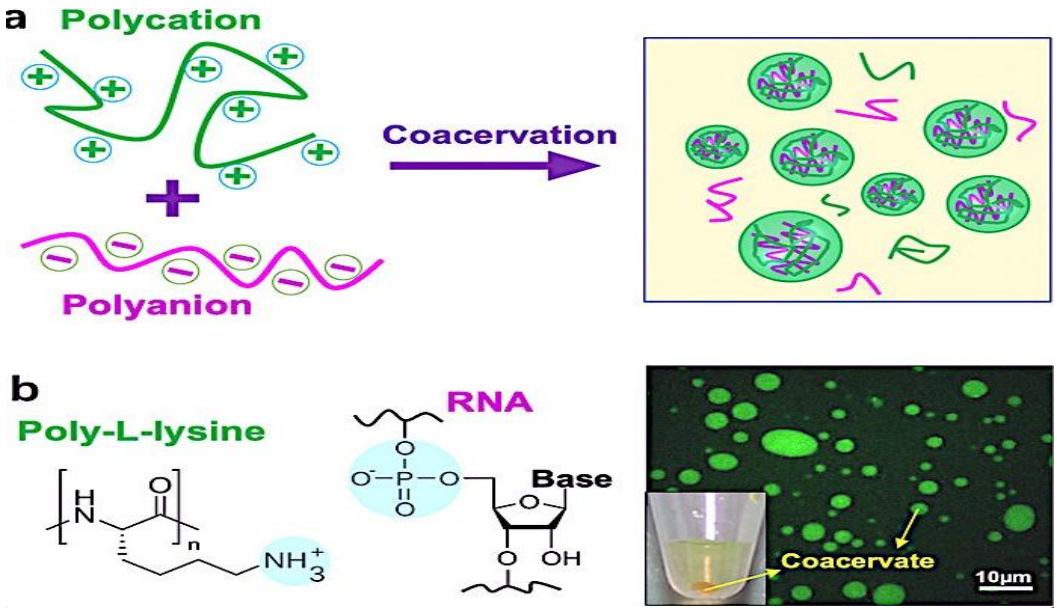

Figure 2: (a) Schematic illustration of the formation of coacervates via mixing pol- ycations and polyanions. (b) An example of coacervates formed from poly-L-lysine and RNA. The right panel shows the as-formed coacervates labeled by fluorescein isothiocyanate. This figure was reproduced from Deng, N.- N. Complex coacervates as artificial membraneless organelles and protocells. *Biomicrofluidics, 14* (5), 051301 (1-6),[58] Copyright 2020, with the permission of AIP Publishing.

The term membrane-free or membraneless organelles (MLOs) refers to a wide variety of subcellular bodies that lack a lipid boundary, with sizes in the order of 0.01–10μm.[59,62] Examples include nucleoli, Cajal bodies and paraspeckles in the nucleus, and processing bodies and stress granules in the cytoplasm. Like the synthetic coacervates these MLOs are dynamic but appear to have significant involvement in essential cellular processes such as replication, signaling, stress response, and disease. Many of those bodies share other distinctive features: they are spherical, deform in flow and show wetting, dripping, and fusion. These are all characteristics of liquids, and increasing evidence suggests that many MLOs are, in essence, liquid droplets dispersed in the cytoplasm or nucleoplasm and formed through LLPS, although some are also reported to be gel-like solids.[63]

From a physicochemical point of view, one of the most relevant aspects to mimic of MLOs are the material properties (Figure 3), which affect not only the deformability and wetting behavior but also the uptake of client molecules by partitioning and catalytic properties. As coacervates and MLOs are both typically formed by phase separation of macromolecules in solution, driven by the same types of underlying interactions, it is not surprising that many material properties are very similar, or at least have a similar range.

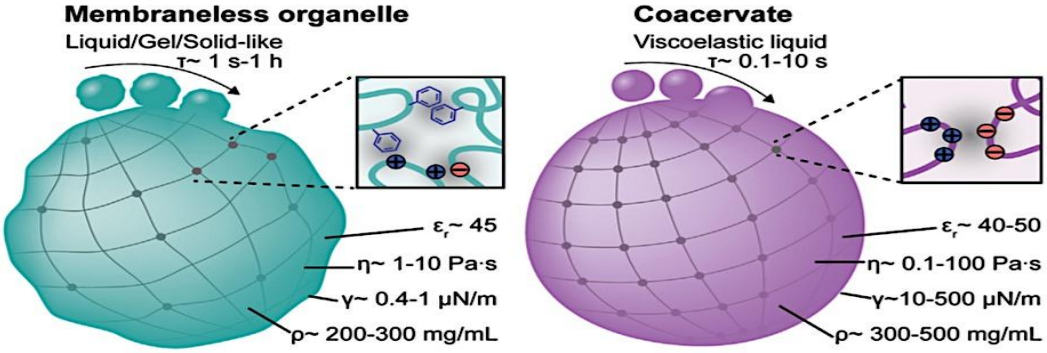

Figure 3: An overview of some relevant physicochemical properties of MLOs versus coacervates, highlighting the parameters: time of coalescence (τ), relative permittivity (ε_r), interfacial tension (γ), viscosity (η), and 'density' (ρ). The similarity in permeability (indicated as mesh) and the higher charge screening of coacervates compared to MLOs (greater number of grey spheres

representing ion pairs) is also indicated. This is in contrast to the more variable interaction mechanisms (π-π, cation- π, and charge–charge) that occur within the more chemically complex MLOs (left box). This figure was reproduced from Yewdall, N. A; André, A. A. M; Lu, T; Spruijt, E. Coacervates as models of membraneless organelles. *Curr. Opin. Colloid Interface Sci.*, *52*, 101416 (1-14), [64] Copyright 2021, with the permission of Elsevier Ltd.

A glance in the hierarchical organization yields numerous similarities between MLO formation in cells and coacervate formation *in vitro* (Figure 4).

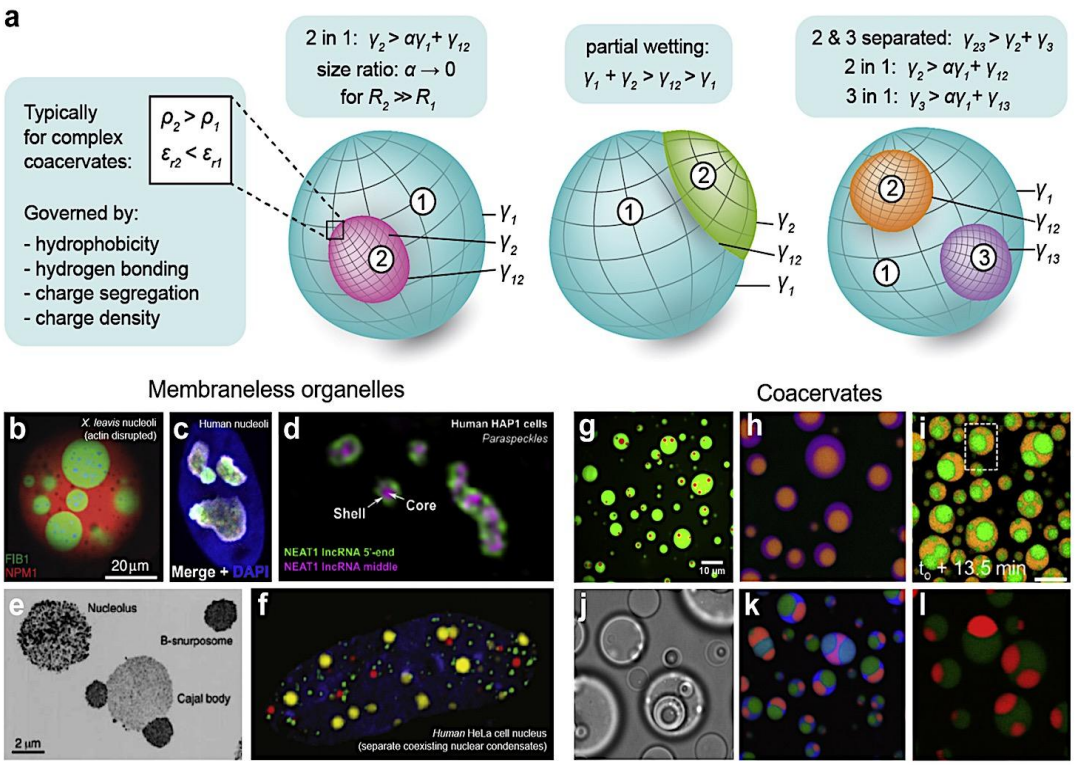

Figure 4: Hierarchical organization in MLOs and coacervates. A schematic illustration of three experimentally observed hierarchical arrangements highlighting the relative magnitude of the interfacial tension (γ), relative permittivity (ε_r), and density (ρ) (a).[64] The parameter α is a measure for the relative size of the domains.[65] Various examples of hierarchical organization in MLOs: the nucleolus (b–c), paraspeckles (d), Cajal bodies (e). By contrast, many MLOs also remain separated (f). Efforts to mimic these structures in coacervates have used a variety of electrolytes. These examples include ssDNA(red)/PLys(Me)$_3$ core coacervates in a ssDNA/GFP-K$_{72}$ (green) outer coacervate phase (g); nested multiphase organization in the 2xRRASL peptide (green)/Prot (red)/pGlu (blue) coacervate system (h), and the pLys (green)/Q-dextran (orange)/ss-oligo system (i); nested triple coacervates with an ATP/PAH inner core, surrounded by a PSPMA/PDDA shell in a PAA/PDDA outer coacervate phase (j); multiphase coacervates with double cores, some appearing partially wetted, observed with PAH, Prot, 2xRRASL, PAA, pGlu, and polyU (k); and partial wetting and lens-shaped domains observed in a pLys (red)/pAsp (green)/polyU coacervate system (l). Nonstandard abbreviations include protamine sulfate (Prot), poly-uridylic acid (polyU), poly-L-glutamic acid (pGlu). This figure was reproduced from Yewdall, N. A; André, A. A. M; Lu, T; Spruijt, E. Coacervates as models of membraneless organelles. *Curr. Opin. Colloid Interface Sci.*, *52*, 101416 (1-14),[64] Copyright 2021, with the permission of Elsevier Ltd.

Cells differ, however, in using active processes to achieve dynamic control over MLO assembly and disassembly.[66] To understand these control mechanisms, we first consider the framework of liquid phase separation that underlies formation of coacervates and many MLOs. The condensation of *chain-like* macromolecules, such as intrinsically disordered proteins (IDPs), into a dense liquid phase *in vitro* is usually described by a mean-field Flory-Huggins theory.[63]

$$\frac{F}{k_B T} = \frac{\phi}{N}\ln\phi + (1-\phi)\ln(1-\phi) + F_{int} \quad (1)$$

where F is the free energy, φ is the volume

fraction, N is the chain length, and F_{int} is the interaction free energy. For simple coacervation, F_{int} is expressed using an effective macromolecule- solvent interaction parameter χ: $F_{\text{int}} = \chi\varphi\ (1 - \varphi)$. For complex coacervation of polymers with an identical length and charge density (σ), F_{int} can be expressed by a Debye-Hückel approximation using an electrostatic interaction constant α: $F_{\text{int}} = \alpha\ (\sigma\varphi)3/2$.

When the interactions are sufficiently strong (large, negative χ, large α, or large σ), a first-order phase transition is predicted, resulting in two coexisting liquid phases: a dense (coacervate) phase and a dilute phase. The width of the two-phase region is set by the relative interaction strength (χ or $\alpha\sigma 3/2$), which is in general a function of temperature, pH, salt concentration, and the chemical groups in the macromolecules.[63]

4. THEORETICAL MODELS

4.1. Voorn-Overbeek theory: The Classical Theory of Coacervation. The earliest theory of complex coacervation, known as the Voorn-Overbeek (VO) theory,[33-35,67,68] established the prevailing conceptual understanding of the phenomenon; here, the translational entropy of the charged species competes with the electrostatic attraction be- tween the same species. The VO model was specifically for two oppositely charged polyelectrolytes — a polycation and a polyanion — and combined the Flory-Huggins theory of mixing for polymer solutions[69] with the Debye-Hückel theory of dilute electrolytes. [64,65] This results in the following expression for the mixing free energy F_{VO}.[33-35,67,68]

$$\frac{F_{VO}}{Vk_BT} = \sum_i \frac{\phi_i}{N_i} \ln\phi_i - \alpha \left[\sum_i \sigma_i \phi_i\right]^{3/2} + \frac{1}{2}\sum_{ij} \chi_{ij}\phi_i\phi_j \quad (2)$$

The first term on the right-hand side is the mixing entropy for each species i (including polyelectrolytes, small-molecule salt ions, and solvent) with volume fraction φ_i and degree of polymerization N_i that drives the system towards miscibility. The second term is a Debye-Hückel free energy that is the correlation- induced attraction between oppositely charged electrolytes.[70,71] Here, the proportionality between the number density and volume fraction of charges is given by the factor σ_i. The strength of the electrostatic energy is given by the quantity $\alpha = \lambda_B/2a$; a is the radius of the charged of species and $\lambda_B = e^2/4\pi\varepsilon k_B T$ is the Bjerrum length, which is distance over which the electro-static energy is larger than the thermal energy $k_B T$. This contribution thus formally considers the attraction between a small, molecular charge and the average distribution of the surrounding oppositely charged species. The original theory only considered these first two terms, however the third term in Equation 1 is often included, [72-74] which captures the short-range interactions included in the Flory χ-parameter between each pair of species i and j.[69]

This model makes predictions for the phase behavior of poly- electrolyte complex coacervation, with phase separation being observed at low salt and polymer concentrations.[67,68] In its original manifestation,[67,68] and in all but a few subsequent studies,[75-78] a major simplification is made that the polyanion and polycation species are symmetric, and can thus be considered a single component. The same simplification is also made for the anion and cation in the added salt, resulting in an effective 3-component system (polyelectrolytes, salt ions, water). The original salt concentration vs. polymer concentration phase diagram for complex coacervation predicted by Overbeek and Voorn (Figure 5) is analogous to the standard solvent-polymer phase diagram from Flory-Huggins, [69] except the ordinate axis plots the salt concentration rather than the temperature. This correspondence is physically appealing, in that it highlights the role of added salt as a way to weaken the driving force for phase separation in the same way that temperature does for standard χ-driven phase separation.

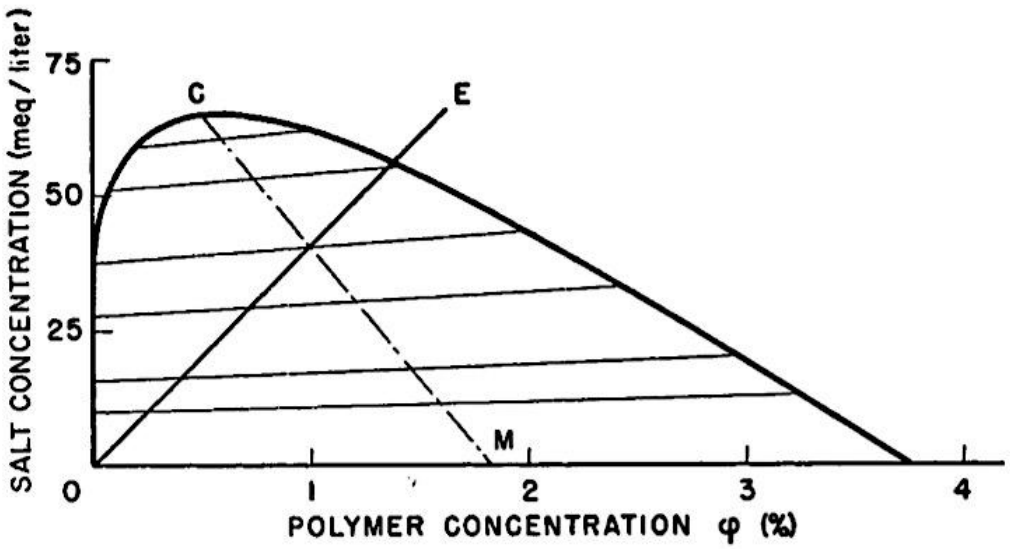

Figure 5. Voorn Overbeek. Original salt concentration vs. polymer concentration phase diagram for complex coacervation predicted by Overbeek and Voorn. Point *C* denotes the critical point, with the line to *M* indicating the center of the tie lines. The line from the origin to *E* indicates conditions where the salt concentration is entirely composed of the polyelectrolyte counterions. This figure was reproduced from Overbeek, J. T. G.; Voorn, M. J. Phase Separation in Polyelectrolyte Solutions, Theory of Complex Coacervation. *J. Cell. Comp. Physiol.*, *49* (S1), 7-26,[79] Copyright 1957, with the permission from John Wiley and Sons, Ltd.

A key difference between the predictions of VO and Flory-Huggins is that, while in the latter the two phases are in thermal equilibrium, the former has two phases in chemical equilibrium. This leads to a subtle difference in the phase diagram, with the two coexisting phases in Flory-Huggins being at the same temperature (so that tie-lines denoting this co- existence are horizontal),[69] while the two coexisting phases in VO are at different concentrations. This leads to tie lines connecting coexisting points in the phase diagram being non-horizontal.[67,68,80,84] Indeed, VO predicts a positive slope for these tie lines,[67,68] because the driving force for phase separation is the favorable electrostatic attraction between the positive and negative species, the small molecule salt ions preferentially partitions into the charge-dense coacervate phase.

The VO expression for the electro-static contribution to the free energy density, F_{el}, was inspired by the Debye- Hückel theory for dilute simple (small ion) electrolyte solutions, but fails to correctly describe free energy density for complex coacervates in any concentration regime. The VO model is based on a picture where all the bound polymer ions, of concentration $\rho\ \sigma$, are detached from the polymers and their electrostatic correlation energy is computed using the Debye - Hückel theory. The VO model neglects finite ion sizes, chain connectivity, and the highly correlated nature of opposite charges at short length scales present in a complex coacervate, including "ion-pair"(IP) and "counterion condensation"(CC), and thus much of the chemistry specificity of the components involved cannot be accommodated. Furthermore, charge densities of either PE chain type remain constant in the VO model, thus neglecting the charge regulation effects induced by the local environment especially in weakly dissociating PEs. Obviously the fact that the charges are bound to the polyelectrolyte backbones is an essential piece of physics that cannot be ignored. It is surprising that this major deficiency in the VO theory has not been appreciated by the colloid and polymer science communities and continues to be applied in the modern literature. Recent literatures argue that although the VO theory makes strong errors in structure and charge aggregation, this is somewhat compensated by excluded-volume effects in some limits. In spite of its conceptual and quantitative inadequacies, the VO theory continues to be widely applied in both experimental and theoretical studies, including very recent publications.[73,85-87] Our opinion however, is that the VO theory is entirely unsatisfactory, both from a conceptual and from a quantitative standpoint.

4.2. 'Beyond VO' Observations in Coacervation: Extensions to VO model and modern developments in theory of complex coacervation. Perhaps the most persistent yet subtle challenge of coacervation is that it is indeed possible to fit simple phase-behavior representations to most candidate theories,

including VO. This is best exemplified by the work of Spruijt *et al*., which used VO theory combined with a Flory-χ parameter to parameterize a number of experimental phase diagrams;[73] successful matching of VO theory to experimental interfacial tension measurements likewise show how challenging it is to determine that a theory is physically meaningful.[88] In an effort to refine the theoretical picture of coacervation, it is thus important to highlight the situations in which VO breaks down experimentally, which must be explained by successful theories.

1. **Salt partitioning.** Inspired by simulation and theory efforts[89-92] discussed in detail later in this review, experiments have recently found that most coacervation-driven phase separations exhibit a higher salt concentration in the supernatant phase than the coacervate phase.[89,93-95] This is opposite of what VO predicts.[33,79]
2. **Entropy versus enthalpy of coacervation.** Thermodynamic characterization of coacervation has demonstrated that mixing of the two oppositely charged polymers is highly entropic, while typically having only minor enthalpic contributions to the overall coacervation process.[96-100] This contrasts with VO theory, which considers coacervation to be an enthalpic process driven by the increased electrostatic attraction between the charged components.[33,79]
3. **Molecular or physical justification for fitting parameters.** Previous efforts to match VO to experiment have been transparent about the fitting parameters used,[73] however it is unclear that the parameters themselves are physically reasonable for the polymers considered. While quantitative, *a priori* prediction of model parameters is not generally a reasonable expectation for simplified theoretical models. Knowledge of the underlying polymer chemistry should be qualitatively consistent with the interpretation of the parameters used in the model.

These experimental observations have, in part, spurred the further development of coacervate theory and thermodynamic study. However, as the candidate theories have proliferated, there has been a concomitant effort from the experimental side to develop more ways to test and probe the regimes of validity for coacervation models, and to decide for a given system the most appropriate physical explanations of coacervation.

Chain connectivity effects missing in the VO model have been addressed utilizing the random phase approximation (RPA) for ideal chains, the accuracy of which is limited to weak and long-ranged fluctuations and low charge densities. Chain connectivity has been recently evaluated explicitly at the Gaussian level in the high wave vector limit and shown to alter the long-ranged electrostatics dramatically at low salt[101] compared to Debye−Hückel (DH) expression derived for simple salts, but CC, IP, and charge regulation were not considered in this work. The short-range electrostatic correlations can be described by treating CC as a reversible chemical reaction. This has been done both for CC in single-PE solutions[102,103] and for IP in oppositely charged PE mixtures.[42,104,105] We note that in their model Jha *et al*. accounted for the size mismatch between components as well as the salt-induced ionization of PEs.[106] They did so by using experimentally obtained acidity constants pKA's treated as explicit functions of salinity. They, however, did not consider CC or IP.

4.3. "Veis" Symmetrical Aggregate Model . In the VO theory[67, 107] the spontaneous formation of a concentrated coacervate phase is driven by a gain in electrostatic free energy at the expense of a decrease in mixing entropy. This model assumes (i) negligible solvent–solute interactions, (ii) the absence of site-specific interactions, and (iii) the absence of soluble complexes.[68] Since previous studies on the polyelectrolyte-micelle systems show the existence of the soluble complexes and soluble aggregates thereof, we turn to the model of Veis *et al*.[39] who described the complex coacervation in gelatin systems as a two-step phase separation and modified the VO equations for complex coacervation and concluded that this occurs in two steps: (i) interaction of oppositely charged polyelectrolytes by electrostatic interaction to form complexes (referred to as "aggregates", a term we reserve for soluble species with more than two macroions) of low configurational entropy, and (ii) re-arrangement of these complexes to form coacervate in equilibrium with the dilute phase (Figure 6).

If bulk stoichiometry does not coincide with local charge neutrality, the macroion in excess can remain in the dilute phase, and this "segregation" to attain complex neutrality can be amplified by system compositional polydispersity. This rearrangement might decrease chain entropy (chains are more ordered in coacervate than in one-phase), increase chain entropy (chains more disordered in coacervate), or have no effect on chain entropy, Veis

proposes the second case. Accordingly, while 1:1 soluble complexes can only approach neutrality given some sort of symmetry with respect to chain length and charge density, more options exist for large multipolymer complex with adjustable stoichiometry (i.e. soluble aggregate) particularly in polydisperse systems. In this way, more macroions can be incorporated into the coacervate. In Veis' description of "random" coacervates, all trace of such multipolymer complexes should disappear via random mixing.

More recently, Veis considered the presence of symmetrical aggregates that might differ in chain length, or excess charge density. The mixtures of the polyions at non-equivalent concentrations led to models, where aggregates were present in both equilibrium liquid and coacervate phases: (1) polyion electrostatic equivalence was required in the concentrated phase, excess polyion remained in the dilute equilibrium liquid;[108] (2) in pauci-disperse mixtures the coacervate phase was partitioned into coexisting separate phases; (3) molecular weight determinations showed that the coacervate phases showed selection by molecular weight or charge density;[36] and (4) in heterogeneous chain length polyion mixtures, the requirement for electrostatic neutrality leads to larger aggregates and at higher mixing concentrations reduces the intensity of coacervation so that the entire mixture remains as a single phase. A schematic illustration of the various options is provided in Figure 6.

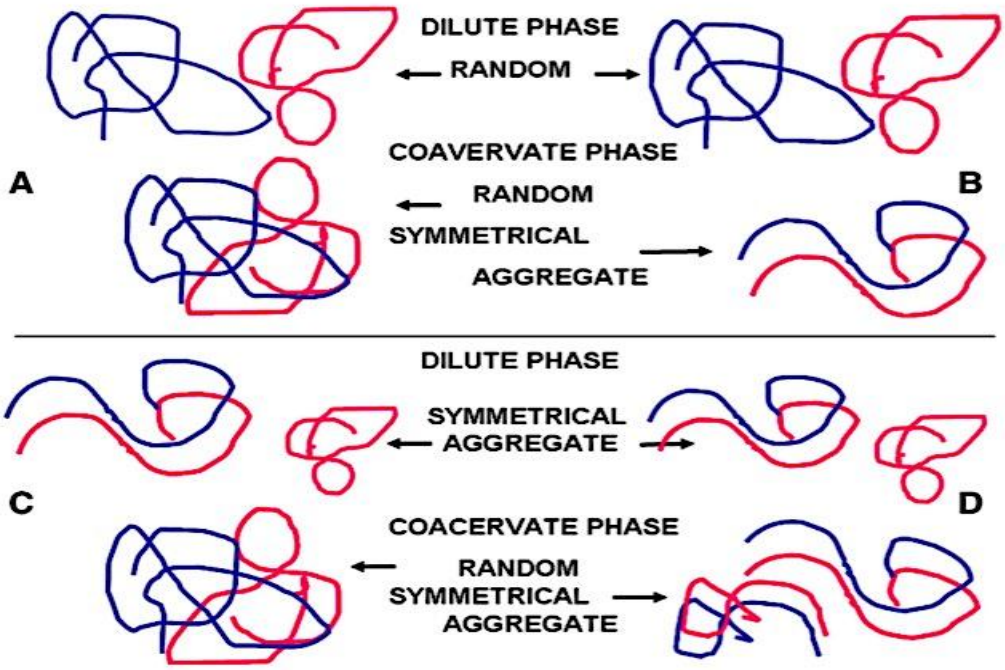

Figure 6: Four possible models for the molecular conformation or aggregated states. A. The Voorn–Overbeek random chain model. B. The initial Veis–Aranyi model — not supported by data showing aggregates in the dilute phase C and D. The two possibilities for the Veis–Gates models. The dilute phase in both cases contains symmetrical aggregates, plus any excess of one polyion or the other. Panels C and D differ in the presence or absence of possible paired aggregates in the coacervate phases. The data appear to support model D the best, based on the fractionation data. This figure was reproduced from Veis, A. A review of the early development of the thermodynamics of the complex coacervation phase separation. *Adv. Colloid and Interface Sci., 167* (1-2), 2–11,[109] Copyright 2011, with the permission of Elsevier Ltd.

The dilute phase, with stoichiometry more biased toward the macroion in excess, may still be susceptible to further coacervation if an intensive variable such as pH or ionic strength provides an additional impetus for coacervation. Progressive depletion of dilute phase macroions in this way may be analogous to MW fractionation of polydisperse polymers by reduction in solvent affinity via e.g. temperature. In the Veis model, the ionic strength is considered primarily as a determinant of complex stability (tendency to resist dissociation), while the enhancement of coacervation by temperature arises from the positive entropy of chain mixing in coacervation. The absence of counterions in the Veis model probably neglects an important contribution to the entropy of coacervation.

5. WHAT ARE THE FORCES DRIVING COACERVATE FORMATION?

In addition to polymer chemistry, the onset of complex coacervation can be modulated by tuning physical−chemical parameters such as ionic strength, temperature, pH, charge density, molecular weight, and weight ratio of the two interacting PEs.[110-112]

Charge neutralization, which plays a central role in coacervation, refers both to bulk charge stoichiometry of the macroions and to microscopic stoichiometry of the spontaneously formed intermacroion complexes. At the macroscopic level, we define the bulk charge stoichiometry as X = [+]/[-], where [+] and [-] are the concentrations of uncompensated charges on the added macroions (polyelectrolytes, micelles, particles, etc.) in the mixture. At the microscopic or mesoscopic scale, we define a charge stoichiometry coming from the intermacroion complexes: (x = Z+ /Z-), where this ratio depends on the contents of the complexes themselves, not including accompanying counterions. Although X and x are precisely equal only in the absence of free macroions, their proximity is attested to by maximal phase separation when the former is near unity. This condition, and hence, the two-phase state, can be approached by changing the weight mixing ratio or by altering the molecular charge of one macroion, most commonly by pH adjustment (The effect of pH on the stoichiometry of complex coacervation in a chitosan (Ch)-gum Odina (GO) system can clearly be observed in Figure 7), or by increasing the inter- macroion binding affinity; for example, by reduction of ionic strength.[6,113,114]

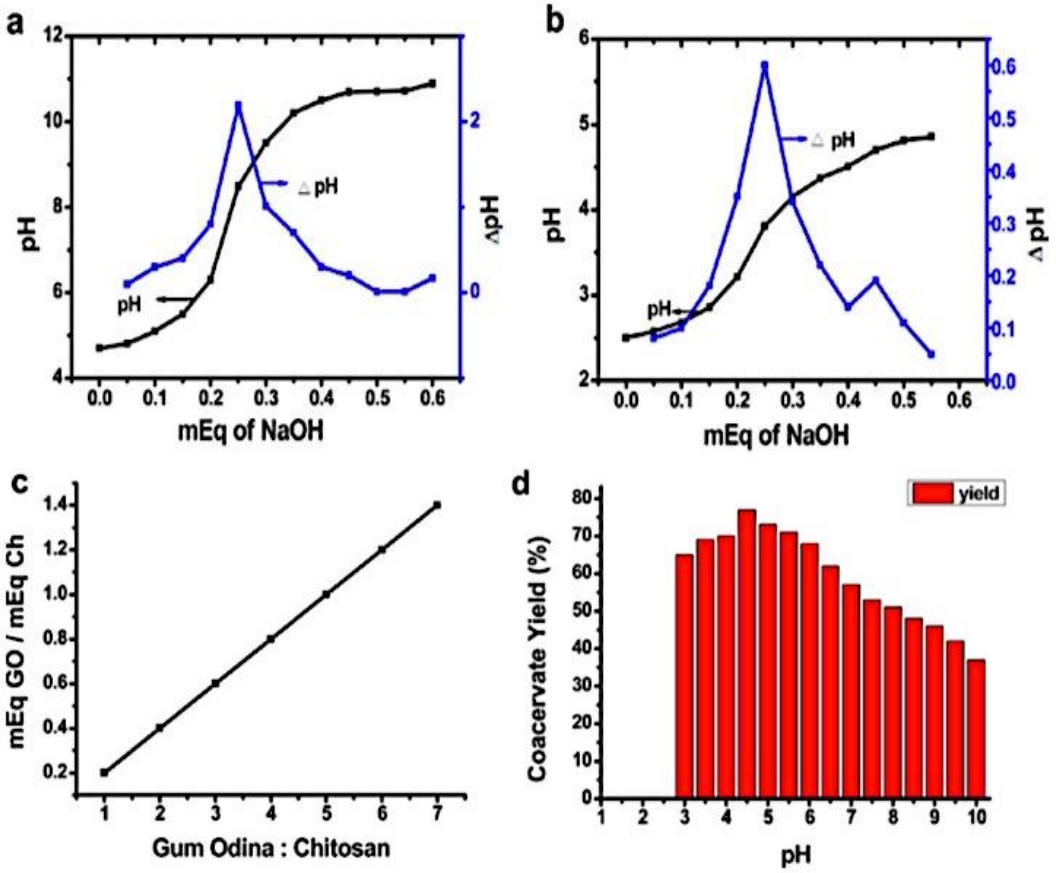

Figure 7: (a) Milliequivalent (mEq) of NaOH per 10 g of gum Odina; (b) mEq of NaOH per 2 g of chitosan (note that both 10 wt % gum Odina and 2 wt % chitosan stock solutions had 0.25 mEq NaOH); (c) mEq ratios of gum Odina (GO)−chitosan (Ch) as a function of initial gum Odina (GO)−chitosan (Ch) ratio (note that at a biopolymers ratio of 5 (5:1 ratio of GO and Ch) the mEq ratio is 1:1); (d) chitosan−gum Odina (1:5 system) coacervate yield as a function of induced pH (1−10) and after 24 h. This figure was reproduced from Roy, P. S.; Samanta, A.; Mukherjee, M.; Roy, B.; Mukherjee, A. Designing Novel pH-Induced Chitosan-Gum Odina Complex Coacervates for Colon Targeting. *Ind. Eng. Chem. Res., 52* (45), 15728−15745, [6] Copyright 2013, American Chemical Society.

There have been relatively few systematic studies of the evolution of species in the one-phase region as the two-phase region is approached, due in part to the difficulty of eliminating kinetic effects when coacervation is attained by a mixing process. Polyelectrolyte-micelle systems appear to display rather unique thermally induced coacervation at an experimentally well-defined temperature, Tφ. This temperature, Tφ, depends on mixed micelle charge, ionic strength, polymer MW, and X, the last being controlled by the ratio of total surfactant/polymer along with the ratio of ionic/nonionic surfactants.[115] It can therefore be adjusted for convenience of study. In most of the models, macroion complexes are assumed to form charge neutral aggregates at 1: 1 stoichiometry.

Zhang and Shklovskii[116] have suggested that non-stoichiometric coacervation can occur by ‘‘intercomplex or intracomplex disproportionation’’ (charge segregation). In intercomplex disproportionation, the charged aggregate experiences a migration of polycations which leads to the coexistence of a neutral coacervate drop with a more highly charged aggregate. Excess charges, on the other hand, migrate to the ‘‘tail’’ of a partially neutral aggregate in intra-complex disproportionation. The effect of nonstoichiometric charge ratios between the polyelectrolyte species can clearly be observed in Figure 8.

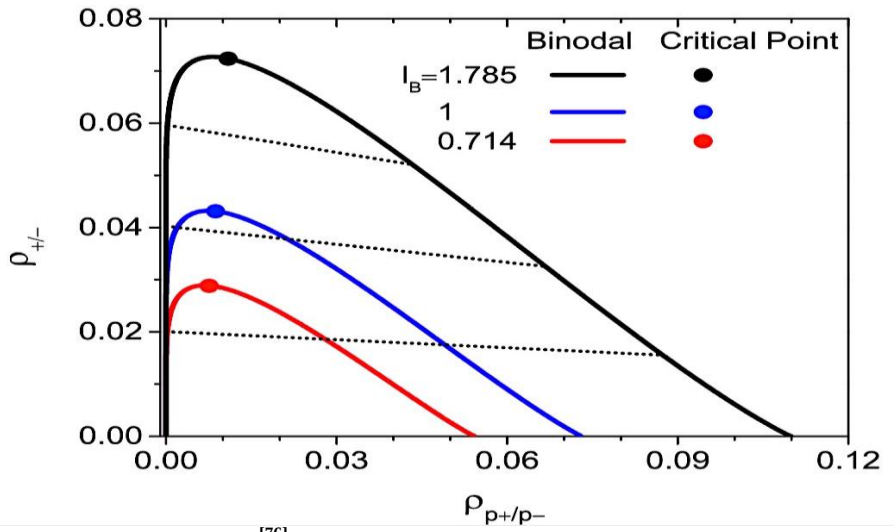

Figure 8. Work by Zhang *et al.*,[76] using a different liquid-state theory to similarly account for charge correlations in a coacervate phase diagram (salt number concentration $\rho_{\pm}$ versus polymer number concentration $\rho_{P\pm}$). This figure was reproduced from Zhang, P.; Alsaifi, N. M.; Wu, J.; Wang, Z.-G. Polyelectrolyte Complex Coacervation: Effects of Concentration Asymmetry. *J. Chem. Phys.*, *149* (16), 163303,[76] Copyright 2018, with the permission of AIP Publishing.

Complex coacervation driven by non-specific electrostatic associations has been the most thoroughly studied, but other types of weak electronic interactions, such as dipole interactions, π–cation, π–π, and metal coordination, can lead to associative liquid–liquid phase separation.[63] Macromolecular ionizable groups in electrostatic systems result in sensitivity of the liquid state to pH and ionic strength. Small changes in such variables can lead to dissolution or solidification of the liquid phase.[117] To date, there have been only a handful of reports that have looked into the effect of combining electrostatics and other interactions. For example, a series of reports from the Tirrell and de Pablo groups described the potential for hydrogen bond formation between the backbones of oppositely-charged polypeptides during complexation.[118-120] In a separate study, Hyman, Alberti, and Pappu used mutagenesis studies of the FUS family of IDPs to demonstrate a hierarchy of interactions driving phase separation.[121] While electrostatic effects enhanced phase separation generally, the distribution of cation-π interactions between arginine and phenylalanine residues affecting the material properties of the resulting coacervate in a manner consistent with the theory of associative polymers.[122-123]

Systems that undergo complex coacervation include polyelectrolyte–polyelectrolyte, polyelectrolyte–colloid, and even colloid–colloid pairs. Two forces drive complex coacervation: enthalpic contributions originating from long-range inter-macroionic electrostatic interactions, and entropic contributions originating from the loss of small ions. Carlsson

et al.[124] studied by Monte Carlo simulations the complexation in model systems composed of protein models (representing lysozyme in aqueous environment) and negatively charged polyelectrolyte. The authors showed that nonelectrostatic protein-protein attraction promoted protein-polyelectrolyte association and facilitated protein- polyelectrolyte cluster formation. This effect could be explained by considering both entropic (mainly due to the polydispersity in size and in molecular mass) and enthalpic (mainly due to the surface properties of aggregates) factors.[67,125]

However, multiple experimental[126-129] and computational studies[130-132] argue that complex coacervation has a strong favorable entropic contribution, which could arise from the gain in translational entropy of the counterions when the polyions are complexed. The driving force for polyion complexation has been investigated in computer simulations by Ou and Muthukumar.[131] They studied uniformly charged polyions in a continuum solvent using Langevin dynamics simulations. Starting with the two polyions far apart, they allowed them to complex and calculated the change in energy, which they identified as the internal energy change of the process. The Hemholtz free energy change was then calculated[120, 133] via thermodynamic integration and the entropy change from the difference between the Helmholtz free energy and the internal energy. The main conclusion of this work was that the driving force was energetic for weakly charged polyions (ξ <1) but become entropic for strongly charged polyions (ξ >1). Similar results have been reported by Rathee *et al*.[130] for associatively charged polyions, where the charge state is determined by conditions of chemical equilibrium.

Briefly, both enthalpic and entropic contributions may be significant, each of which depends markedly on the ionic strength of the solution. A polyelectrolyte chain is surrounded by a cloud of its counterions. At low ionic strength, the concentration of ions surrounding the polyion is high compared to the bulk ion concentration. The large Debye length leads to dilute counterion clouds as a compromise between Coulombic attraction and the counterion entropy. Upon addition of an oppositely charged polymer, tight complexation brings the charges closer together (Coulombic attraction; exothermic) and the counterions are released into the solution (entropy gain). On the other hand, at high ionic strength, the counterion clouds are denser, so that addition of, and complexation with, the second polymer becomes endothermic (Figure 9). Still, the entropy gain from counterion release results in a net energy gain for complex formation.

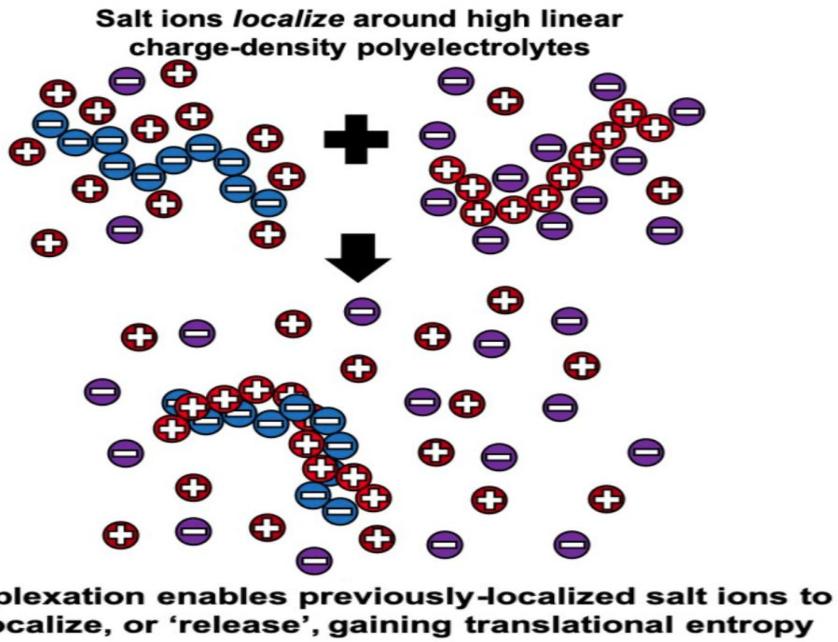

Figure 9: In counterion condensation and release,[134] salt ions localize around isolated high linear charge-density polyelectrolytes at the cost of their translational entropy.[135,136] This translational entropy can be regained if two oppositely-charge polyelectrolytes localize around each other, such that they no longer need to localize small molecule ions. This figure was reproduced from Sing, C. E.; Perry, S. L. Recent progress in the science of complex coacervation. *Soft Matter*, *16* (12), 2885–2914,[57] Copyright 2020, with the permission of The Royal Society of Chemistry.

However, above a critical salt concentration the net driving force for complexation vanishes and complex coacervation no longer takes place. Besides the salt concentration, the chemical nature of the components can affect the energy balance. In addition to electrostatic interactions, hydrophobic interactions and hydrogen bond formation are often contributing driving forces.[86] Coacervation of polyelectrolytes that exhibit these additional interactions enhances the entropic and enthalpic contributions of complexation, resulting in an elevated critical salt concentration.[137,138]

If the linear charge density of the polyelectrolyte is high enough and the charges on the polymer chain are fixed (quenched, not ionizable), phase separation usually results in flocculates and/or precipitates rather than coacervates.[8] The higher water content of coacervates is due to the hydration of excess small ions. Coacervates provide several advantages relative to precipitates: (1) the macroscopically homogeneous and cohesive coacervate fluid is easier to handle, and (2) it has a low interfacial tension. Phase separation is often described as the consequence of an insolubilization of aggregated complexes. It was previously found that phase separation occurred when the net charge of interpolymer complexes was close to 0.[139] We have to remember that, besides entropic contributions, stability of mixed biopolymer dispersions is much determined by the balance between biopolymer-biopolymer and biopolymer-solvent interactions. According to the Veis-Aranyi theory,[39] attractive interactions between biopolymers and low biopolymer-solvent interactions are favorable to coacervation. When neutral aggregated complexes are formed, as a consequence of strong attractive interactions, aggregated complexes-solvent interactions become low and phase separation occurs. Nevertheless, Xia *et al*.[140] found that the requirement of neutrality at phase separation was not a general rule and was only observed for complexes formed by protein-polycationic polymers. For protein-polyanionic polymers, phase separation occurred for complexes with a negative total charge. No explanation was provided.

The optimum conditions for complex coacervation are achieved when the pH is adjusted to a point at which equivalents of oppositely charged molecules of the two polyelectrolytes/colloids are present, because the greatest numbers of salt bonds form at this point. The intriguing question of the rheological properties of the coacervate phase was already raised some years ago after several authors hypothesized that the coacervate could behave either like an elastic gel or like a concentrated solution (viscous behavior). Most commonly, the viscoelastic response is described with respect to the storage (or elastic) modulus *G'*, and the loss (or viscous) modulus *G"*.[6]

$$\frac{s(w,t)}{g^o} = G'\sin(wt) + G''\cos(wt) \quad (3)$$

The storage modulus *G'* describes the "in-phase" response of the shear stress to a periodic shear strain of amplitude γ^o on the material (*i.e.*, effectively a cosinusoidal response), while the loss modulus *G"* describes the "out-of-phase" response, related to the ability of the material to dissipate energy (*i.e.*, a sinusoidal response). These two material functions can also be expressed in terms of a complex modulus *G** and the phase angle difference between the applied strain and the resultant stress δ.[141]

$$|G^*| = \sqrt{G'^2 + G''^2} \quad (4)$$

$$\tan(\delta) = \frac{G''}{G'} \quad (5)$$

From a rheological viewpoint the storage modulus (G′) and loss modulus (G″) in the elastic gel state have the characteristics G′ (ω) > G″ (ω), and in the viscous fluid (sol state) G″ > G. It could be clearly seen from Figure 10a and 10b, at a given strain percent in the linear viscoelastic region, the value of G′ was significantly greater than G″, indicating a dominant elastic character of the chitosan-gum Odina polyelectrolyte complex coacervate systems. The frequency sweep curves show the highest elastic mechanical response to be exhibited by the coacervate (1:5) formed at pH 4.5 (Figure 10c).[6]

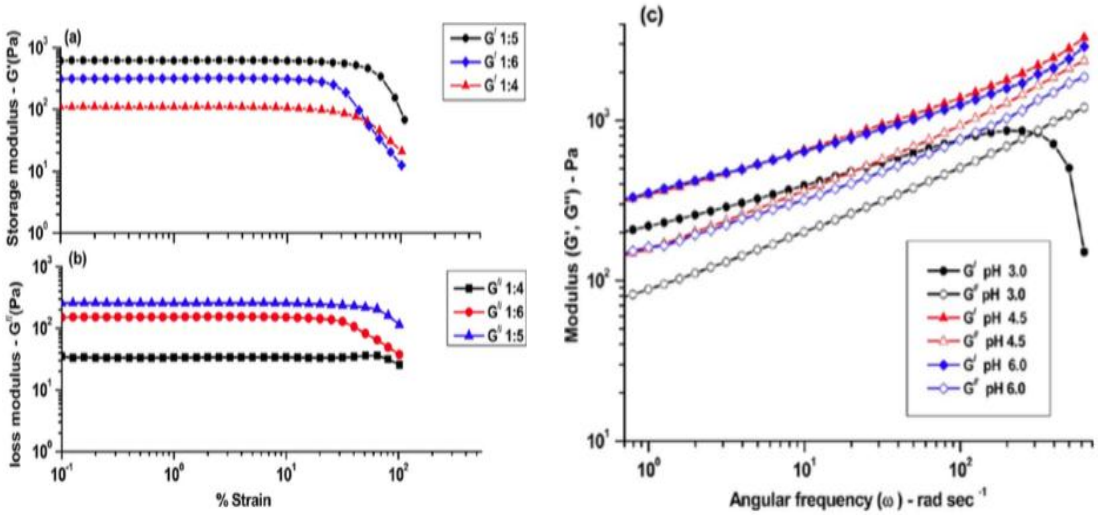

Figure 10: Variation of pH-independent Ch−GO [1:4 (initial pH value, 4.7 ± 0.0), 1:5 (initial pH value, 4.3 ± 0.1), and 1:6 (initial pH value, 3.9 ± 0.0)] PEC coacervates rheological properties as a function of strain %: (a) storage modulus G′; (b) loss modulus G″; (c) frequency sweeps of the pH-induced (3.0, 4.5, and 6.0) chitosan−gum Odina (1:5) PEC coacervates at 25 °C. This figure was reproduced from Roy, P. S.; Samanta, A.; Mukherjee, M.; Roy, B.; Mukherjee, A. Designing Novel pH-Induced Chitosan-Gum Odina Complex Coacervates for Colon Targeting. *Ind. Eng. Chem. Res., 52* (45), 15728−15745, [6] Copyright 2013, American Chemical Society.

The viscous fluid state (sol) reportedly contains only finite branched clusters, whereas an elastic solid state (gel) contains an infinite network. The network may be produced from covalent structure (chemical or irreversible gels), or it may be produced from noncovalent interactions such as electrostatic/ionic interactions, helical domains, micro- crystalline bundles, hydrogen bonding, coordination, crystallization, hydrophobic effect, and so forth (physical or reversible gels).[6] Reports on the phase behavior of complexation have described the occurrence of both liquid complex coacervates (polyelectrolyte coacervates/PECOV) and solid precipitation (polyelectrolyte complexes/PECOX), and recent efforts have attempted to better elucidate these relationships between PECOX and PECOV. It is now known that all of the properties of PECOX in contact with aqueous solutions are controlled by their salt and water content. The fundamental unit of interaction in a PEC is the ion pair Pol^+Pol^- between two charged monomer units. These interactions are broken with the addition of salt, transforming "intrinsic" charge compensation to "extrinsic", where polyelectrolyte segments are paired with, and compensated by, salt counterions, M^+ and A^-.[142-144]

$$Pol^+Pol^- + M_{aq}^{\ +} + A_{aq}^{\ -} \leftrightharpoons Pol^+A^- + Pol^-M^+ \quad (6)$$

The "doping level," y, is the fraction of polyelectrolyte compensated by counterions.

$$y = \frac{[Pol^+A^-]}{[Pol^+Pol^-] + [Pol^+A^-]} \quad (7)$$

Recognizing that $[Pol^+A^-] = [Pol^-M^+]$. A nice example of salt-controlled properties in PECOX is the strong dependence of bulk modulus on the density of Pol^+Pol^-pairs,[145] since they are physical cross-links which can be broken by salt. Pressing the salt "doping" represented in eq 6 to the extreme breaks more and more ion pairs and eventually dissociates polyelectrolyte chains from each other completely.[73,146-147] Just before this critical dissociation point, polyelectrolytes should be associated extremely loosely. These weakly associated PECs, which are, in fact, coacervates and, with salt, connect the entire spectrum of the same associated polyelectrolytes from complex to coacervates. A boundary between complex and coacervate states was defined by the crossover point between loss and storage modulus.[6]

The design of new materials based on coacervates would require an understanding of how these parameters control *inter alia* the onset of phase separation, but theoretical treatments of coacervation have investigated few of these parameters. Voorn[107] and Overbeek[68,79] suggested that coacervation can take place only beyond a critical charge density and/or chain length. On the other hand, the model by Tainaka[148] proposes that precipitation rather than coacervation will occur if the charge density

is too high or the chain length is too long, while a stable solution (single phase) will result for very low charge densities and short chain lengths. Experimental systems with much lower critical charge densities and chain lengths are better treated in the ‘‘dilute phase aggregate model’’ developed by Veis and Aranyi.[39] All these early models predict the suppression of coacervation at high ionic strengths, but all fail to predict the suppression of coacervation at low salt concentrations.[149] Recent theories have also focused on the mechanism of coacervation. According to a theory developed for weak polyelectrolytes,[150]coacervation was enhanced when the difference between the p*K* values of the polyacid and polybase groups was lowered. This result is in agreement with the stability diagrams for the coacervation of gum Arabic with gelatin. The chemical mechanisms and conditions for PEs complex coacervation have been widely explored by different authors.[151-160] Yet, only a handful of theoretical and simulation studies have investigated the influence of polymer−solvent interactions on the phase behavior of complexes.[106,161] Sato and Nakajima included the Flory interaction parameter χ to account for interaction between water and polyelectrolyte salt in the classical VO theory and deduced the limiting conditions of charge density and chain length for complexation.[161,162] Larson and co-workers extended the VO theory by incorporating the χ parameter between protonated poly(acrylic acid) and solvent molecules to explain the unusual high salt resistances of PECs measured in acidic environments.[163,164] A recent theoretical study by Rumyantsev *et al*. outlined a salt concentration−solvent quality diagram of PECs based on scaling laws. [160] The diagram of coacervate regimes in c_s−*v* coordinates is shown in Figure 11.

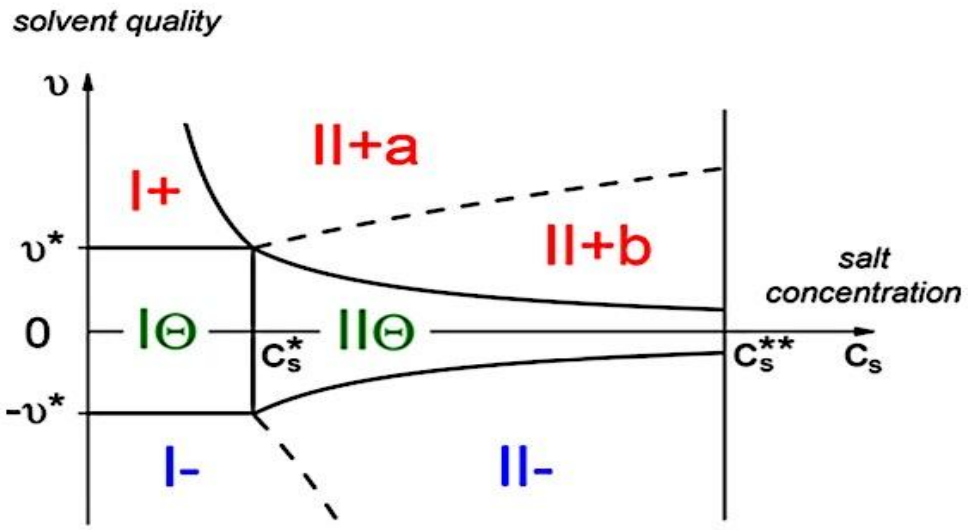

Figure 11: Diagram of states of coacervate in salt concentration−solvent quality coordinates, c_S−v. Boundaries between regimes and subregimes are indicated by solid and dashed lines, respectively. Consideration applicability limits are $c_S < c^*_S$ * ≃ u-3 and |v| < 1 (not shown in diagram). This figure was reproduced from Rumyantsev, A. M.; Zhulina, E. B.; Borisov, O. V. Complex Coacervate of Weakly Charged Polyelectrolytes: Diagram of States. *Macromolecules, 51* (10), 3788−3801.[160] Copyright 2018, American Chemical Society.

Concomitantly, experimental investigations have begun to investigate the influence of parameters such as the unique chemical attributes of the individual polymers and solvent effects on complexation.[106,138,160] Sadman *et al*. have demonstrated mechanical tunability for poly (styrene sulfonate) (PSS) and poly (4-vinyl pyridine) (QVP) complexes by varying the hydrophobicity of the quaternized poly (4-vinylpyridine) through methyl, ethyl and propyl substitutions (PSS: QVP-C1, C2 & C3 Complexes).[138] Figure 12 demonstrates that PSS: QVP complexes behave like liquids at high salt concentrations and low frequencies, and appear to approach a power-law behavior at low salts and high frequencies.

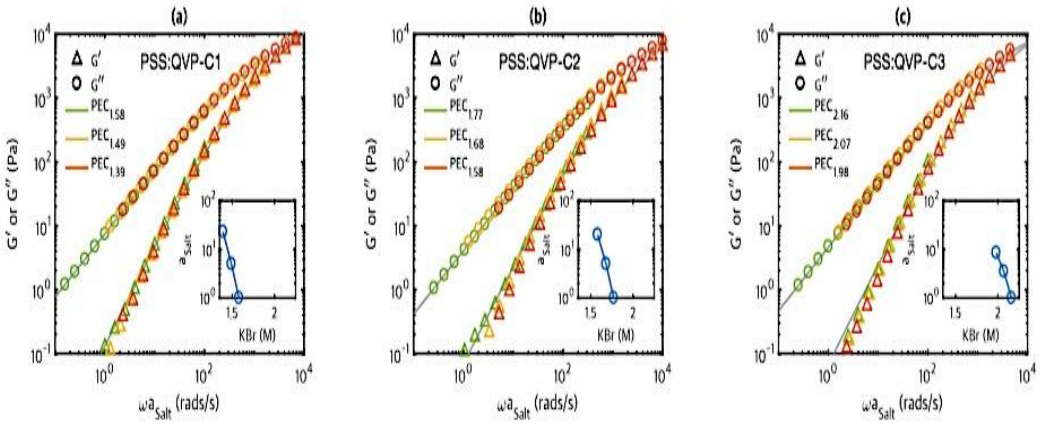

Figure 12: Time-Salt Superposition of frequency sweeps at 20 °C of (a) PSS: QVP-C1; (b) PSS: QVP-C2; (c) PSS: QVP-C3. This figure was reproduced from Sadman, K.; Wang, Q.; Chen, Y.; Keshavarz, B.; Jiang, Z.; Shull, K. R. Influence of Hydrophobicity on Polyelectrolyte Complexation. *Macromolecules, 50* (23), 9417−9426,[138] Copyright 2017, American Chemical Society.

Spruijt *et al*. included the χ parameter in calculations based on VO theory to describe experimentally determined polymer contents in PECs.[73] Figure 13 predicts that complexation takes place even for a chain length of 1 for $\chi r > 0$. It shows that for a value of $\chi r = 0.1$, the correct critical salt concentrations are predicted based on mapping of the associative phase separation onto segregative phase separation. There is a strong dependence of the critical salt concentration on the choice of χ_r, indicating that slightly more hydrophobic polymers might have a significantly higher critical salt concentration for identical chain lengths.

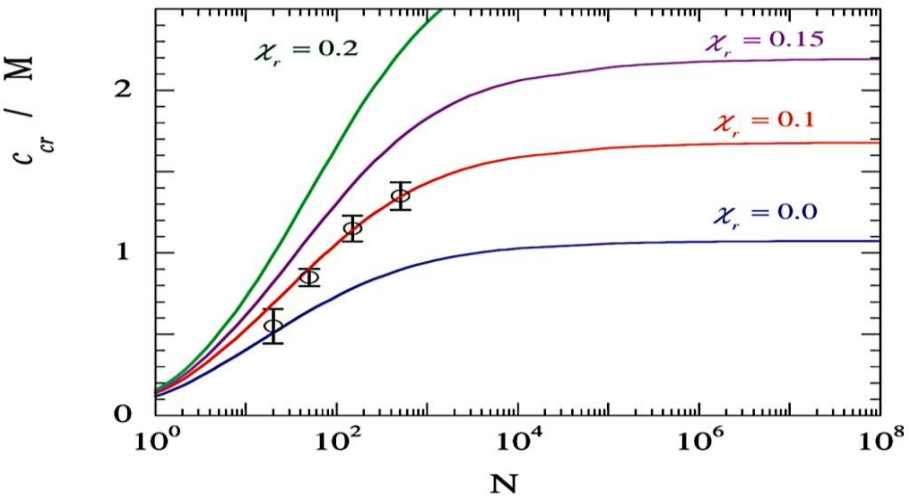

Figure 13: Critical salt concentration of complex coacervation between poly(acrylic acid (PAA) and poly(N,N-dimethylaminoethyl methacrylate) (PDMAEMA) at pH 6.5 (σ = 0.95) as a function of polymer chain length. This figure was reproduced from Spruijt, E.; Westphal, A. H.; Borst, J. W.; Cohen Stuart, M. A.; van der Gucht, J. Binodal Compositions of Polyelectrolyte Complexes. *Macromolecules, 43* (15), 6476-6484,[73] Copyright 2010, American Chemical Society.

More recently, the influence of polymer−solvent interactions on the phase behavior and complex morphology in PECs has been discussed in various polyelectrolyte systems ranging from natural polymers[165] to polypeptides[166] to synthetic polymers.[167,168]

Despite the progress in the description of the influence of solvent interactions on complexation, detailed datasets describing the phase behavior quantitatively to illustrate the effect of hydrophobicity and other prevailing physical non-covalent interactions on polyelectrolyte complexation are still elusive. These more realistic aspects of complexation are essential to advance our current understanding of

selecting polyelectrolyte pairs for PEC materials and to harness such materials into products and end-use technologies.

Most recently, "field- theoretic" simulations have been used to examine the conditions under which oppositely charged polymers produce complex coacervates.[169,170] Prabhu and co-workers have reported a lower critical solution temperature for PEC systems (potassium-poly (styrenesulfonate) (KPSS) and poly (diallyl dimethylammonium bromide) (PDADMAB) with added KBr salt)[171] that were described in a mean-field theory formalism to identify the ranges of the solvent dielectric constant and the χ parameter justifying these observations.[172] Figure 14 has the appearance of a lower critical solution temperature. T_{cp} corresponds to the point where the kinetics of phase separation becomes observable, rather than an exact thermodynamic phase boundary.

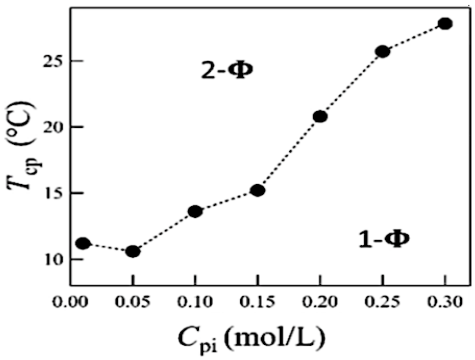

Figure 14: Cloud-point temperature vs initial polymer concentration with fixed C_{KBr} = 2.15 mol/L. This figure was reproduced from Ali, S.; Bleuel, M.; Prabhu, V. M. Lower Critical Solution Temperature in Polyelectrolyte Complex Coacervates. *ACS Macro Lett., 8* (3), 289−293,[171] Copyright 2019, American Chemical Society.

Complex theories (as shown by numerical simulations) that account for many of the factors, that can affect coacervation, such as sequence specificity,[173-175] charge correlation,[176,177] and soluble complex formation,[178] have recently been developed (Figure 15, 16).[178,179]

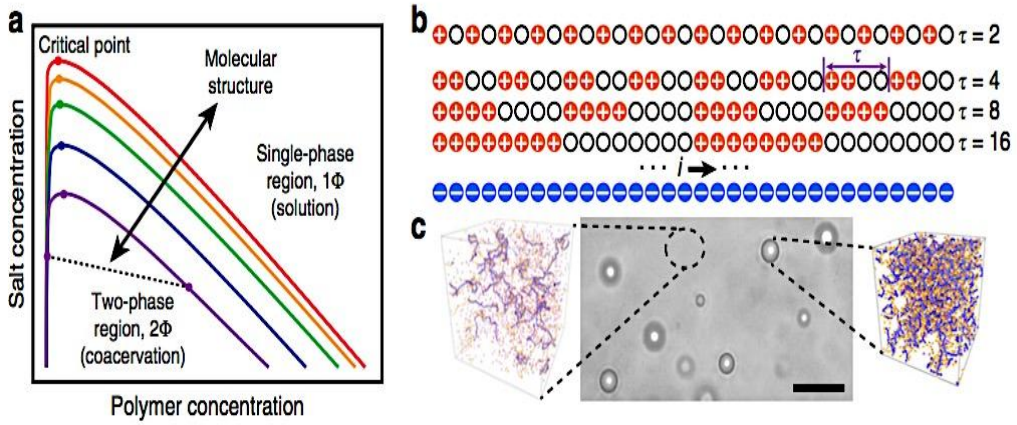

Figure 15: Molecular structure and sequence affects charge-driven phase separation. (a) Qualitative sketch of a typical phase diagram of complex coacervate- forming polyelectrolytes. Coacervation occurs at low salt and polymer concentrations, where oppositely charged polyelectrolytes undergo a liquid-liquid phase separation into polymer dense (coacervate) and polymer-dilute (supernatant) phases. The different curves qualitatively represent how the immiscible region changes with different molecular features (charge monomer sequence, spacing, ion size, degree of polymerization, valency, etc.), (b) Figure shows that charge monomer sequence is a molecular feature, which can be used to tune coacervation behavior. This simulation and experimental result is based on coacervation between a homopolyanion and a series of model, sequence-defined polycations with half of their monomers charged. These polycations are characterized by the periodic repeat of the monomer sequence, τ, (c) Coacervation is experimentally observed as droplets of a polymer- dense 'coacervate' dispersed in a polymer-dilute 'supernatant' phase. Simulation images correspond to conditions (salt concentration, 25 mM and τ = 2) shown in Figure 16. Scale bar is 25 µm. This figure was reproduced from Chang, L. W.; Lytle, T. K.; Radhakrishna, M.; Madinya, J. J.; Vélez, J.; Sing, C. E. Sequence and entropy-based control of complex coacervates. *Nat. Commun., 8* (1), 1273 (1 – 8),[177] Copyright 2017, Springer Nature.

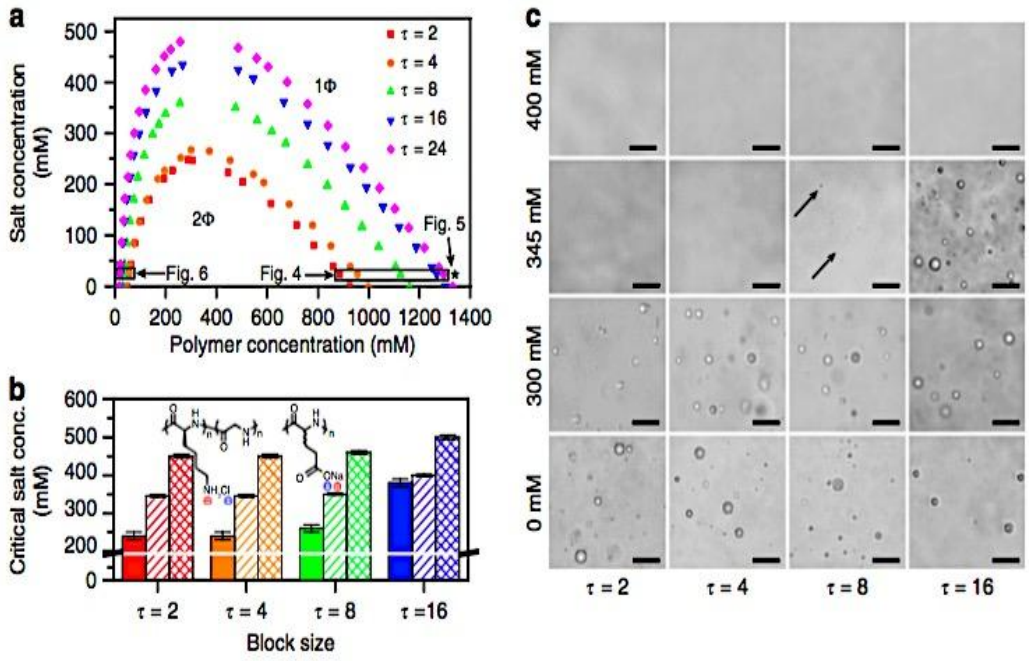

Figure 16: Coacervate phase behavior is affected by charge sequence in both simulation and experiment. (a) Simulations demonstrate that the size of the coexistence region 2Φ increases with τ, (b) The experimental critical salt concentration (CSC) for sequence-defined coacervates at a variety of total charged monomer concentrations (solid 1 mM, stripes 5 mM, crosshatch 50 mM), plotted as a function their periodic block size (τ = 2 to τ = 24). Increasing τ leads to a marked increase in the CSC, qualitatively changing by as much as 50–150 mM, consistent with simulations in a. Error bars reflect the intervals between samples in these experiments, (c) A selection of optical micrographs corresponding to the data in a, highlighting that the region of coacervation increases with τ. Arrows indicate the presence of tiny coacervate drops. Scale bars are 25 μm. This figure was reproduced from Chang, L. W.; Lytle, T. K.; Radhakrishna, M.; Madinya, J. J.; Vélez, J.; Sing, C. E. Sequence and entropy-based control of complex coacervates. *Nat. Commun.*, *8* (1), 1273 (1 – 8),[177] Copyright 2017, Springer Nature.

However, none of these provides a quantitative explanation for all types of liquid phase separating proteins and polymers, and the relative simplicity of the classical mean-field model, which can provide semi-quantitative agreement with experimental phase diagrams based on a single effective interaction parameter (χ or α), is therefore still attractive.[63, 176]

In the context of polyacid/polybase polyelectrolyte complexes, the use of acid-base interactions to overcome the free energy barrier to the mixing of rods and coils, originating primarily from the reduced entropy of mixing in the presence of rods, has to be mentioned, too. The mixing of solutions of rigid-rod macro-molecules with random coil macromolecules of opposite charge gives molecular polymer-polymer composites upon precipitation or film casting from solution. Introducing a negative χ-parameter into the original Flory theory[180] was used to model the experiments.[181]

More recently, Qin and de Pablo[182] used a Gaussian-fluctuation analysis and demonstrated how the inclusion of chain connectivity — in particular the fractal dimension of the connectivity (*e.g.*, rods versus coils versus branched polymers) plays a significant role on coacervation, and Shen and Wang[183] developed a renormalized Gaussian fluctuation field theory that self-consistently accounts for polymer chain conformation and connectivity in formulating a description of electrostatic correlations.

In particular, the RPA model for electrolytes is related to Debye–Hückel theory, and thus serves as the basis to systematically improve field theoretic models of coacervation.[184] Specifically, Borue and Erukhimovich[185,186] pioneered the application of the random phase approximation (RPA) for concentrated systems of weakly charged polyelectrolytes, and this was further elaborated for the specific case of complex coacervation by Castelnovo and Joanny.[184] Olvera de la Cruz[104] included short-range correlations via a diagrammatic representation of ion pairs as 'reversible cross-links' and also included a high-q modification to approximate the effect of finite excluded volume.

They explicitly included the effect of excluded volume via a modification to the form of the Coulomb potential. This result is an *ad hoc* addition, mathematically chosen to be straightforwardly incorporated into the RPA formalism.[125] This advance crucially captures the experimentally-observed phenomenology of salt-partitioning to the supernatant,[75] however the magnitude of the effect is sensitive to the highly-approximate form of the excluded volume. The possibility of finite-sized aggregates in the dilute regime, either by ion-pairing of individual charges or by non-specific electrostatic correlations, has been considered by numerous authors including Kudlay, Ermoshkin, and Olvera de la Cruz,[187] Shusharina, Zhulina, Dobrynin, and Rubinstein,[188] Castelnovo and Joanny,[189] and Zhang and Shklovskii (Figure 17).[116]

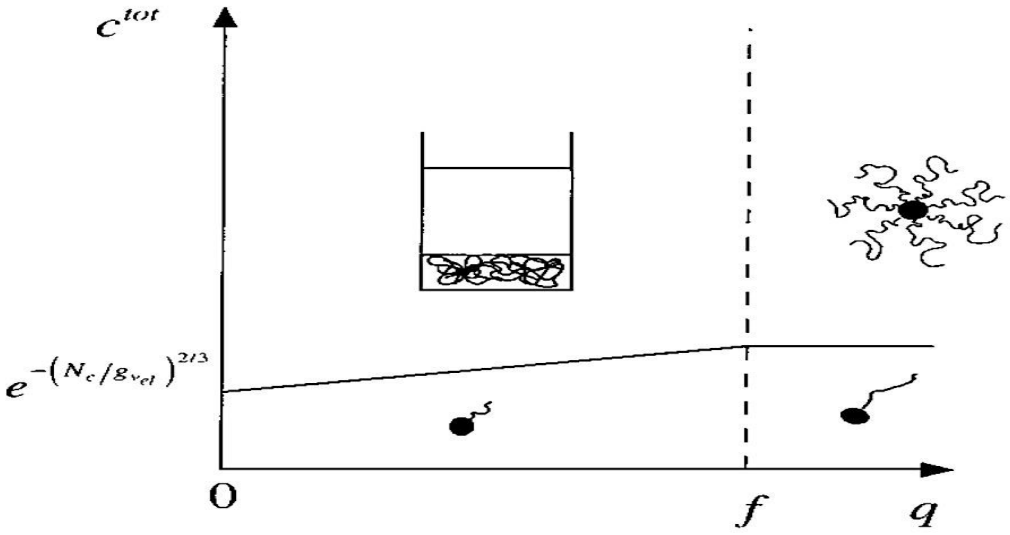

Figure 17: Phase diagram (c^{tot} vs q) in the limit of high ionic strength. The macroscopic phase separation takes place first when $q/f \leq 1$ and $c^{tot} > c_{sep}$. For higher asymmetries $q/f \geq 1$, spherical micelles are formed when $c^{tot} > c_{mc.}$ Therefore it can be predicted that the only aggregates to be observable when the solution is macroscopically stable are spherical micelles. This figure was reproduced from Castelnovo, M.; Joanny, J. F. Phase Diagram of Diblock Polyampholyte Solutions. *Macromolecules*, *35*(11): 4531–4538,[189] Copyright 2002, American Chemical Society.

Ultimately, RPA and related analytical field theory approaches elucidate the physical couplings between chain connectivity and electrostatics, and can introduce corrections to account for excluded volume and correlation effects.[92,187] These are highly sophisticated theories, yet their sophistication limits both their adaption by experimentalists and the transparency of their assumptions. Indeed, there are well-known challenges with regard to both electrostatics and polymers treated in RPA and related perturbative approaches.[190] In particular, such theories do not converge when the electrostatic interactions are strong or the ion valency is large.[165] This is an important limitation; high charge densities along a polymer chain remain a challenge because multivalent ions are in the limit of high charge densities. Approaches to circumvent these challenges have been widely proposed for polyelectrolyte systems, typically relying on the supposition of an alternate 'highly-ordered' state such as an ionic solid,[191,192] effective chi-parameters,[193,194] and/or ion condensation.[195-198] While motivated by strong physical intuition, these invoke assumptions about the system that decreases their predictive power or limits their regime of applicability. Nevertheless, these understandings have been instrumental in progressing the state of complex coacervation.

The first theoretical study for ordered morphologies is given by Audus *et al*. [199] They developed a modified self-consistent field theory (SCFT) with an embedded fluctuation (EF) model in which the one-loop random phase approximation (RPA) is used in order to capture the electrostatic correlations. Using this EF model, they investigated the phase diagrams of salt-free triblock copolyeletrolyte solutions as a function of end-block fraction and polymer concentration.

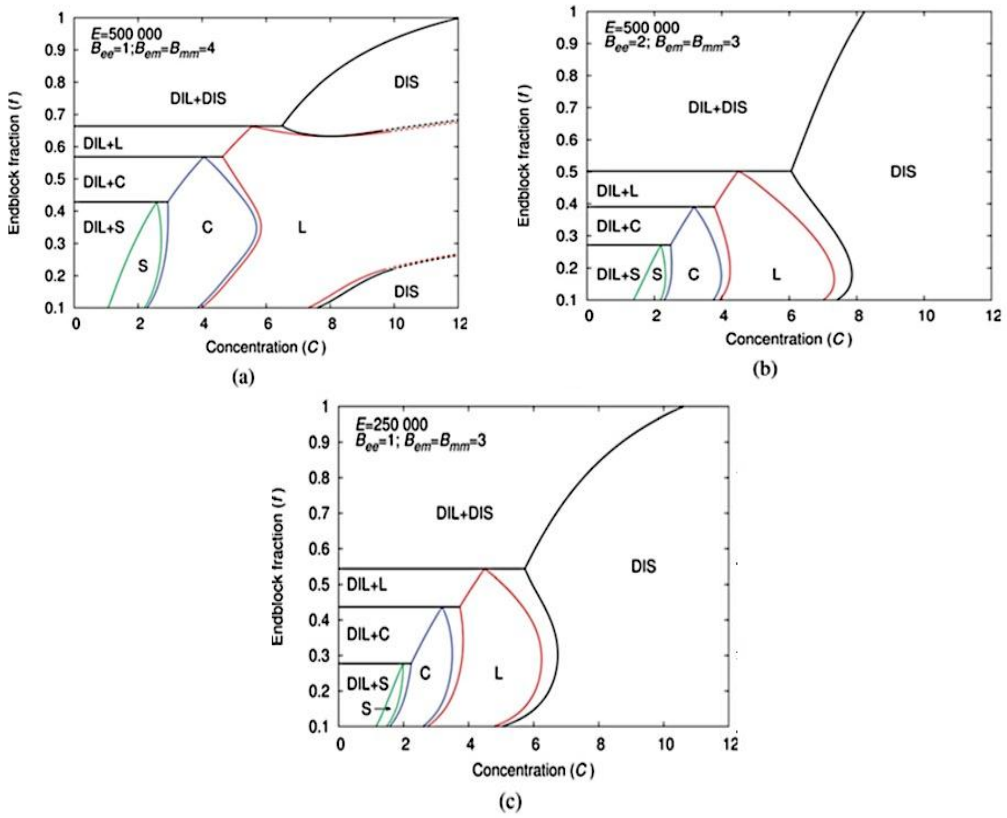

Figure 18: Phase diagram for various parameters using the EF model. Observed phases included disordered (DIS), dilute (DIL), either body- centered cubic spheres or face-centered cubic spheres (S), hexagonally packed cylinders (C), lamellae (L) and regions of phase coexistence. This figure was reproduced from Audus, D. J.; Gopez, J. D.; Krogstad, D. V.; Lynd, N. A.; Kramer, E. J.; Hawker, C. J.; Fredrickson, G. H. Phase behavior of electrostatically complexed polyelectrolyte gels using an embedded fluctuation model. *Soft Matter*, *11* (6), 1214–1225,[199] Copyright 2015, with the permission of The Royal Society of Chemistry.

The calculations using the EF model were consistent with small angle x-ray scattering (SAXS) measurements on an experimental system. In spite of the great success on understanding the hydrogel with an ordered structure, such an EF model containing Gaussian fluctuation contributions breaks down when the line charge density is relatively high, which limits its application. Significant progress for coacervate self-assembly with high charge density polymers was achieved by Sing's group. They proposed a hybrid "Monte Carlo-single chain in mean field" (MC-SCMF) method to handle charge-dense scenarios (Figure 19).[200]

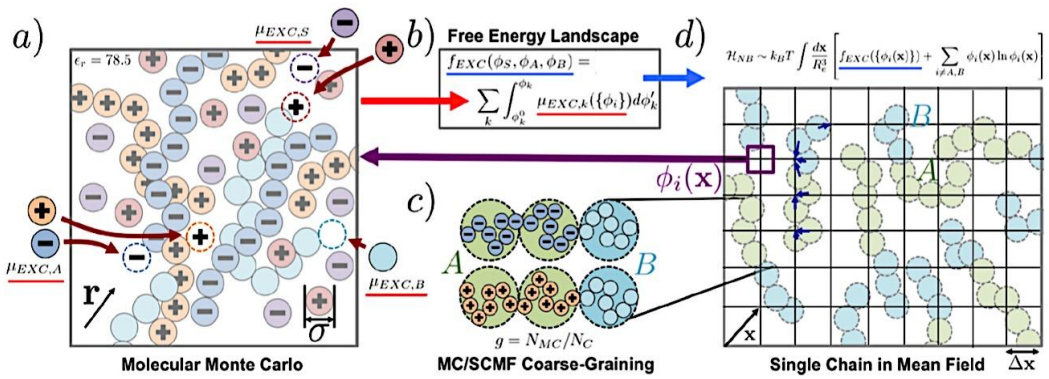

Figure 19: Schematic of the hybrid MC-SCMF scheme. (a) Molecular MC simulates solutions of polymer (polycation, orange; polyanion, blue; neutral polymer, cyan) and salt (cation, red; anion, purple). The RPM is used, with charged species represented as hard spheres of diameter σ in a dielectric solvent medium with ε_r = 78.5. Spatial coordinate is r. Widom insertion of salt/polymer

species (dark red arrows) yields $\mu_{EXC,i}$ of species *i*. (b) $\mu_{EXC,i}$ is an input into the calculation of the free energy landscape $f_{EXC}(\varphi_S,\varphi_A,\varphi_B)$; (c) SCMF simulations consider coarse-grained representions of (for example) block copolymers. *g* monomers make up individual coarse-grained beads, which are connected by Gaussian springs. In this scheme, polycation versus polyanion beads are indistinguishable. (d) f_{EXC} from (b) contributes to a nonbonded Hamiltonian H_{NB} calculated by assigning beads to grid points (blue arrows). Grid has coordinate x and informs MC updates of coarse-grained polymers. These chains do not interact except through the contribution of each coarse-grained bead to the φ_A or φ_B at a given grid point. The f_{EXC} informs the distribution of SCMF chains, which set the values of φ_i at a grid point x used to calculate f_{EXC}, establishing consistency between the two simulation methods. This figure was reproduced from Lytle T. K.; Radhakrishna, M.; Sing, C. E. High charge density coacervate assembly via hybrid Monte Carlo single chain in mean field theory. *Macromolecules, 49*(24): 9693–9705,[200] Copyright 2016, American Chemical Society.

Then, they embedded molecular-level Monte Carlo (MC) simulations into field theoretic calculations, leading to a multiscale, coarse-grained description to such systems. Their calculations match well with previous experimental and theoretical results. Recently, Ong and Sing developed a transfer matrix (TM) theory, and incorporated it into a SCFT calculation to provide predictions for both the macroscopic phase behavior and microscopic charge correlations present in complex coacervates (Figure 20).[201]

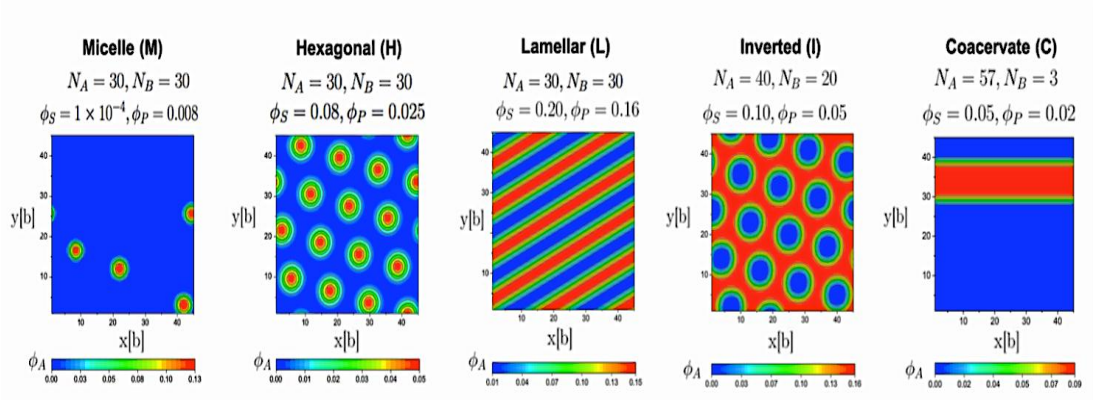

Figure 20: Representative contour plots of the morphologies observed in two-dimensional TM-SCFT calculations, showing the density of the polyelectrolyte block φ_A. Micelle phases (M), hexagonally-packed micelles (H), lamellar (L), and inverse hexagonally-packed micelles (I) as self-assembled phases were observed. Also bulk phase separation into a coacervate phase (C), distinguished as a phase separated region that is significantly larger than the H or M structures were occasionally observed. This figure was reproduced from Ong, G. M. C.; Sing. C. E. Mapping the phase behavior of coacervate-driven self-assembly in diblock copolyelectrolytes," *Soft Matter, 15*(25): 5116–5127,[201] Copyright 2019, with the permission of The Royal Society of Chemistry.

The transfer matrix theory is based on a one-dimensional adsorption model and accounts for charge correlations related to ion pairing, counterion condensation, and release (Figure 21).[202]

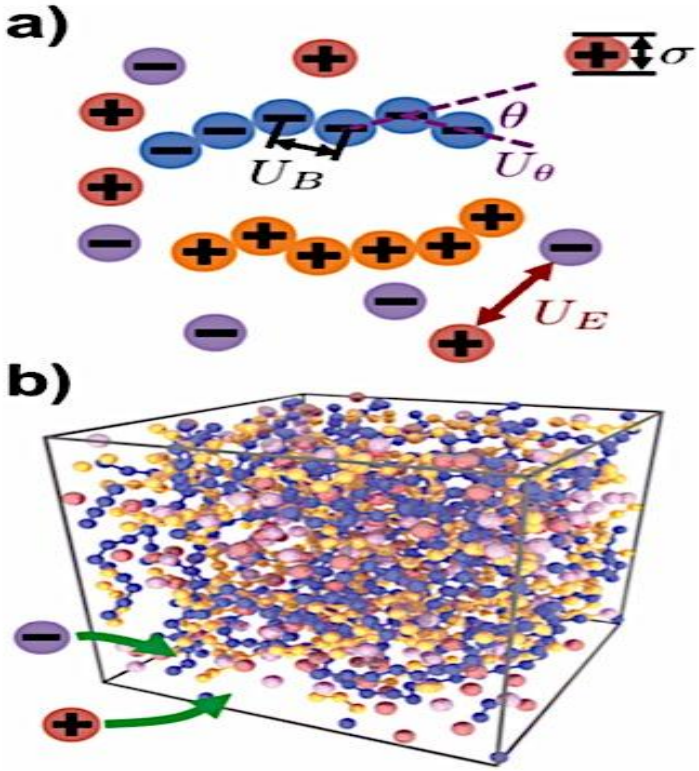

Figure 21: (a) Schematic of the simulation model. The RPM is used, with all hard-sphere particles of diameter σ and electrostatic interactions between all charged species U_E. Polymers are connected charges with a bonding potential U_B and a bending potential U_0. (b) Simulation snapshot of a coacervate phase using this model. A method known as Widom insertion measures the energy change associated with adding pairs of charged particles into a simulation box, yielding excess chemical potentials that can be integrated to calculate f_{EXC}. This figure was reproduced from Lytle, T. K.; Sing, C. E. Transfer matrix theory of polymer complex coacervation. *Soft Matter*, *13*(39): 7001–7012,[202] Copyright 2017, with the permission of The Royal Society of Chemistry.

Their phase diagram predictions for the two dimensional system are analogous to experimental results in the literature.[203] This theory is easy to calculate and shows its novelty. However, their transfer matrix method involves a phenomenological parameter to describe the three-order term that captures excluded volume interaction between polymer species and salt ions in the coacervate phase, and it also neglects the spatial dependence of the transfer matrix of each segment along the chain in practical calculation.[201] In addition, a more accurate handling to the transfer matrix needs the help of simulations.[204]

One important aspect of coacervate formation, relevant to modern polymer science, is its relationship to the construction of polyelectrolyte multilayer films by sequential adsorbed layers of weak polyelectrolytes. It has been established that polymer and salt concentration as well as pH affect the structure and composition of the multilayer composite sheet, similarly as discussed for bulk coacervate formation, and common features have been specifically addressed.[205-210] Layer-by-layer growth is an arrested, nonequilibrium form of PEC. The associative electrostatic interactions driving complex coacervation are an obvious parallel to those used to drive the formation of layer-by-layer (LbL) films.[211-213] While the field has long been cognizant of these parallels,[86,214,215] the difficulties associated with predicting the dynamics of polyelectrolyte complex systems has limited the amount of progress that has been made. Recent experimental work by Salehi *et al.* has suggested a possible correlation for predicting the growth rate of LbL films based on measurements of coacervate phase behavior.[216] Depicted in Figure 22 is the growth kinetics of LbL films composed of Poly (acrylic acid) (PAA) and poly (N,N- dimethylaminoethyl methacrylate) (PDMAEMA) along with corresponding bulk phase behavior at various pH values and in the absence of salt. However, further validation of this approach with a broader range of polymer systems is still needed.

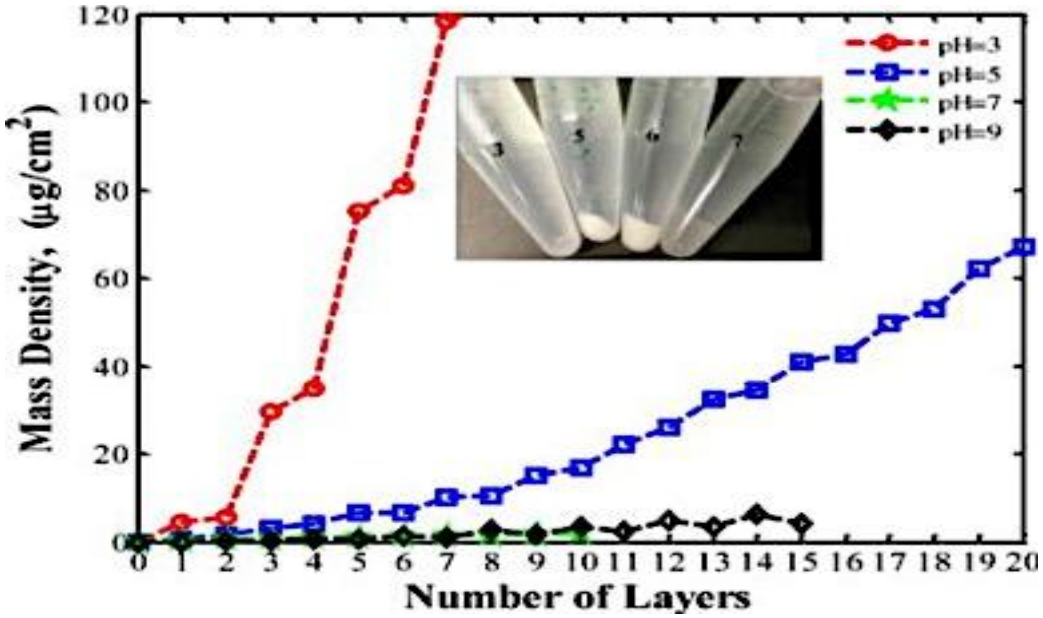

Figure 22: Effect of pH on PEM growth kinetics for PAA/PDMAEMA in the absence of KCl at room temperature. The inset illustrates the physical form of the complex phases corresponding to LbL experiments. Numbers on the vials in the inset denote the pH of the contents. PAA was deposited at the odd-numbered steps and produced larger increments in mass than the deposition of PDMAEMA on the even-numbered steps. This figure was reproduced from Salehi, A.; Desai, P.; Li, J.; Steele, C. A.; Larson, R. G. Relationship between Polyelectrolyte Bulk Complexation and Kinetics of Their Layer-by-Layer Assembly. *Macromolecules*, *48* (2), 400–409,[216] Copyright 2015, American Chemical Society.

Complex coacervation might fruitfully be considered from the perspective of colloidal clustering,[126] though this idea has not been widespread in part because the field developed from the vantage point of the association of flexible polyampholytes (i.e. gelatin) not viewed as colloidal particles. It is clear—at least for colloid-polyelectrolyte coacervation—that well-defined and thermodynamically stable intermacroionic aggregates exist near the point of phase separation and that repulsive and attractive interactions among them play a role in their coalescence. These clusters possess structural hierarchies far more subtle than conventional colloids: at the largest scale, multipolymer aggregates arise from the association of intrapolymer complexes, which in turn arise from the binding to polymers of micelles, which themselves are surfactant aggregates.[217] The primarily electrostatic repulsive and attractive forces operating over different length scales determine the cluster sizes and structures of the resulting dense phases. The competition between short-range attraction and longer-range repulsion (SALR) operating over different length scales determine the cluster sizes and structures of the resulting dense phases.[218-223] Colloidal systems interacting via SALR possess a rich phase behavior and may exhibit one or more stable liquid-liquid phase transitions. The effect of the repulsion has been found to be analogous to the liquid-vapor critical point and a portion of the associated liquid-vapor transition line, with two first-order phase transitions: one from the vapor to a fluid of spherical liquid- like clusters and the other from the liquid to a fluid of spherical voids (Figure 23).[224-226] The possible retention of aggregate structural features within the macroscopically homogeneous dense phase, an interesting question that has yet to be resolved.

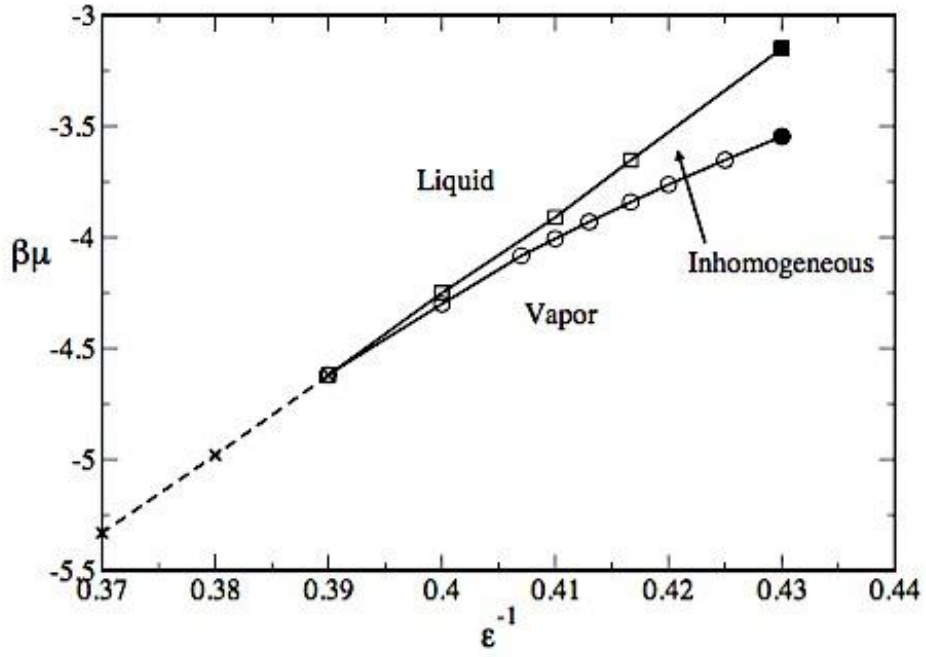

Figure 23: Estimates of the phase diagram. Circles are the vapor-spherical cluster transition, squares are the spherical bubble-liquid transition. Crosses lie on the liquid-vapor coexistence line, lines merely guide the eye. Filled symbols locate the putative critical points. Uncertainties do not exceed the symbol sizes. This figure was reproduced from Archer, A. J.; Wilding, N. B. Phase Behavior of a Fluid with Competing Attractive and Repulsive Interactions. *Phys. Rev. E*, *76* (3), 031501,[225] Copyright 2007, with the permission of American Physical Society.

Those concepts can be applied to the case of polyelectrolyte - micelle complexation and coacervation, where the long-range electrostatic repulsions among complexes of like charge, subject to screening, compete with short-range attractions between complexes due to polarization or disproportionation. Temperature is the parameter that ameliorates the Coulomb repulsion among polyelectrolyte complexes, by promoting the entropy of counterion expulsion, as clustering or phase separation of complexes leads to the replacement of macroion-bound counterions by intermacroionic ion-pairing. This colloidal model in which the polyelectrolyte-micelle complexes are viewed as intricately hierarchal soft colloidal particles, would then predict the coexistence of supernatant droplets (voids) in a coacervate dense medium at high volume fractions with coacervate droplets (liquidlike clusters on micrometer or submicrometer scale) in the supernatant at low volume fraction. This scenario implies the retention of micelle- polyelectrolyte aggregate structural features within the macroscopically homogeneous dense phase that finds only limited experimental evidence so far.[227-229]

6. pH INDUCED STRUCTURAL AND MORPHOLOGICAL TRANSITIONS.

Structural and morphological transitions were highlighted in polymer-polymer and protein-polyelectrolyte dispersions by using a variety of experimental techniques such as turbidimetric titration,[17,139,151, 230-233] quasi-elastic and static light scattering,[17,139,140,151,230,233] and electrophoretic light scattering,[140,233] upon changing gradually the pH. Two remarkable pH values, pH_c and pH_φ, were identified and correspond to structural and morphological changes.[17,230,231] Determined by a slight increase of scattered light intensity in dispersion, the critical pH, pH_c, is related to the primary complexation of macromolecules and the formation of intrapolymeric complexes. The pH_c can be considered as a phase transition on the molecular scale. The pH_φ is determined by a significant increase of the dispersion turbidity, indicating, according to most of authors, the first step of phase separation at the microscopic level, leading to the coacervate droplet formation. In addition to the two pH values already defined, Kaibara *et al.*[17] established on bovine serum albumin (BSA)-poly(di-methyldiallylammonium chloride) (PDADMAC) dispersions other characteristic pH transitions using light scattering and spectrophotometric measurements. The formation of soluble primary complexes was initiated at pH_c and completed at "pH'_{crit}". An afterward increase in scattering

intensity at "pH_{pre}" may arise from the assembly of quasi-neutralized primary complexes. The pH region between pH'_{crit} and pH_{pre} was identified as the region of stable intrapolymer complexes as spectrophotometric data and pH values remained constant once the titration of the BSA-PDADMAC dispersion was interrupted. At pH_{φ}, a maximum in scattering intensity was concomitant with both the appearance of turbidity and the first microscopic observation of coacervate droplets. Contrary to the previously mentioned definition, the pH_{φ} corresponds in this case to a late stage of phase separation since droplets appeared. Coacervates displayed morphological changes at "pH_{morph}", observed by phase contrast microscopy, followed by the transformation to solid or flocculant substances at "pH_{precip}" (Figure 24).

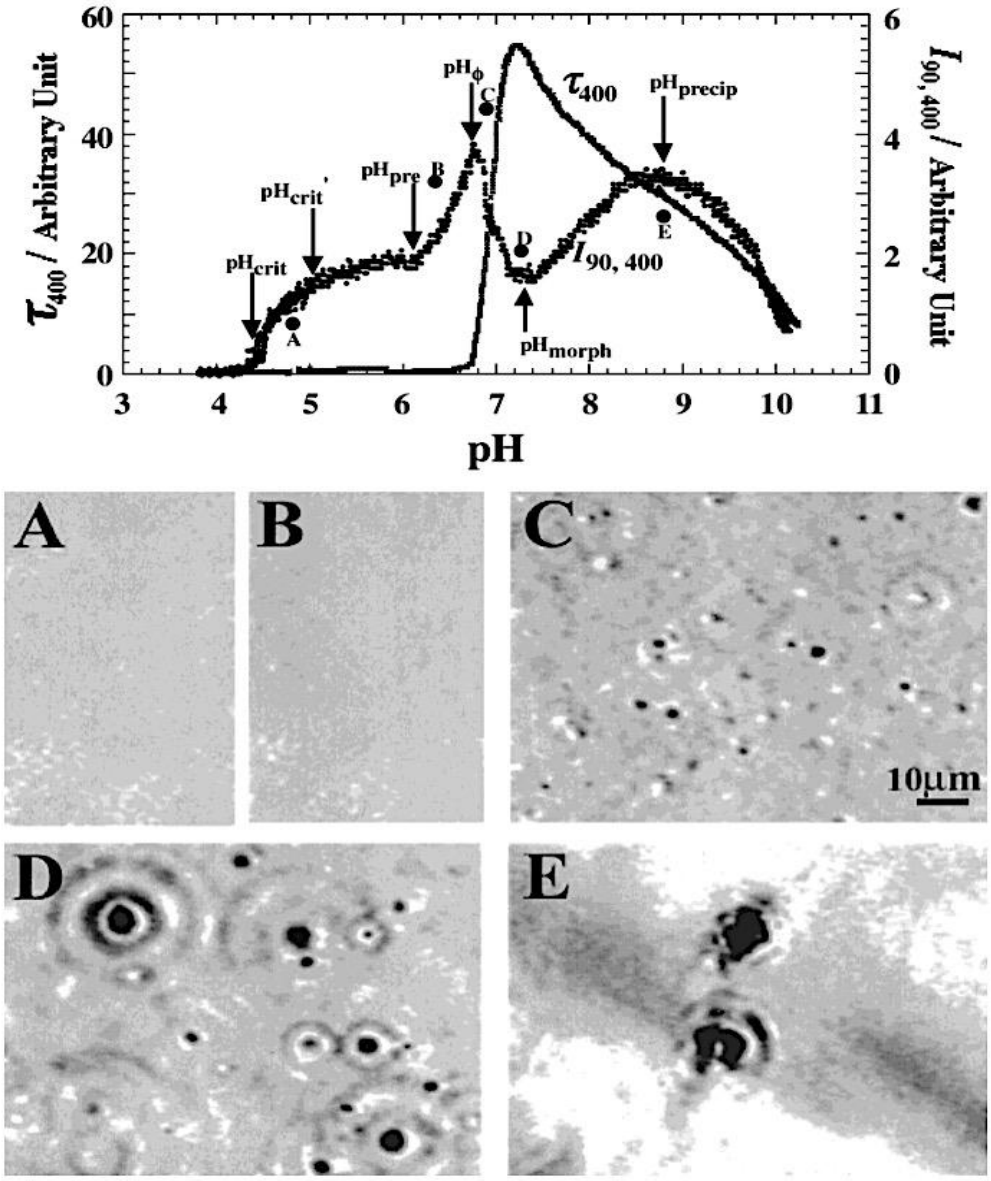

Figure 24: Typical pH profile of turbidity, τ, and scattering intensity, I_{90}, for r = 22.4 and NaCl concentration of 100mM at 25°C. Arrows indicate specific pH points, pH_{crit}, pH'_{crit}, pH_{pre}, pH_{φ}, pH_{morph}, and pH_{precip}. Black dots identified by A-E refer to the point where the phase contrast microscope images A-E are taken. The scale bar in the microscope image is 10 μm. This figure was reproduced from Kaibara, K.; Okazaki, T.; Bohidar, H. B.; Dubin, P. L. pH- Induced Coacervation in Complexes of Bovine Serum Albumin and Cationic Polyelectrolytes. *Biomacromolecules*, *1* (1), 100–107,[17] Copyright 2000, American Chemical Society.

Except for this study, all analyses of the kinetic mechanism of phase separation on a great number of polymer-polymer and protein-polymer systems, and on a more limited number

of protein-polysaccharide systems,[151,234,236] revealed that pH_c and pH_φ were the most important pH of structural transitions. This description seems to be incomplete with regard to the several transitions described above in the protein- polymer phase separation process, especially considering that soluble intrapolymeric complexes have to interact in order to form, more or less, neutral aggregated (inter- polymeric) complexes before phase separation occurs. It may be expected that in the complexation of biopolymers, more than two pH values corresponding to structural transitions will be identified. A great challenge concerns in particular the crucial transition region between complexation and phase separation. More detailed information on the structure of the different entities formed and energetic of assembly are also needed, using for instance high-resolution cryo- TEM microscopy and modern calorimetric techniques.

We could then wonder whether these forces determine a specific structure of coacervates; it is not, by definition, possible to speak of an intrinsic common structure because we are at least initially dealing with liquid phases that may proceed to completely different endpoints. There have nevertheless been attempts to capture 3D structural elements by cryoelectron microscopy (cryo-EM) methods. For example, a distinct 'sponge structure' was described in droplets by cryogenic temperature high-resolution scanning EM (cryo-HRSEM) (Figure 25).[237]

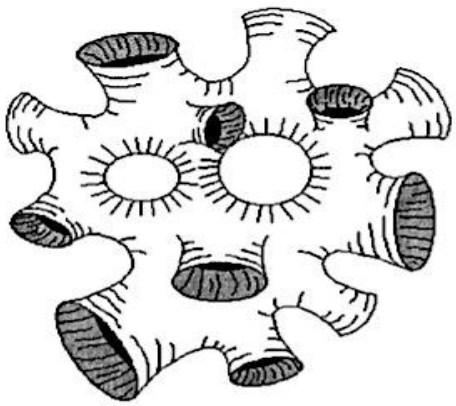

Figure 25: Schematic drawing of the sponge phase. This figure was reproduced from Menger, F. M.; Seredyuk, V. A.; Caran K. L.; Apkarian, R. P. A Sponge Morphology in an Elementary Coacervate. *Langmuir*, *16*(24): 9113–9116.[237] Copyright 2000, American Chemical Society.

7. APPLICATIONS.

Recent interest in coacervation as a phenomenon has led to deep questions that influence – and are influenced by – other emerging areas in polymer physics, materials engineering, and biophysics. Complex coacervates represent a wide class of materials with applications ranging from coatings and adhesives to pharmaceutical technologies, and they also underpin multiple biological processes, which are only now beginning to be deciphered.

In the scope of these larger trends in soft matter, it is apparent that the electrostatic interactions that drive complex coacervation are broadly relevant due to their sensitivity to molecular structure and chemical identity. Great interest was shown in complex coacervation because of its implication in many biological processes like self-assembly of biological macromolecules.[238-240] The outlook of coacervation thus exists at the interface between polymer science, molecular engineering, and biology, and because of their interesting interfacial and bulk material properties, complex coacervates find applications in many industrial applications, including the pharmaceutical and food industries. Complex coacervates are used for microencapsulation, drug delivery and tissue engineering,[241-248] biomaterials, [249-251] underwater adhesives,[252-254] protein purification,[255] enzyme immobilization,[256] cosmetic formulations,[257] flavors,[258] and oil[259,260] with applications in biomedical adhesives,[261] food science[262] and electronic ink.[263] Because of these applications and because of some fascinating biological implications,[264] there has recently been a resurgence of interest in coacervation. (The number of papers with coacervation/coacervate in their titles in the last three years surpassed the total published during the preceding decade). In the following sections, we highlight a few directions that show the use of coacervate-based materials across the broad field of biomedicine.

7.1. Encapsulation. A highly interesting characteristic of complex coacervates is their ability to host a great variety of so-called client molecules.[265] This characteristic has been exploited to encapsulate proteins and small molecules inside the coacervate phase to study biological processes in a simple and highly controlled environment.[265-269]

In particular, complex coacervates exhibit very low interfacial energy in aqueous solution,[270,271] a property that enables them to engulf a variety of materials.[47] Encapsulation was one of the first applications of acacia gum- gelatine coacervates since papers and patents are reported as early as in 1970s.[126]

The unique gelling-melting profile of gelatine generates interesting properties for microencapsulation. Viscous coacervates can be prepared at 50–60 °C, a temperature higher than

gel point of gelatine while on cooling interface's rigidity increases resulting in a stable gelled shell around the microcapsule. During consumption, the shell will be disrupted as gelatine is readily melted in the mouth. Since then, these two macromolecules have been used to encapsulate various materials of liquid and/or solid nature. Recently, Yeo *et al*.[272] used gelatine–acacia gum coacervates to encapsulate flavours to be released during cooking in baked goods.

Compared with spray drying which is the most widely used microencapsulation technique, complex coacervation has advantages including high encapsulation efficiency (up to 99%), high loading of the "core" material (>50%) and significantly improved controlled-release characteristics.[273]

The ability to sequester high amounts of biologically relevant macromolecules is also important for the application of coacervate-based synthetic cells in the biomedical field. In fact, encapsulation of cargo in complex coacervates has already been demonstrated across a range of biomedical disciplines, including the development of sensors, nanoreactors, biomimetic adhesives, delivery platforms[274,275] and has been widely used in food science and medicine.[276-293]

Encapsulation can be achieved by using the cargo as part of the coacervate matrix,[294] as a result of specific interactions,[295] or by preferential partitioning.[296-300] In all of these cases, two major advantages of coacervation are (i) the ability to perform encapsulation in a purely aqueous environment,[250,301-305] and (ii) the potential for dramatically enriching the molecule of interest in the macromolecule-rich coacervate phase, as compared to the original solution. These methods result in the significant enrichment and protection of cargo inside the aqueous environment but also allow for their controlled release upon dissociation of the coacervate phase or as a reaction to external triggers. Overall, the development of programmable complex coacervate−synthetic cells shows great potential for creating novel delivery strategies, provided they are compatible with living cells.[306]

Upon encapsulation, it is critical to test whether the coacervation process adversely affected the guest molecules. This consideration is particularly important for proteins, as opposed to small molecules, and can be assayed using spectroscopic methods such as circular dichroism (CD) and FTIR, which are sensitive to the protein secondary structure. Fortunately, coacervation is a relatively gentle method for encapsulation that maintains proteins in an aqueous environment. Typical reports have shown minimal evidence for adverse effects of coacervation on protein structure.[250, 294, 307]

Encapsulation of charged proteins into complex coacervate core micelles (C3Ms) can be accomplished by mixing them with oppositely charged diblock copolymers. However, these micelles tend to disintegrate at high ionic strength, often as a result of the low charge density of proteins. Lindhoud *et al*. showed, using dynamic light scattering (DLS), that the most stable enzyme-containing C3Ms could be obtained by adding a homopolymer with the same charge sign as the protein to the two-component system, in excess over the protein concentration.[308]

While complex coacervates have a tremendous history of applications related to the encapsulation of both hydrophobic and hydrophilic cargo,[250, 309-318] there have been few systematic studies that investigate how the molecular properties of small molecules drive encapsulation and/or modulate the phase behavior and properties of the coacervate itself.[319] Recent work by Zacharia and co-workers demonstrated the importance of charge and hydrophobicity in driving the partitioning of small molecule dyes into various polymer-based coacervates.[320,321] The encapsulation of proteins within a coacervate phase can represent a particular challenge due to the fact that not all proteins of interest are strongly charged. A strategy for overcoming this limitation was recently reported for the case of binary, protein-polyelectrolyte coacervates. In this work, the natural charge state of various proteins was supplemented through the use of conjugation chemistry to create artificially supercharged proteins using succinic anhydride.[322] Furthermore, the authors were also able to elegantly demonstrate that the degree of supercharging necessary to effect coacervation (as defined by the ratio of the number of negative to positive charged groups, for subsequent coacervation with a polycation) is relatively low – on the order of 1.1 to 1.4 (Figure 26).

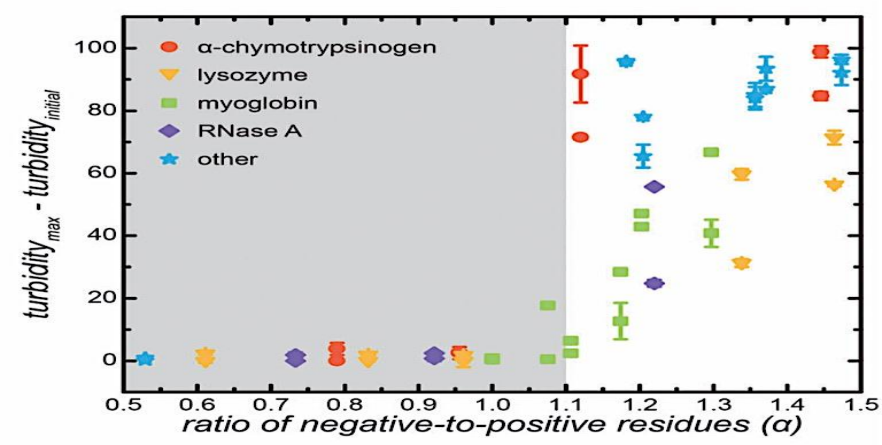

Figure 26: Plot of changes in turbidity as a function of the ratio of negative-to-positive residues on the protein. The grey shaded region corresponds to proteins that do not undergo phase separation. This figure was reproduced from Obermeyer, A. C.; Mills, C. E.; Dong, X.-H.; Flores, R. J.; Olsen, B. D. Complex coacervation of supercharged proteins with polyelectrolytes. *Soft Matter*, *12* (15), 3570–3581,[322] Copyright 2016, with the permission of The Royal Society of Chemistry .

While most of the reports on the complex coacervation of proteins take advantage of the charge nature of the protein itself, Kapelner and Obermeyer[323] recently reported a strategy that takes advantage of recombinantly expressed short ionic peptide tags (6-18 amino acids) to facilitate the phase separation of tagged proteins via complex coacervation. Of particular note was the result that proteins with the same total amount of charge distributed isotropically on the protein surface showed lower stability against dissolution by salt than proteins where coacervation with a strong polyelectrolyte was driven by the presence of an ionic tag. These results suggest a range of interesting potential applications, from protein purification to the colocalization of enzymes and more. Ternary systems of coacervates have also been reported as an effective strategy for encapsulating proteins.[250,324]

Rather than relying on the charge of the protein itself to drive coacervation, the use of a ternary system of proteins and polymers allows for the initial formation of an intermediate complex between the protein of interest and an oppositely-charged polyelectrolyte, the overall charge of which is dominated by the polyelectrolyte. Coacervation is then induced by the addition of a second polyelectrolyte, which interacts directly with the intermediate complex (Figure 27).[250] While a broad exploration of ternary composition space has not been performed, preliminary reports suggest a trade-off between encapsulation efficiency and total protein loading, as would be expected given the need to maintain charge neutrality in the coacervate phase. Further exploration of ternary composition space represents an exciting area for further investigations.

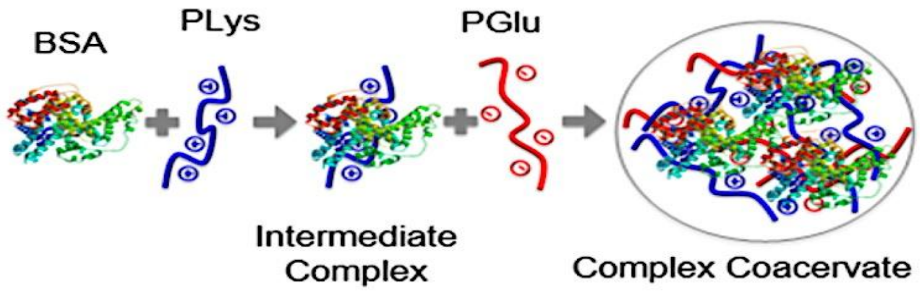

Figure 27: Encapsulation of bovine serum albumin (BSA) into a coacervate. Positively-charged poly(*L*-lysine) (PLys) is added to the negatively-charged protein to form an intermediate complex. Negatively-charged poly(*D,L*-glutamate) (PGlu) is then added to form the complex coacervate. This figure was reproduced from Black, K. A.; Priftis, D.; Perry, S. L.; Yip, J.; Byun, W. Y.; Tirrell, M. Protein encapsulation via polypeptide complex coacervation. *ACS Macro Lett.*, *3* (10), 1088−1091, [250] Copyright 2014, American Chemical Society.

7.2. Delivery Platforms. Building on the strengths of complex coacervation for encapsulation, several examples of ionically cross-linked colloidal polyelectrolyte (PE) coacervates-mostly conceived for biomedical applications-are reported in the literature. More recently, systems of complex coacervation have been explored for drug delivery using such naturally occurring polymers as alginate, chitosan, and heparin.[325,326] For instance, chitosan/nucleic acid polyplexes were designed for the in vitro delivery of RNA or DNA in mammalian cells.[327-329] Similarly, hybrid PEGylated nanoparticles formed via the complex coacervation mechanism have been shown to enhance the in vivo gene transfection efficiency compared with traditional carriers.[330] On the other hand, protein encapsulation via polypeptide complex coacervation has been recently reported with the aim of delivering protein therapeutics.[250] The ability of complex coacervates to contain high concentrations of aggregation-free and fully active proteins has been exploited in the formulation and delivery of growth factors and monoclonal antibodies. Li *et al*.[331] showed the use of zein−chitosan complex coacervate particles in the slow release of curcumin. Zein−chitosan complex coacervation was studied by Ren *et al*.[332] to investigate the effect of ultrasound frequency in the encapsulation of resveratrol. Thermodynamics and wetting kinetics of zein coacervate was studied by Li *et al*.[333] Their study also revealed the formation of zein coacervate in a water/propylene glycol solvent and its ability to encapsulate limonene. Injectable hydrogel coacervate was used by Lee *et al*.[334] for the delivery of anticancer drug bortezomib. Huei *et al*. [335] have reported iron cross-linked carboxymethyl cellulose complex coacervate beads for the sustained release of ibuprofen drug. Chenglong *et al*.[336] reported a dextran-based coacervate nanodroplet as potential gene carriers for efficient cancer therapy. A water-soluble starch derivative anionic and cationic polymer that undergoes nanoparticle formation via coacervation was reported by Barthold *et al*.[337] The group discussed the potential use of the nanoparticles in pulmonary delivery of protein/peptides.

From a delivery standpoint, bulk and hydrogel-like coacervate-based materials are typically the most useful in circumstances that allow for bolus-style delivery (*i.e.*, direct application or injection of the material to the site of interest). For example, coacervate-based hydrogels composed of alginate and chitosan were shown to enhance the proliferation of cells *in vitro* while accelerating healing efficiency and wound closure in a rat model.[338] In another series of reports, the cationic polymer poly(ethylene argininylaspartate diglyceride) (PEAD) was used in concert with the glycosaminoglycan heparin to form coacervate-based delivery vehicles that take advantage of the strong binding affinity between heparin and various growth factors to enable cargo encapsulation and protection. Applications included the use of heparin-binding epidermal growth factor-like growth factor (HB- EGF) to accelerate wound healing,[339] fibroblast growth factor-2 (FGF2) to enhance angiogenesis in both surface wounds and after myocardial infarction (Figure 28),[340,341] stromal cell-derived factor (SDF)-1a for vascular regeneration,[342] bone morphogenetic protein-2 for stem cell differentiation and bone formation,[343] nerve growth factor (NGF) for nerve regeneration,[344] and the anti- inflammatory cytokine interleukin-10 (IL-10).[345]

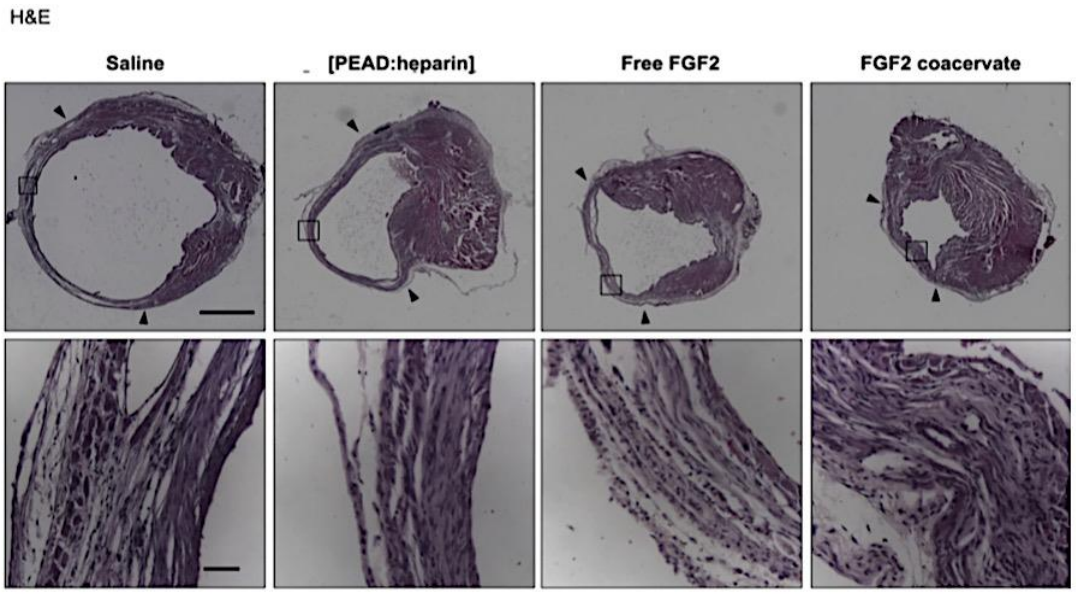

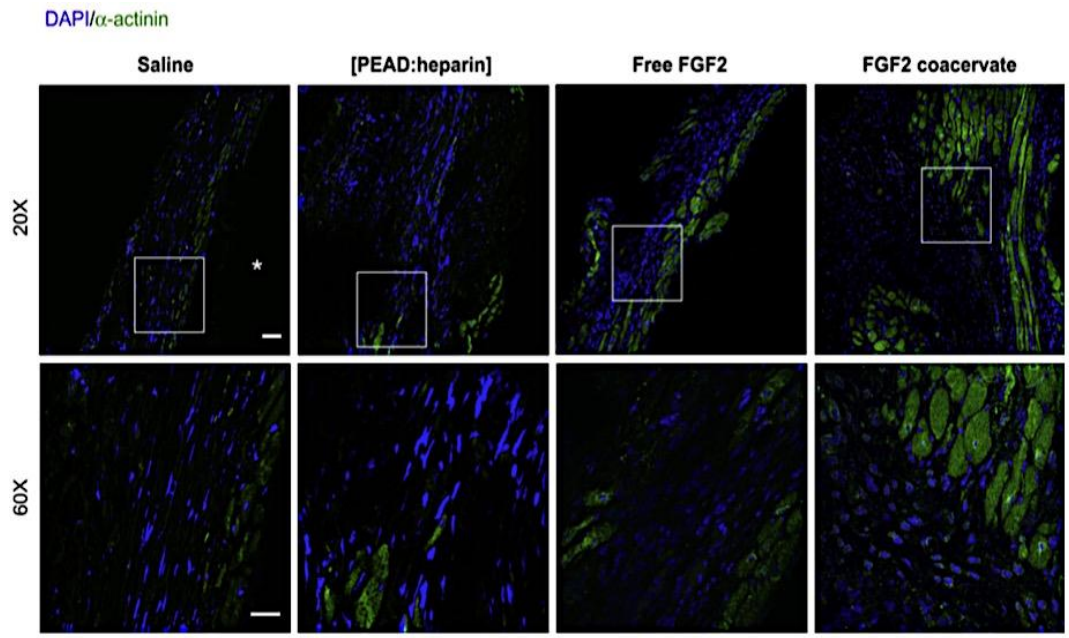

Figure 28: Comparison of H&E (scale bar is 1 mm) and α-actinin (scale bar is 50 µm) stained tissues for infarcted myocardium receiving treatments of saline, [PEAD:Heparin], free FGF2 and FGF2 coacervate. Application of the coacervate FGF2 formulation significantly reduced the infarct area, preventing ventricular dilation and preserving cardiac fibers, compared with the other treatment strategies. α-actinin stained tissues demonstrate enhanced preservation of cardiomyocites in the infarct zone for the FGF2 coacervate treatment. This figure was reproduced from Chu, H.; Chen, C.-W.; Huard, J.; Wang, Y. The effect of a heparin-based coacervate of fibroblast growth factor-2 on scarring in the infarcted myocardium. *Biomaterials*, *34* (6), 1747–1756,[341] Copyright 2013, with the permission of Elsevier Ltd.

While exploring the efficiency of coacervates in drug delivery, a very interesting work was carried by Lim *et al.*[346] They showed that a Humboldt squid beak-derived biomimetic peptide coacervate can be used for encapsulating insulin with high efficiency along with its controlled release. Chitosan-based coacervates for propolis encapsulation and its release and cytotoxic effect was reported by Sato *et al*.[347]
The lack of organic solvents in coacervation has added benefits in the context of drug delivery, beyond those related to the gentle encapsulation of biomolecules. Drug delivery platforms typically address multiple challenges, including (i) protection and/or isolation of the cargo, (ii) enabling targeted delivery and uptake into the cells or tissues of interest, and (iii) controlled release of therapeutics over time. A variety of reports have demonstrated the efficacy of coacervation as the basis of a drug delivery platform, taking advantage of the flexible and modular capabilities of charge-driven self-assembly to address each of these challenges. Reports of coacervate-based platforms for gene delivery include bulk complexes[348-351] and micellar[352-358] systems for the delivery of plasmid DNA, microRNA,[353] and siRNA[226] (small interfering RNA). Specific diseases targeted by these approaches include atherosclerosis[353]and cancer.[358]

The issue of cargo protection is often coupled with strategies to facilitate cellular uptake. For instance, the vast majority of non-viral strategies for gene delivery rely on electrostatic complex formation between the negatively-charged DNA or RNA and a positively-charged carrier polymer, surfactant, or lipid.[359-362] Such complexation helps to protect against attack from nucleases.[354,355] The positively-charged carrier materials also help to facilitate cellular uptake by masking the negative charge of the DNA or RNA363 and facilitating an attractive interaction with the negatively-charged cellular membrane.[364]

While the idea of targeted delivery is typically associated with medical applications, food scientists have recently begun to adapt older concepts where complex coacervation has been used to entrap flavors and oils for the delivery of proteins, nutraceuticals, and other water-soluble actives.[365-367] Just as delivery platforms in biomedicine can be harnessed to facilitate uptake, materials design strategies are being utilized to enable more efficient absorption of nutrients, vitamins, and antioxidant molecules during digestion.[292,293] Here, the design

parameters are limited in terms of biocompatibility, the availability of bulk quantities of food-grade, cost, and the need to generate a delicious product.

7.3. Adhesive Technology. Adhesive technology, despite being known and exploited since the middle Pleistocene is rarely applied when dealing with adverse environments.[368] Most commercially available adhesives fail to offer a proper performance in wet and dynamic environments and do not achieve the required bonding strength.[369,370] Many surgical procedures are performed worldwide and the number continues to grow every year. In a recent study, over 300 million surgeries were performed in 2012; an increase of 33.6% over the last 8 years.[371,372] Currently, no tissue adhesive has been approved for clinical use that complies with all the requirements, including: easy delivery, fast setting time, strong adhesive and cohesive properties, and biocompatibility.[373,374] Due to these difficulties, in medicine, adhesive technology has been applied primarily for stopping bleeding and gluing skin externally, while current surgical closure techniques involve the use of invasive techniques like sutures, staples, or clips, which often result in secondary tissue damage, microbial infection, fluid or air leakage, and poor cosmetic outcome.[375] The development of effective surgical glues would dramatically reduce the incidence of such complications. A different, largely unexplored, strategy for the development of surgical glues is based on complex coacervation,[376-382] which is involved in the processing of natural adhesives employed by several organisms to attach to different surfaces underwater.[383-385] Coacervate-based adhesives were first observed in natural systems, such as the sandcastle worm and mussels. In the case of sandcastle worms and mussels, the coacervation phenomenon was found to play an important role in the formation of adhesive in a wet environment.[386-389]

Complex coacervates as being polymer-rich, water-insoluble complexes of oppositely charged polyelectrolytes with a low surface tension that makes them compliant with surfaces. [86, 271] After delivery, additional interactions need to be introduced to transition the viscous liquid into a strong and tough material to prevent flow under an applied stress.[390] Work on biomacromolecule-based complex coacervates has revealed that they have great potential as wet adhesives.[252, 278] Several research groups have employed the electrostatic interactions of complex coacervation to fabricate viscous glues, most of which set underwater due to covalent cross-linking reactions, providing the strength required to oppose detachment.[391-396] The higher water content of coacervates is due to the hydration of excess small ions. For all water-containing adhesives, the adhesive performance and the mechanical properties heavily depend on water content. The optimization of the water content and, consequently, of the polymer concentration is necessary to enhance the adhesion performance. For instance, commercial poly(ethylene glycol) (PEG)-based glues, such as DuraSeal and CoSeal, bind to tissues with a low adhesive strength, which is mainly attributable to the high water content, ranging from 90% to 99% w/v.[397] Water may also act as plasticizer, which can improve the adhesion performance.[398] Feldstein *et al*. studied how water content affects the adhesive properties of poly(N-vinylpyrrolidone)−poly(ethylene glycol) (PVP−PEG)blends.[399-400] By increasing the content of PEG, the water content increased and adhesion was enhanced, enabling the material to sustain higher deformations without considerably affecting the ultimate tensile strength. The optimal performance, in terms of peel force, was observed when the PEG concentration was increased to 36%, with the mode of failure transitioning from adhesive to cohesive, allowing fibrillation within the material.

More recently, attempts to develop an effective underwater adhesive have been made using complex coacervates that are based on recombinant mussel adhesive proteins (MAPs) due to the water immiscibility of complex coacervates and the adhesiveness of MAPs.[401] Lim and co-workers developed MAP-based encapsulated coacervates as smart tissue adhesives with drug carrier ability. In this study, an adhesive was formed by complex coacervation between cationic recombinant hybrid MAPs (fp-131 or fp-151) and the anionic hyaluronic acid (HA). The bulk adhesive strengths of coacervates were twice as strong compared to the protein itself on aluminum substrates.[402] Cha and co-workers used the recombinant expression method to obtain rfp-1 MAP (AKP- SYPPTYK) for hydrogel formation by coordination (Fe^{3+}) or covalent cross-linking (NaIO4). The hydrogel system showed maximum adhesion strengths of ~130 and ~200 kPa when cross-linked with Fe^{3+} and NaIO4 respectively. The difficulty in synthesizing the rfps in bulk limit the clinical application of these adhesive hydrogels.[403] In another study, they engineered a residue-specific DOPA-incorporated recombinant mussel adhesive protein (dfp-3 and dfp-5) with DOPA content up to 23 mol%. The recombinant protein showed strong dry and underwater adhesion along with

significant water resistance.[404] They also developed a light-activated, mussel protein-based bioadhesive (LAMBA) hydrogel using a photo-oxidative reaction in the presence of blue light involving Ru(II)bpy3^{2+} as the activator and sodium persulfate (SPS) as the oxidizing agent with recombinant MAP. LAMBA demonstrated strong adhesion to wet porcine skin and also promoted wound healing in addition to wound closure in a rat model.[405] Lu and co- workers developed a hybrid molecular adhesive by fusing Mfps found in DOPA from mussel adhesives with the CsgA proteins found in the amyloid-based adhesives in E. coli (monomeric, CsgA-Mfp3; Mfp5-CsgA and copolymer constructs, (CsgA- Mfp3)-co- (Mfp5-CsgA)) (Figure 29). The molecular hybrid self-assembled in which the β-sheet amyloid protein formed the core, whereas the disordered Mfps were exposed on the exterior. The (CsgA-Mfp3)-co-(Mfp5-CsgA) copolymer demonstrated impressive adhesion energy of 20.9 mJ/m2, which made it a strong competitor for application in medical adhesives.[406]

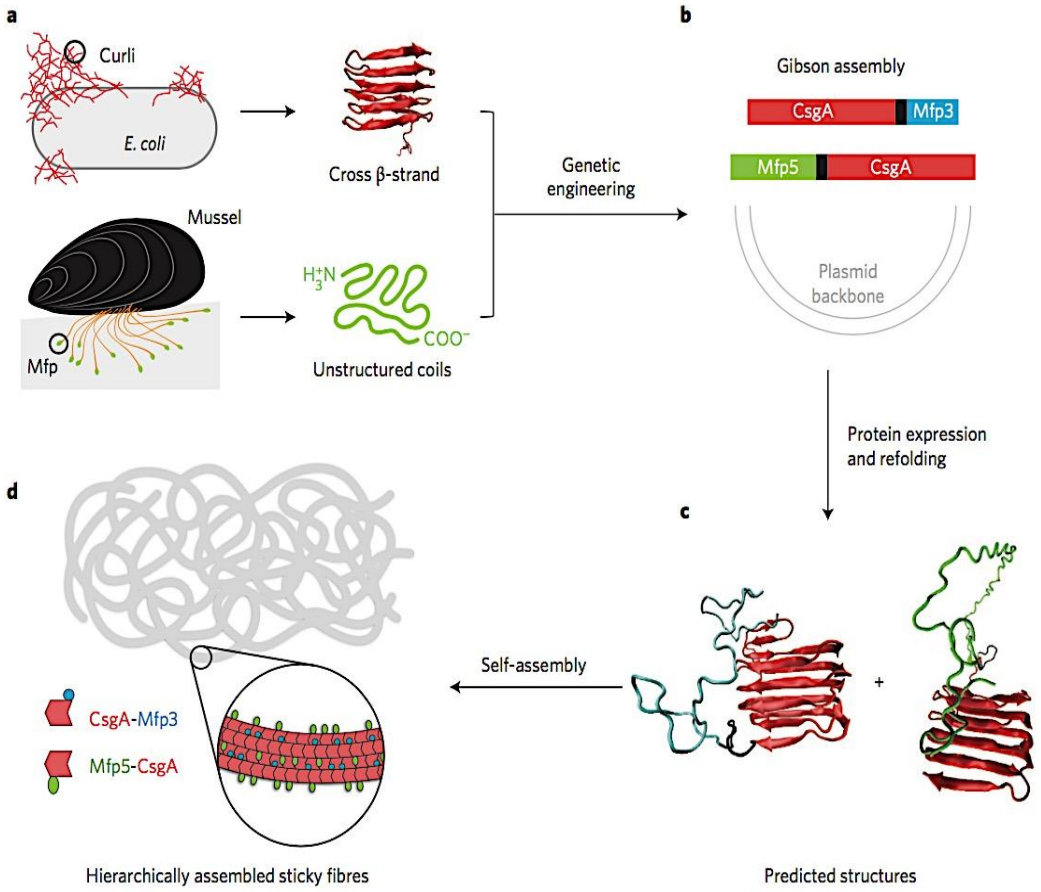

Figure 29: (a-c) Genetically engineered molecular hybrids of mussel adhesive proteins (Mfps) and amyloid-based adhesive proteins in E. coli (CsgA). (d) Adhesive molecular hybrids self-assemble with β-sheet amyloid protein forming the core and the Mfps flanking the exterior. http://www.nature.com/nnano/index.html. This figure was reproduced from Zhong, C.; Gurry, T.; Cheng, A. A.; Downey, J.; Deng, Z.; Stultz, C. M.; Lu, T. K. Strong underwater adhesives made by self- assembling multi-protein nanofibres. *Nat. Nanotechnol., 9* (10), 858− 866,[406] Copyright 2014, with the permission of Nature Publishing Group.

Biomimetic adhesives is another class of tissue adhesives inspired from the examples of adhesion in nature and rapidly gaining momentum in the field of biological adhesives. Stewart and co-workers described an electrostatically driven coacervate formation by using alternating anionic and cationic block copolymers. As a mimic of caddisfly silk, these block copolymers are functionalized with amine, phosphate groups, divalent cations, and also dihydroxyl aromatic groups for oxidative cross-linking.[407]

The main biomedical areas for such adhesives include bone,[278, 408] cartilage,[409,410] and tissue repair,[408, 410-416] as well as implants.[417] For example, coacervate-based adhesives composed of poly (acrylamide-co-aminopropyl methacrylamide)-poly (ethylene glycol diacrylate) and poly (2- (methacryloyoxy) ethyl

phosphate dopamine methacrylamide)-poly (ethylene glycol diacrylate) were used in vitro to seal an iatrogenic defect in a fetal membrane patch. The adhesives were able to function, as well as withstand traction and turbulence without leakage of fluid or slippage.418 Cytotoxicity tests revealed the adhesive to be non-toxic and may help prevent iatrogenic preterm premature rupture of the membranes.[418] In another example, craniofacial reconstruction via a non-cytotoxic coacervate adhesive of gelatin and phosphodopamine in rats was conducted (Figure 30).[278] The adhesive was used to attach a piece of circular bone in the skull and, after recovery from anaesthesia, were allowed to move freely. The adhesive was observed to effectively hold the bone in place despite free movement of the animals. Furthermore, as the adhesive material was resorbed by the body, it was replaced by new bone without affecting alignment.[278] Though these and other examples have demonstrated the potential for coacervate-based adhesives, further in vivo testing and ultimately clinical experiments are still needed to fully validate their safety and efficacy.[410] However, one particular advantage of bio-inspired coacervate-based adhesives would be the potential for repairing tissue and bone without the need to remove the adhesive at a later time.

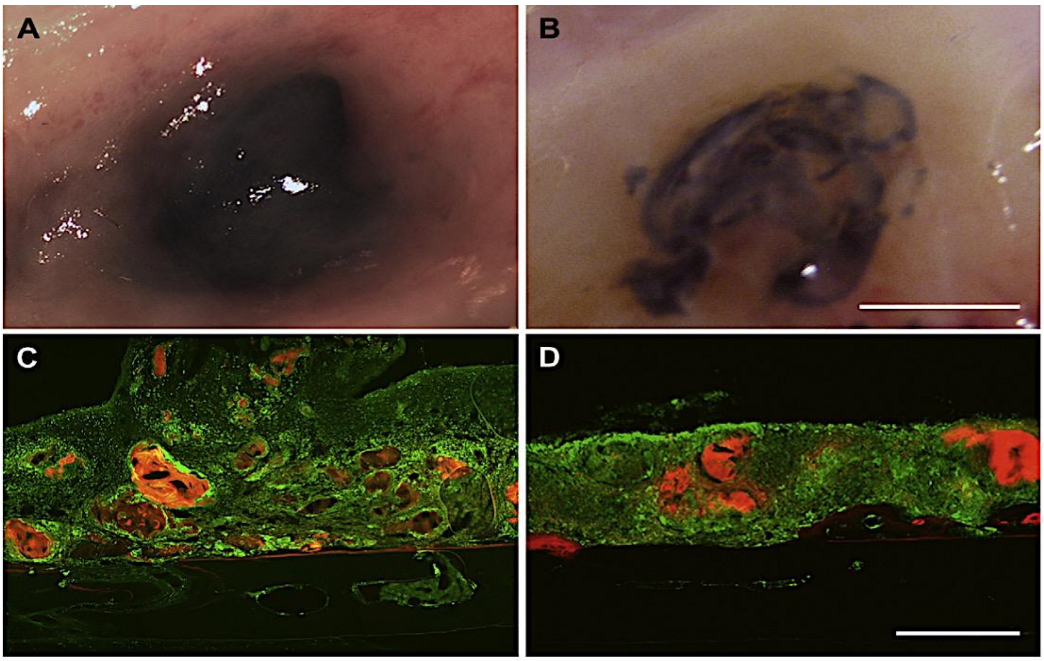

Figure 30: Adhesive complex coacervate adhesive analysis on skull surface (left) and CD68 immunoreactivity (green) associated with adhesive (red). Scale bars represent 500 µm. This figure was reproduced from Winslow, B. D.; Shao, H.; Stewart, R. J.; Tresco, P. A. Biocompatibility of adhesive complex coacervates modeled after the sandcastle glue of Phragmatopoma californica for craniofacial reconstruction. *Biomaterials, 31* (36), 9373–9381,[278] Copyright 2010, with the permission of Elsevier Ltd.

Our knowledge of underwater adhesion is still quite limited and considerable efforts are being invested to study adhesion in natural systems. Deeper understanding of the interplay of environmental and chemical factors, chemistries, and mechanisms of natural adhesion will open numerous possibilities for further advancement in biomimetic tissue adhesives. Currently, biomimetic adhesives involve coacervate formation or functionalization with an adhesive group like DOPA, catechol, or phosphates.[419,420] Although these strategies have shown satisfactory adhesion under dry conditions, they often tend to fail under humid and/or wet conditions.[421]

Recent studies have looked at incorporating a range of cross-linking chemistries to strike a balance between the adhesive and cohesive strengths (see above). Despite such extensive research on tissue adhesives, we have been unsuccessful in developing adhesive mimics capable of rivaling natural adhesives that are scalable, nontoxic, biocompatible, easy to use and degradable. There is still a need to explore the effect of backbone chemistry, polymer hydrophilicity/hydrophobicity, combination of different amino acids, and charged side groups on adhesion strengths. It is also necessary to widen the scope of adhesives beyond tissue adhesion toward drug delivery, tissue grafts, wound healing, and tissue reconstruction via

addition of peptides. In addition, long-term studies and clinical trials are essential before these adhesives can be realized in medical or surgical applications.

Another focus of future work should be to better understand processing methods used by marine creatures to store, process, and deliver the adhesive to the interface. Indeed, biomimicry of sandcastle worm complex coacervate formation is an early example of this. However, further research into coacervate formation is necessary to relate phase behavior to mechanical properties as a function of pH, concentration, temperature and ionic strength.

7.4. Protocells and Membraneless Organelles. Complex coacervation has a long history in the field of cell biology. The first protocells may have been complex coacervates of abiotic macromolecules that served as liquid containers for early anabolic processes.[422] Historically, one particularly contentious topic surrounding complex coacervation was the potential for these phase-separated compartments to serve as a type of protocell that could form the basis for the evolution of life.[47,53,423-430] Despite this hypothesis, originally put forth by Oparin,[425, 430-432] has had on many studies on the origin of life, the importance of coacervates declined rapidly, mainly because it seemed in stark contrast with the presence of well-defined membranes that separate cells from the outside world as well as those that separate the cellular interior into organelles. It is only over the past few decades that evidence has accumulated observing the existence of organelles not enclosed in membranes, 50 so much so that membraneless organelles (MLOs) are now considered essential components of eukaryotic cells.[433-435] They have been shown to constitute a more dynamic way to sequester (sometimes temporarily and reversibly) cellular components from the rest of the cell. Membrane and MLOs can be respectively assimilated by analogy to a grape (membrane organelle) that encloses its seeds and to oil droplets in an aqueous solution (MLOs). These findings have thus renewed broad interest in Oparin's proposal[436] and have led to new experimental efforts to address the origin of life. For instance, in 2019 Jia et al. started with prebiotically available α-hydroxy acids and prepared polyester droplets that would segregate proteins and RNA in a fashion compatible with origin-of-life conditions.[437] More recently, it was shown that phase separation may help in transforming abiotic ornithine residues into arginines, thus allowing the formation of a dsDNA-binding protein.[438] In modern cell biology, regulated intracellular liquid–liquid phase separation of bio- macromolecules is known to play fundamental roles in organizing the cytoplasm, assembling transient signaling complexes, and sequestering metabolic pathways.[439]

In the past few years, coacervate research has seen a tremendous development, in part inspired by the rapid advances in the field of MLOs and the need for model systems that are simple enough to allow systematic and quantitative investigation of MLO characteristics. MLOs represent a rich and still poorly understood variety of phase-separated subcellular structures such as the nucleolus and germ granules.[61, 440-442] These indispensable organelles are formed as a result of liquid−liquid phase separation (LLPS), primarily by the process of complex coacervation, i.e., interactions between charged polyelectrolytes such as proteins and nucleic acids.[61] MLOs exhibit liquid-like material properties[443] and tend to be highly dynamic, as there is a continuous internal diffusive rearrangement of the coacervate material as well as an exchange of components with the surroundings.[442, 444] A number of cytoplasmic and nucleoplasmic MLOs comprised of RNA and protein, such as nucleoli[445] and P granules,[442] have been reported to have liquid phase characteristics.[440, 446-453] An increasing number of other MLOs are candidates for liquid phase separation, including Cajal bodies, nuclear speckles, para-speckles, and PML bodies in the nucleoplasm and stress granules and germ granules in the cytoplasm.[454,455] Since coacervates and most MLOs are both formed through liquid-liquid phase separation, driven by the same attractive interactions, coacervates have a clear potential to mimic material properties, hierarchical organization, and sequestration of MLOs. This has inspired scientists to utilize the self-assembling and crowded nature of coacervates to engineer synthetic cells[456] and artificial organelles,[439, 457,458] which are capable of mimicking specific biological features including compartmentalization and communication.[459,460]

Beyond the historical debate, phase-separated and coacervate-like materials have been increasingly discussed in the context of cellular compartmentalization. Improvements in microscopy and labelling strategies has led to the discovery of a tremendous range of membraneless cellular compartments that harness liquid-liquid phase separation to drive functionality. Such compartmentalization has been typically associated with interactions between intrinsically disordered proteins (IDPs) and oligonucleotides. The formation of stress

granules has been observed as a mechanism for cells to arrest certain metabolic pathways while retaining the enzymatic machinery for later use.[461] Granule formation has also been associated with loci of transcription[440,462–465] and ribosome biogenesis, such as nucleoli (Figure 31a,b).[173,440] Compartmentalization also enables passive noise filtration, which can further help to increase the predictability of transcriptional outputs.[465]

In addition to the potential benefits of compartmentalization, aberrant phase transitions have also been correlated with disease states. FUS is a prion like IDP associated with the neurodegenerative disease ALS that has been shown to form liquid compartments as a result of stress and/or DNA damage. However, aging experiments demonstrated that mutations in FUS associated ALS resulted in an accelerated liquid-to-solid transition (Figure 31c).[466] While it should be noted that complex coacervation is not the driving force behind the formation of all membraneless organelles,[173] there is tremendous potential for parallel scientific exploration in the space between pure biology and pure materials science.

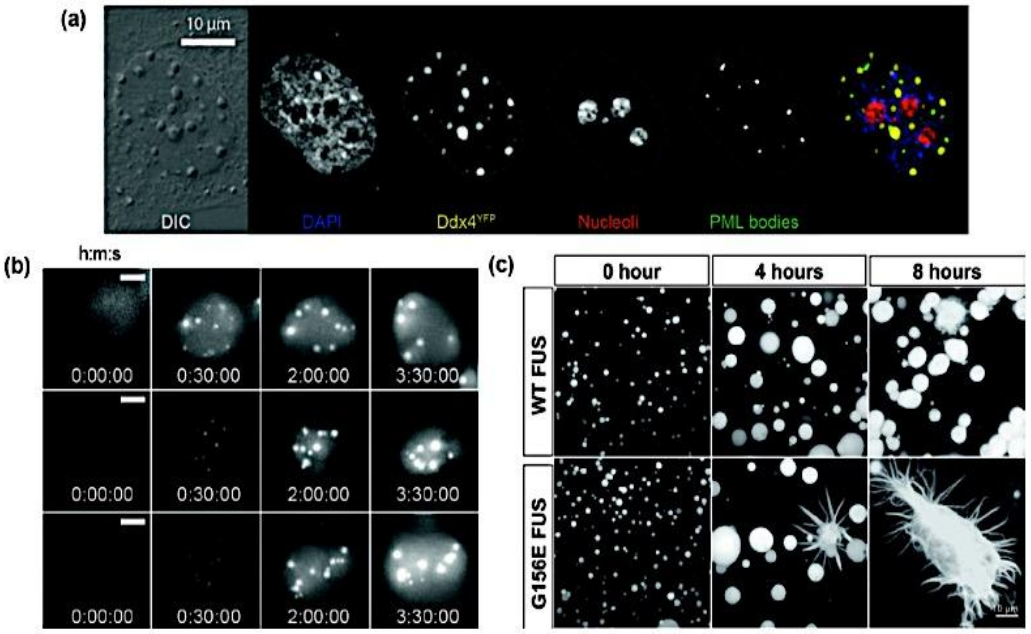

Figure 31: (a) Differential interface contrast (DIC) and fluorescence micrographs of a HeLa cell expressing Ddx4^{YFP}. Ddx4^{YFP} forms dense, spherical organelles in the nucleus. Cells were stained with antibodies to visualize nucleoli, PML bodies, nuclear speckles, and Cajal bodies. This figure was reproduced from Nott, T. J.; Petsalaki, E.; Farber, P.; Jervis, D.; Fussner, E.; Plochowietz, A.; Craggs, T. D.; Bazett-Jones, D. P.; Pawson, T.; Forman-Kay, J. D.; Baldwin, A. J. Phase Transition of a Disordered Nuage Protein Generates Environmentally Responsive Membraneless Organelles. *Mol. Cell*, *57* (5), 936−947,[440] Copyright 1969, Elsevier; (b) Time-lapse imaging of a nuclear body assembly in transiently transfected HeLa cells expressing Nephrin intracellular domain (NCID). Scale bar represents 5 µm. This figure was reproduced from Pak, C. W.; Kosno, M.; Holehouse, A. S.; Padrick, S. B.; Mittal, A.; Ali, R. Sequence determinants of intracellular phase separation by complex coacervation of a disordered protein. *Mol. Cell*, *63*(1), 72–85,[173] Copyright 2016, with the permission of Elsevier Inc.; (c) Representative images of the morphological changes in *in vitro* droplets of wild-type (WT) and G156E FUS during an "aging" experiment over 8 hr. This figure was reproduced from Patel, A.; Lee, H. O.; Jawerth, L.; Maharana, S.; Jahnel, M.; Hein, M. Y.; Stoynov, S.; Mahamid, J.; Saha, S.; Franzmann, T. M.; Pozniakovski, A; Poser, I.; Maghelli, N.; Royer, L. A.; Weigert, M.; Myers, E. W.; Grill, S.; Drechsel, D.; Hyman, A. A.; Alberti, S. A liquid-to-solid phase transition of the ALS protein FUS accelerated by disease mutation. *Cell*, *162* (5), 1066–1077,[466] Copyright 2015, with the permission of Elsevier Inc.

The compartmentalization afforded by coacervation can also be harnessed to define micro- or nanoscale reaction chambers. Coacervate droplets and coacervate-core micelles have been used to entrap enzymes to create nanoreactors and potentially increase the

reaction efficiency and/or operational stability of the encapsulated proteins.[467-469] In one example, a higher thermal tolerance was achieved for encapsulated trypsin, along with an increased reaction rate when compared to native trypsin.[467] In another example, the encapsulation of such constructs have the potential to be used to enable enzyme replacement therapies. Alternatively, these reactors can selectively uptake nanoparticles or other small molecules to enable *in situ* chemical synthesis.[469,470] For instance, nanoreactors containing poly(ethylene glycol)-*b*-poly(*α,β*-aspartic acid) (PEG-*b*-PAsp) and homo-catiomer poly([5-aminopentyl]-*α,β*-aspartamide) (Homo-PAsp-AP) were capable of activating prodrugs on location at tumor tissue sites.[469]

MLOs play versatile roles in regulating the cellular biochemistry, and their malfunctioning is associated with protein-aggregation diseases including Alzheimer's disease.[471-474] With new examples being discovered at a rapid pace, it is increasingly becoming clear that liquid−liquid phase separation (LLPS), primarily by the process of complex coacervation, plays a crucial role in an especially wide variety of cellular processes such as DNA compaction and chromatin organization,[475-478] selectively filtering specific biomolecules,[479] stress regulation,[440, 480] transcription regulation,[481-484] polarity establishment,[442] photosynthesis,[485] endocytosis,[486] cell signaling,[487] and cell adhesion.[488] While some functionalities such as sequestering and concentrating specific molecules to assist biochemical reactions are recurring and established themes, many other questions are just starting to get investigated. For example, it is as of yet quite unclear whether, and if so how, MLOs physically manipulate their local environment, e.g., mechanically remodel membranes. The interaction between MLOs and membranes is gathering interest but has not yet been widely studied. Recent work has indicated the role of coacervates in endocytosis and cell adhesion,[488,489] pointing out the potential of MLOs in exerting forces on lipid membranes.

In *Caenorhabditis elegans* (*C. elegans*), the liquid-like P granules that act as mRNA exporters have been reported to directly wet the nuclear membrane,[490] possibly enhancing transport. Membrane-bound phase-separated protein cluster shave also been shown to be involved in a variety of signaling pathways, modulating signal transduction as well as recruiting cytoskeletal elements.[405,491-494] These recent studies indicate previously unknown roles served by MLOs, including that of mechanical work.[495] Membrane-bound coacervates could serve as localized sites for the production of lipids or membrane proteins and could, due to their strong interaction with the membrane, perhaps even be engineered for transmembrane transport that would otherwise require complicated machinery. Future research on coacervate−membrane interactions could produce more refined manifestations of the interplay between cell-sized compartments and condensates. However, most contemporary coacervate models lack the chemical and compositional richness of MLOs, which explains why there remains a gap between coacervates in MLOs in terms of selectivity, regulation, and metastability. We need to identify some intrinsic limitations of coacervates and the current gaps between coacervates and MLOs, which will hopefully inspire future research. Most coacervate models are based on compositionally simple components whose phase separation is driven by a single type of interaction (e.g., charge complexation). They lack the chemical and compositional richness of many MLOs, which often contain many co-assembled proteins, each with a unique arrangement of amino acids and potential for interactions. This complexity explains, to a large extent, the superior selectivity, actively regulated formation and dissolution, and even the metastability seen in some MLOs. In order to mimic these features of MLOs better, reconstituted and designer proteins are being used to successfully create *in vitro* droplets with the same molecular composition as MLOs.[496, 497] Using principles from polymer coacervation, a wide range of de novo synthetic peptides were designed with tunable coacervation properties. By systematically analyzing the coacervate phase behavior, Dzuricky[498] provide fundamental insights into the link between sequence and coacervate properties, bridging the gap between condensates *in vitro* and *in vivo*. With increasing complexity, the boundaries between coacervates and (artificial) MLOs slowly fade away, and the more protein-based coacervate droplets will be capable of mimicking the characteristics of MLOs. By using such a bottom-up approach, we will be able to establish which level of complexity is required to mimic each property of an MLO.

Additionally, one crucial aspect that has so far been lacking in almost all *in vitro* models is the out-of-equilibrium nature of the cellular environment. Cells are fundamentally active, and a constant turnover of chemical energy governs the formation, stability, and arrangement of cytoskeletal structures, protein complexes, and also MLOs. Active processes can keep droplets stable or proteins soluble,[499] and they can

literally shape MLOs[500,501] and alter their physical state by fluidization. Recapitulating these processes in coacervate models to understand the underlying physical effects is a major challenge for the coming years, of which the first steps are being made. Spoelstra[502] described an alternative strategy to use a UDP-polymerizing enzyme to create enzyme-controlled active coacervates, and the first study in which transient, nonspherical coacervate shapes are reported, depending on enzyme activity. Additionally, Donau[503] reported active peptide-RNA coacervates that are formed transiently upon the addition of a carbodiimide chemical fuel. This is the first report of enzyme-free active coacervate droplets, which display emerging self-dividing behavior shortly before they dissolve.

7.5. Coacervate Rheology: Applications of Dynamics. There has also been increasing interest in understanding the rheological properties of coacervates[504,505] in order to improve and optimize applications. For this purpose, a series of biopolymers[506,507] and/or synthetic polymer systems 508 have been considered previously. Complex coacervates typically exhibit a viscoelastic response,[509] and rheological studies have shown that the viscoelasticity and viscosity of coacervates are affected by a number of parameters, including salt concentration, mixing stoichiometry, and chain length.[128, 271]

7.5.1. Encapsulation and Release. In addition to characterization of the properties of the base material, rheology has been used to understand the impact that a guest molecule has on the structure of a complex coacervate. Tiwari *et al*., examined both the encapsulation and release of salbutamol sulfate, a bronchodilator used in the treatment of asthma and other chronic airway diseases, from coacervates formed from a pair of protein molecules, gelatin-A and gelatin-B.[510] Linear viscoelastic characterization showed that drug encapsulation caused a significant decrease in the storage modulus (G'), suggesting that the coacervate matrix was disturbed and weakened by the presence of the drug, and a slight increase in the loss modulus (G"), suggesting a commensurate fluidization of the material. Such changes in material properties can be critical for modeling of release processes for more advanced therapeutics.

7.5.2. Connection to Layer-by-Layer Films and solid PECOX. The associative electrostatic interactions driving complex coacervation are an obvious parallel to those used to drive the formation of layer-by-layer (LbL) films.[211-213] LbL films are assembled by the sequential deposition of oppositely-charged polyelectrolytes on a surface.[511] While complex coacervation is an equilibrium phase separation, LbL films are a kinetically-trapped assembly. Such films can be formed onto a variety of surfaces, including bubbles and droplets to create capsules for delivery. LbL assembly can be used either as a method for creating a capsule, or as a layered structure that allows for the direct release of therapeutics upon disassembly. Careful design of the layered structures can enable both spatial and temporal control over the release of therapeutics. Alternatively, the materials of the films themselves could be harnessed as active coatings, such as antibacterial and/or antifouling surfaces.[512] While LbL films can be formed as free-standing films, they are much more commonly presented as coatings. However, recent reports have demonstrated the utility of bulk PECOX solids as well. PECOX may be extruded into large articles if sufficiently plasticized with salt and water ("saloplasticity") has introduced yet another processing dimension.[513,514] This idea of salt-driven plasticization, or 'saloplasticity' has opened up a tremendous range of opportunities for using salt to process polyelectrolyte complex materials as liquid coacervates, and then solidify the materials by the removal of salt, and a range of accounts describing ultracentrifuged[515-518] or extruded materials, 513 spin-coated films,[519,520] 3D printed structures,[521] and electrospun fibers[522,523] have been reported. However, thus far saloplastic materials have only been reported for synthetic polymer systems. Expanding this class of materials to include biopolyelectrolytes such as proteins, hyaluronic acid, chitosan, or chondroitin sulfate has tremendous potential to further enhance their utility.

7.5.3. Self-Healing and Structural Recovery. Another interesting material property conferred by the non-covalent nature of the molecular interactions defining complex coacervates is the potential for self-healing and structural recovery after complete network disruption.[505,524] This can be assayed by the application of a large strain (*i.e.*, 100% oscillatory shear strain, well beyond the linear range for the material) to break the sample, followed by continuous measurements back in the linear strain regime to track the ability of the material to recover its original elasticity, and the requisite timescale to do so. An example of this type of experiment is given for a fish gelatin/sodium montmorillonite coacervate system (Figure 32).[524]

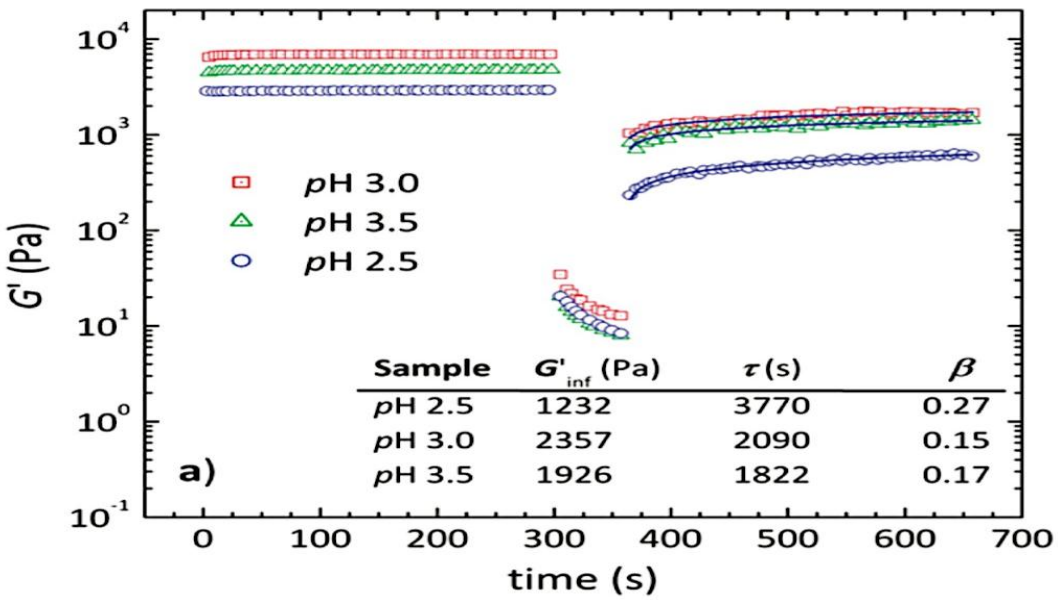

Figure 32: Structural recovery behavior as a function of time, assessed by monitoring G' after the application of a 100% oscillatory shear strain. The solid lines in regime III are fitting of $G' = G'_\infty (1 - \exp(t/\tau)\beta)$ to the data points. The inset table lists the fitting parameters. This figure was reproduced from Qazvini, N. T.; Bolisetty, S.; Adamcik, J.; Mezzenga, R. Self-Healing Fish Gelatin/Sodium Montmorillonite Biohybrid Coacervates: Structural and Rheological Characterization. *Biomacromolecules, 13* (7): 2136–2147,[524] Copyright 2012, American Chemical Society.

From an initially high value for the equilibrium storage modulus (G'), the application a high strain decreases the modulus of the material, breaking the internal elastic network of electrostatic interactions and converting it into a liquid-like material. Five minutes after the application of this high strain, the sample was able to recover 20-30% of its original modulus – a process that could be modeled by an exponential function. Examination of the effects network disruption in the example by Qazvini *et al.*,[524] suggested that the liquid-like behavior was not the result of free- flowing individual nanoplatelets, but rather the result of domain fracturing. Upon removal of strain, these domains are then able to quickly recover the percolated elastic behavior of a network to give a solid-like response, followed by a slower rearrangement of the gelatin network. This self-healing capability suggests that these types of materials could be easily processed as low viscosity materials, for example as thin films or injectables, followed by a recovery time to allow for the formation of an elastic gel.

7.5.4. Microrheology Techniques. Elbaum-Garfinkle *et al.*, recently reported the use of microrheology techniques to coacervate-like materials formed as a result of the self-interaction of LAF-1, a DDX3 RNA helicase found in the P granules of *Caenorhabditis elegans* (Figure 33).[525]

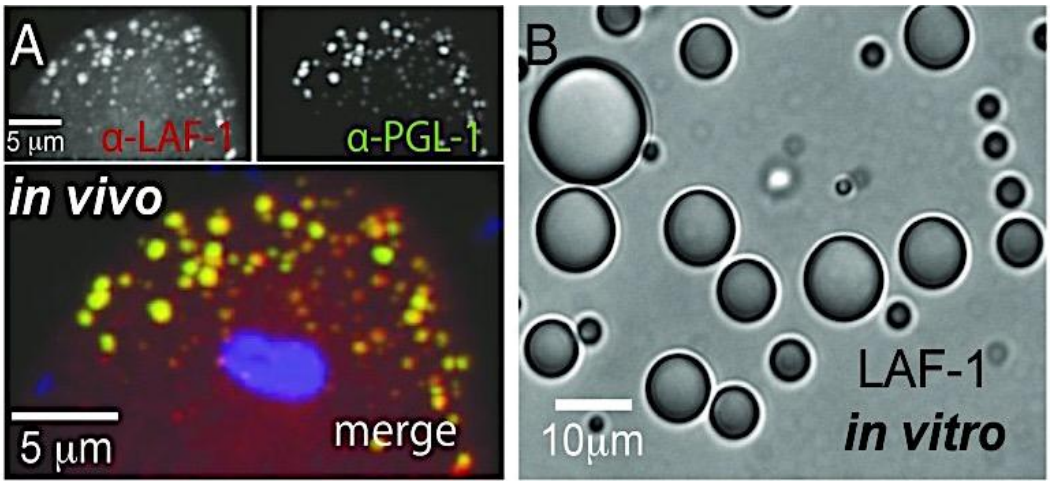

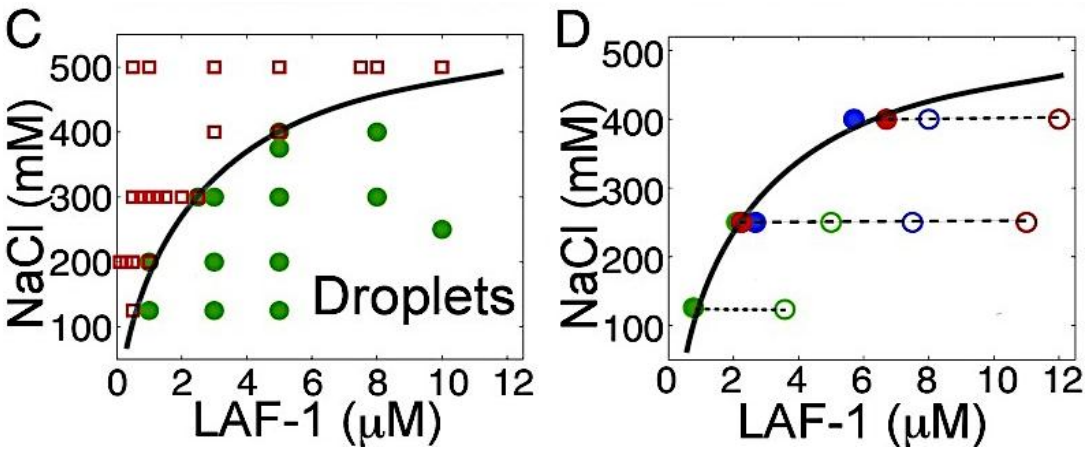

Figure 33: LAF-1 colocalizes to P granules in vivo and phase separates into droplets in vitro. (A) Confocal images of two-cell embryo posterior immunostained for LAF-1 (*Upper Left*) and PGL-1 (*Upper Right*). In the dividing P1 cell, LAF-1 localizes to PGL-1–marked P granules; DAPI-stained nucleus is included in the merged image. (B) DIC image of phase separated LAF-1 droplets. (C) Protein/NaCl concentrations scoring positive (green circles) or negative (red squares) for optically resolvable droplets are plotted, resulting in a phase boundary (line drawn to guide the eye). (D) The protein concentration in the dilute phase (●) is plotted for varying total protein concentrations (○) at three different salt concentrations. For all conditions, the concentration of the dilute phase falls directly onto the LAF-1 phase boundary from *C* (solid line). This figure was reproduced with permission from Elbaum-Garfinkle, S.; Kim, Y.; Szczepaniak, K.; Chen, C. C.; Eckmann, C. R.; Myong, S.; Brangwynne, C. P. The disordered P granule protein LAF-1 drives phase separation into droplets with tunable viscosity and dynamics. *Proc. Natl. Acad. Sci. U. S. A.* 2015, *112* (23), 7189-7194.[525]

Here, confocal fluorescence microscopy was used in conjunction with particle tracking methodologies to measure the viscosity of coacervate-like droplets of LAF-1 both with and without RNA. A more detailed treatment of this type of microrheological characterization is beyond the scope of the current work. However, adoption of these types of techniques has the potential to enable the analysis of a vast array of coacervate-based materials that would otherwise be inaccessible to larger-scale rheological measurements.

7.6. Medical Science. To relate complex coacervation to medical science, disruption of normal intracellular complex coacervation, or gain of function mutations leading to abnormal complex coacervation, can cause disease. Benedek[526] used the term "molecular condensation disease" to broadly describe cataracts and other pathologies associated with abnormal protein phase separation. "Cold" cataracts are the reversible opacification of the lens by liquid–liquid phase separation of cytoplasmic crystallin proteins. As another example, the leading cause of fronto-temporal dementia may be a protein condensation disease caused by mistranslated arginine-rich dipeptide repeat proteins that insert or dissolve into liquid phase- defined intracellular compartments, disrupting their normal function.[527] Conceivably, better understanding of the physical chemistry of complex coacervation of biomacromolecules and the role of specific functional groups could lead to treatments for pathological intra- cellular phase separations.

Abnormal accumulation of TAR DNA-binding protein43 (TDP-43) is a pathological hallmark of amyotrophic lateral sclerosis (ALS), a fatal neurodegenerative disease characterized by a selective loss of motor neurons, and a subtype of frontotemporal lobar degeneration (FTLD-TDP).[528] Recently, a number of studies revealed that many kinds of RNA-binding proteins (RBPs), including TDP-43, spontaneously develop granule-like structures via a liquid–liquid phase separation (LLPS) mechanism.[529,530] LLPS is a process in which proteins and nucleotides abruptly segregate into two distinct phases, enabling the formation of intracellular membrane-less organelles,[531] such as p-bodies[532] and stress granules.[533,534] Under physiological conditions, LLPS enables to achieve high local concentrations for molecular interactions and rapid chemical reactions, and allow fast changes of molecules upon signaling for facilitating various intracellular biological processes, e.g., transcriptional regulation and signal transduction.[535] However, once excess amounts of proteins are accumulated together with dysregulation of LLPS, the complexes quickly transform into pathological inclusions that are often found in neurodegenerative

diseases[536,537] ALS causative gene products, including FUS, TIA-1, and, of course, TDP-43, are proposed to form aggregates via LLPS. Consistent with this hypothesis, recent studies have discovered that optical multimerization of cytoplasmic TDP-43 induces the aggregation and sequestration of endogenous nuclear TDP-43 into the cytoplasmic aggregates that are dependent on LLPS.[538,539] As shown in Figure 34 A, B, 1,6-hexanediol (1,6-Hd) drastically dissociated the cytoplasmic aggregates of RBPs, mutant FUS and TIA1. Consistent with the decreased number of RBPs-induced aggregates, sequestration of TDP-43 into the aggregates was also significantly prevented (Fig. 4C). These observations suggest that LLPS drives the cytoplasmic co-aggregation of RBPs and TDP43. In contrast, 1,6-Hd did not influence either the number of aggregates of microtubule-related proteins (MRPs; mutant PFN1 and UBQLN2) or coaggregates with TDP-43 (Fig. 34A–C), suggesting that a mechanism independent of LLPS drives the co-aggregation of MRPs and TDP-43.

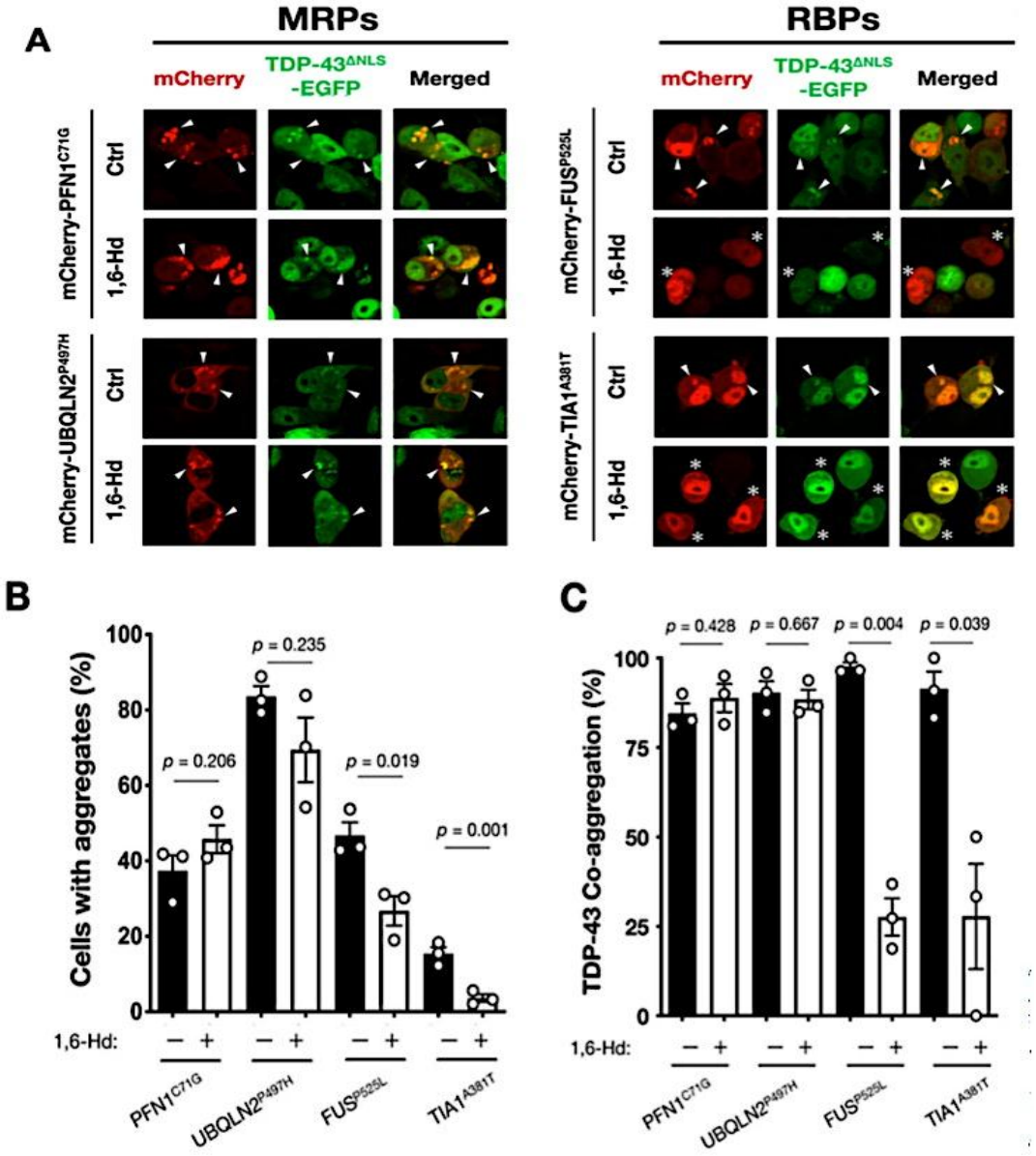

Figure 34: Liquid–liquid phase separation (LLPS) is involved in RBPs-induced TDP-43 co-aggregation. Administration of 1,6-hexanediol (1,6-Hd), an inhibitor of LLPS, dissociated TDP-43 co-aggregates with RBPs but not with MRPs in Neuro 2a (N2a) cells expressing TDP-43$^{\Delta NLS}$-EGFP. Representative images are shown in A. Both the ratio of the cells with TDP-43 aggregates (B) and TDP-43 co-aggregation (C) were reduced, specifically in the cells expressing RBPs with 1,6-Hd. Arrowheads indicate co-aggregates of the RBPs and MAPs with TDP-43$^{\Delta NLS}$ -EGFP. Whereas, asterisks indicate the cells without co- aggregates of the RBPs by the 1,6-Hd treatment. More than 50 cells in each condition were analyzed for the quantification. Data are expressed as

mean ± SEM (n = 3). This figure was reproduced from Watanabe, S.; Inami, H.; Oiwa, K.; Murata, Y.; Sakai, S.; Komine, O.; Sobue, A.; Iguchi, Y.; Masahisa Katsuno, M.; Yamanaka, K. Aggresome formation and liquid–liquid phase separation independently induce cytoplasmic aggregation of TAR DNA-binding protein 43. *Cell Death Dis., 11* (10), 909 (1-15),[540] Copyright 2020, Springer Nature.

The C9orf72 mutation is an expansion of a GGGGCC (G4C2) repeat in intron 1 of the gene. In unaffected individuals the G4C2 is repeated 2 to 23 times, whereas in those with the mutation, the sequence is expanded to contain hundreds to thousands of repeats.[541,542] Due to its location upstream of the coding region, the mutation can lead to a reduction in the levels of the protein that it encodes,[543,544] which is involved in the regulation of endo-lysosomal trafficking and autophagy.[545-547] However, a common finding from murine C9orf72 knockout models is the lack of neurodegeneration or TDP-43 pathology—a key pathological feature of C9orf72- ALS/FTD (frontotemporal dementia).[548-553] There is now substantial and clear evidence that a disruption in the phase separation behavior of proteins and RNA involved in the formation of liquid-like membraneless organelles explains much of the major pathological phenomena associated with C9orf72-ALS/FTD (Figure 35). Gain-of-function mechanisms associated with the G4C2 repeat expansion in C9orf72–G4C2 repeat RNA and the arginine rich DPRs poly-GR and poly-PR—undergo phase separation themselves and perturb the phase separation of LCD (low complexity sequence domains) containing proteins, resulting in abnormal membraneless organelle formation and dissolution, impairing their physiological functions and leading to neurodegeneration. Further pathological phase separation induced by the arginine rich DPRs is strongly associated with TDP-43 dysfunction and aggregation, the major pathological hallmark of C9orf72-ALS/FTD correlating with neuronal cell death. The targeting of abnormally phase separated condensates using small molecules or gene therapy provides a novel strategy for future therapeutics, although a greater understanding is needed of phase separation in order to design targets which are both beneficial and precise. [554]

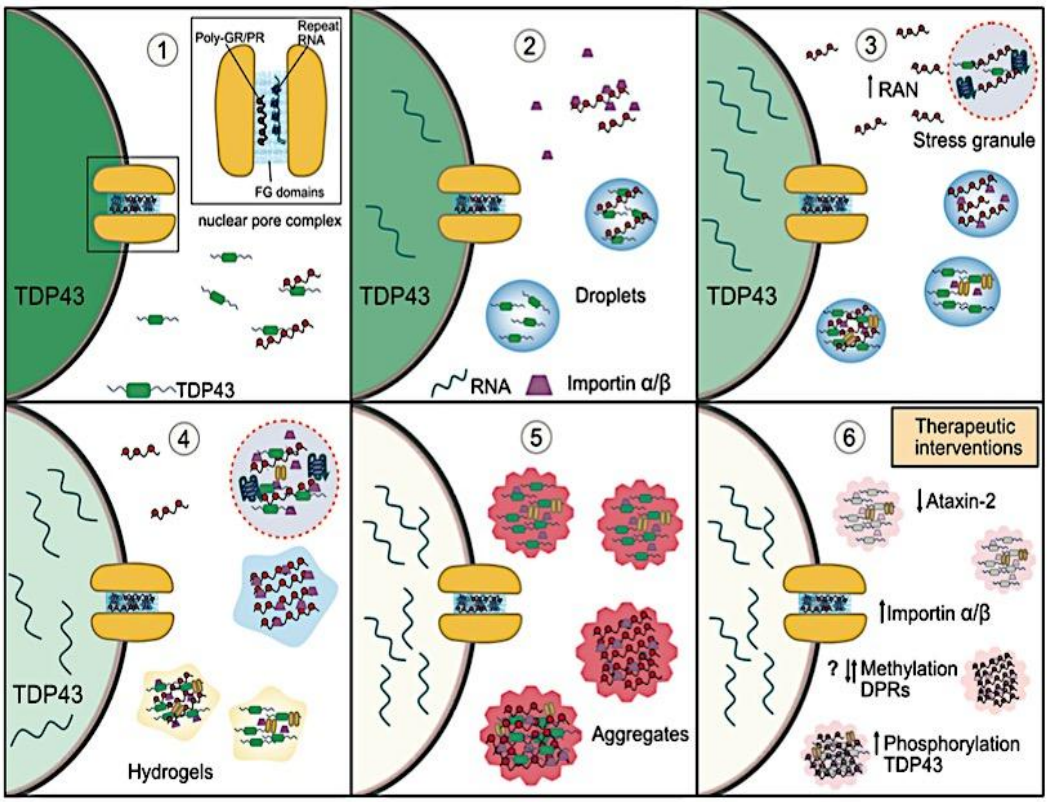

Figure 35: How disruptions in phase separation and membraneless organelles may lead to TDP-43 aggregation in *C9orf72*-ALS/FTD and possible therapeutic strategies. (1) *C9orf72* arginine rich DPRs and G_4C_2 repeat RNA bind nuclear pore proteins with phenylalanine rich repeats (FG domains) and result in nucleocytoplasmic transport dysfunction and mislocalization of TDP-43 to the cytoplasm. (2) Interaction between cytoplasmic TDP-43 and the arginine rich DPRs results in the LLPS of TDP-43 in the cytoplasm. Impaired nucleocytoplasmic transport also results in an

accumulation of the importin-α/β complex (the import receptor for TDP-43) in the cytoplasm where it is also bound by the arginine rich DPRs and results in their reduced solubility. This begins a vicious feedback loop as impaired nuclear import of TDP-43 further increases levels of cytoplasmic TDP-43, whose LLPS is potentiated by a nuclear retention of mRNA from impaired nuclear export. (3) Cellular stress and the direct interaction of arginine rich DPRs and G_4C_2 RNA with stress granule proteins (including TDP-43) promotes phase separation and the formation of stress granules. The arginine rich DPRs also induce condensation of importin-α/β. TDP-43 droplets recruit importin-α/β complexes and nuclear pore proteins further impairing nucleocytoplasmic transport, resulting in more TDP-43 accumulation in the cytoplasm and depletion of nuclear TDP-43. Both stress granule accumulation and cytoplasmic TDP-43 also enhance RAN translation of the arginine rich DPRs. (4) The stress granules induced by the arginine rich DPRs and repeat RNA have reduced dynamics which entraps TDP-43, import receptors and nuclear pore proteins. Persistent TDP-43 and DPR-importin-α/β droplets are likely to mature into more solid-like states such as hydrogels, further immobilizing these proteins. (5) TDP-43 in solid-like states and within stress granules, and also DPRs, mature into pathological insoluble aggregates which further sequester proteins involved in nucleocytoplasmic transport. Thus, the disruption of phase separation and membraneless organelles leads to a cascade of vicious feedback loops which result in depletion of nuclear TDP-43 and its accumulation and aggregation in the cytoplasm in disease. (6) Therapeutic targeting of stress granules by reducing ataxin-2 levels, manipulating post-translation modifications such as methylation of the DPRs and phosphorylation of TDP-43, or increasing importin-α/β to reduce excessive LLPS may enhance the solubility of TDP-43, help to reduce its aggregation and ameliorate the pathological cascade in *C9orf72*-ALS/FTD and other TDP-43 proteinopathies. This figure was reproduced from Solomon, D. A.; Smikle, R.; Reid, M. J.; Mizielinska, S. Altered Phase Separation and Cellular Impact in C9orf72-Linked ALS/FTD. *Front. Cell. Neurosci.*, *15*, 664151 (1-24),[554] Copyright 2021, Solomon, Smikle, Reid and Mizielinska.

9. CONCLUSION AND FUTURE PERSPECTIVES

In this review, we have shown that recent advances in the science and engineering of complex coacervates has provided the foundation for their practical use in a variety of applications, ranging from self-assembled, functional materials to tunable material encapsulants and industrially-practical viscosity modifiers. For all, little is understood about the mechanism and kinetics of complex coacervation, few theories are quantitatively supported by experiment, phenomenology alone fails to predict coacervate stability, and equilibrium behavior is sometimes not confirmed. Investigation of the mechanisms of complex formation between polyelectrolytes and oppositely charged colloids, and of coacervate structures formed at different length scales represents an active and important research area. Although mechanisms of coacervation have been deduced from observations of self-organized microscopic structures, the true relationship between coacervation mechanism and the resultant structure remains to be further explored. There is still a need for more connection between experimental and theoretical work. Experimental efforts have largely focused on phase behavior as the primary point of comparison, however this is not always a direct probe of the molecular-level features such as charge correlations, charge density effects, excluded volume, and specific ion effects. This makes it difficult to distinguish between VO theory and more sophisticated theories, which as a result are not often compared to experiment. Conversely, there is a need from the theoretical side to expand the palette of models relevant to the coacervate-driven assembly that is at the forefront of experimental work in the field. Joint efforts will expedite the convergence on an overall picture of coacervation; this will hopefully enable polymer scientists to fully exploit their complexity to make truly exciting and biologically inspired materials. Further levels of understanding require incorporation of knowledge regarding the molecular structure of coacervate-based materials, and the development of more detailed theories and models. For example, to the author's knowledge the rheological behavior of coacervates has not been widely studied from a theoretical perspective. This is despite the regular use of rheology as a tool to characterize coacervates.[112,555] Hybrid techniques, such as simultaneous small-angle X-ray or small-angle neutron scattering, coupled with rheology (rheo-SAXS/SANS),[504] rheo-optics,[141,556-558] calorimetry, and/or other methods have tremendous potential to further expand our understanding of this class of materials. Subsequent interpretation of the resulting data will require the further development and validation of theoretical predictions to couple observation with molecular models. For instance, the systematic linear viscoelastic analysis of polymer chemistry effects on complex

coacervation would enable further testing of the "sticky" Rouse model proposed by Spruijt *et al*.[509,558] Such efforts could also be coupled with advancements in the modeling of coacervation in general.

It is important to note, that the vast majority of experimental and theoretical efforts have focused on understanding small-amplitude oscillatory shear (SAOS) data because of the strong theoretical background of such measurements. However, from an applications perspective, most processing operations subject materials to deformations that are well beyond the limits of linear viscoelasticity. Extension of theoretical treatments of polymer behavior into the non-linear large- angle oscillatory shear (LAOS) regime, has tremendous potential to elucidate critical mechanisms related to the large-scale disruption and rearrangements of polymer networks. The application of such non-linear techniques to the characterization of complex coacervate-based materials is an open challenge for the future.

Polyelectrolyte coacervates and complexes are a class of materials that are being increasingly used for self-assembly[199, 555, 559-561] however there are fundamental challenges in understanding them from a theoretical point of view. Many if not most of the most pressing challenges in polymer modeling today affect have profound implications for complex coacervates–highly correlated electrostatics,[190, 562] multiple length scales, kinetic traps and glassy dynamics,[117, 199, 563,564] water,[564] dielectric,[565] and specific ion effects.[10, 74, 566] The diversity of modern theoretical approaches typically address some but not all of these issues. A comprehensive picture of the state of the theory shows that while a patchwork of many theories collectively captures a number of limiting cases, there is not a single theory capable of simultaneously addressing the full spectrum of features observed in complex coacervation. Ideally, such a theory would be able to predict coacervate properties over a broad range of parameters and length scales. At the atomistic and/or molecular level, the organization of charges and even solvent would be characterized by (for example) pair correlation functions. Larger length-scale effects, such as the overall polymer conformation, phase behavior, and self-assembled structures, would be simultaneously predicted. Out-of-equilibrium behavior should also be captured in a complete physical picture of coacervation. Finally, such a theory would ideally provide a consistent conceptual picture of coacervation that is useful for experimental design of coacervate-based materials. Looking forward, we anticipate that the need to reckon with the role of hydration and atomistic detail, the possibility of higher-order molecular self-assembly with sequence-defined polyelectrolytes, and the importance of non-electrostatic interactions in biology are all emerging areas in both coacervation as well starting points for deeply challenging questions in molecular engineering and chemical physics.

The cytomimetic approaches to address three aspects of MLOs that are still poorly understood are dynamic assembly, partitioning of client molecules and reaction kinetics inside MLOs. Coacervates serve as model systems to investigate these aspects systematically *in vitro*. However, most coacervates are still far from resembling cellular MLOs, and significant progress is needed to develop coacervate- based cytomimetic systems that capture the full complexity of spatiotemporal organization in cells. In particular, such studies should be used to shed light on three aspects of MLOs that are still poorly understood: (1) how can the assembly and dissolution of MLOs be controlled, (2) what rules govern the partitioning of biomolecules into MLOs, and (3) how are rates of reactions and other biochemical processes affected by MLOs? As multicomponent complexes composed of polyelectrolytes, biomacromolecules, or other charged species (e.g., DNA and RNA) become increasingly important in materials and biomaterials research, the ability to understand the complexation process of multicomponent mixtures and control the structure and properties of the resulting material will provide further means to enhance their functionality. Multicompartment coacervates have recently been developed based on ELPs with different chain lengths,[567] and different IDPs derived from nucleoli,[500] in an attempt to better understand the hierarchical organization of the numerous different components found in many MLOs. A related aspect that has not been experimentally addressed yet, is how different types of coacervates or MLOs could coexist in the same cytosol, without mixing,[500, 568] as has long been known for many other multicomponent liquid mixtures.[569,570] This could be connected to amphipathic biomolecules that adsorb at the liquid-liquid interface to stabilize it,[567, 571] or to a continuous turnover of coacervate material, away from thermodynamic equilibrium, in order to suppress Ostwald ripening.[572] Such aspects represent the oncoming challenges on the road to artificial organelles and cells.

Thus, despite the extensive efforts of the community to date, there remain endless

opportunities for polymer scientists — both experimentalists and theorists — to find interesting problems the study of complex coacervation.

ACKNOWLEDGMENT

P.S.R acknowledges UGC, Government of India, New Delhi, India, for granting doctoral fellowship in the form of a Junior Research Fellowship (JRF) in Engineering and Technology [Fellowship 10-01/2008 (SA-I)] and postdoctoral fellowship under RUSA 2.0 scheme (Ref. No. R-11/214/19). P.S.R greatfully acknowledges University of Missouri-Kansas City (UMKC), U. S. A., and University of the Pacific-Stockton, California, U. S. A., for granting postdoctoral research assistantship.

REFERENCES

1. Kruyt, H. R.; Bungenberg de Jong, H. G. Chemistry – Coacervation (Partial miscibility in colloid systems). *Proc. K. Ned. Akad. Wet*, 1929; *32*: 849–856.
2. Skepoe, M.; Linse, P. Complexation, Phase Separation, and Redissolution in Polyelectrolyte-Macroion Solutions. *Macromolecules*, 2003; *36*(2): 508-519.
3. Kayitmazer, B.; Seeman, D.; Minsky, B. B.; Dubin, P. L.; Xu, Y. Protein–polyelectrolyte interactions. *Soft Matter*, 2013; *9*(9): 2553-2583.
4. Tsuchida, E.; Abe, K. *Inter macromolecular Complexes*; Springer: Heidelberg, Germany, 1982.
5. Tiebackx, F. W. Gleichzeitige Ausflockung zweier Kolloide. *Z. Chem. Ind. Kolloide*, 1911; *8:* 198–201.
6. Roy, P. S.; Samanta, A.; Mukherjee, M.; Roy, B.; Mukherjee, A. Designing Novel pH-Induced Chitosan-Gum Odina Complex Coacervates for Colon Targeting. *Ind. Eng. Chem. Res*, 2013; *52*(45): 15728−15745.
7. Bungenberg de Jong, H. G. Crystallization-coacervation-flocculation. In *Colloid Science*; Kruyt, H. R., Ed.; Elsevier Publishing: Amsterdam, The Netherlands, 1949a; Vol. II, Chapter VIII, pp 232−258.
8. Bungenberg de Jong, H. G. Complex colloid systems. In *Colloid Science*; Kruyt, H. R., Eds.; Elsevier: Amsterdam, 1949b; Vol. II, Chapter X, pp 335-432.
9. Singh, S. S.; Siddhanta, A. K.; Meena, R.; Prasad, K.; Bandyopadhyay, S; Bohidar, H. B. Intermolecular complexation and phase separation in aqueous solutions of oppositely charged biopolymers. *Int. J. Biol. Macromol*, 2007; *41*(2): 185-192.
10. Weinbreck, F.; Rollema, H. S.; Tromp, R. H.; de Kruif, C. G. Diffusivity of whey protein and gum arabic in their coacervates. *Langmuir*, 2004; *20*(15): 6389-6395.
11. Gupta, A. N.; Bohidar, H. B.; Aswal, V. K. Surface patch binding induced intermolecular complexation and phase separation in aqueous solutions of similarly charged gelatin-chitosan molecules. *J. Phys. Chem. B*, 2007; *111*(34): 10137-10145.
12. Gao, J.; Dubin, P. L.; Muhoberac, B. B. Capillary Electrophoresis and Dynamic Light Scattering Studies of Structure and Binding Characteristics of Protein-Polyelectrolyte Complexes. *J. Phys. Chem. B*, 1998; *102*(28): 5529–5535.
13. Kayitmazer, A. B.; Bohidar, H. B.; Mattison, K. W.; Bose, A.; Sarkar, J.; Hashidzume, A.; Russo, P. S.; Jaeger, W.; Dubin, P. L. Mesophase separation and probe dynamics in protein–polyelectrolyte coacervates. *Soft Matter*, 2007; *3:* 1064–1076.
14. Arfin, N.; Bohidar, H. B. Condensation, complex coacervation, and overcharging during DNA-gelatin interactions in aqueous solutions. *J. Phys. Chem. B*, 2012; *116*(44): 13192-13199.
15. Strauss, G.; Gibson, S. A. Plant Phenolics As Cross-Linkers of Gelatin Gels and Gelatin-Based Coacervates for Use As Food Ingredients. *Food Hydrocoll*, 2004; *18*(1): 81–89.
16. Mohanty, B.; Aswal, V. K.; Kohlbrecher, J.; Bohidar, H. B. Length Scale Hierarchy in Sol, Gel, And Coacervate Phases of Gelatin. *J. Polym. Sci. Polym. Phys*, 2006; *44*(12): 1653–1665.
17. Kaibara, K.; Okazaki, T.; Bohidar, H. B.; Dubin, P. L. pH- Induced Coacervation in Complexes of Bovine Serum Albumin and Cationic Polyelectrolytes. *Biomacromolecules*, 2000; *1*(1): 100–107.
18. Antonov, M.; Mazzawi, M.; Dubin, P. L. Entering and Exiting the Protein-Polyelectrolyte Coacervate Phase via Nonmonotonic Salt Dependence of Critical Conditions. *Biomacromolecules*, 2010; *11*(1): 51–59.
19. Kayitmazer, A. B.; Strand, S. P.; Tribet, C.; Jaeger, W.; Dubin, P. L. Effect of Polyelectrolyte Structure on Protein-Polyelectrolyte Coacervates: Coacervates of Bovine Serum Albumin with Poly-(diallyidimethylammonium chloride) versus Chitosan. *Biomacromolecules*, 2007; *8*(11): 3568–3577.
20. Liu, S. H.; Cao, Y. L.; Ghosh, S.; Rousseau, D.; Low, N. H.; Nickerson, M. T. Intermolecular Interactions during Complex Coacervation of Pea Protein Isolate and

Gum Arabic. *J. Agric. Food Chem*, 2010; *58*(1): 552–556.
21. Gupta, S.; Biswas, P. Conformational properties of complexes of poly (propylene imine) dendrimers with linear polyelectrolytes in dilute solutions. *J. Chem. Phys*, 2020; *153*(19): 194902.
22. Wang, Y. L.; Kimura, K.; Dubin, P. L.; Jaeger, W. Polyelectrolyte-Micelle Coacervation: Effects of Micelle Surface Charge Density, Polymer Molecular Weight, and Polymer/Surfactant Ratio. *Macromolecules*, 2000; *33*(9): 3324–3331.
23. Feng, X. H.; Dubin, P. L.; Zhang, H. W.; Kirton, G. F.; Bahadur, P.; Parotte, J. Critical Conditions for Binding of Dimethyldodecylamine Oxide Micelles to Polyanions of Variable Charge Density. *Macromolecules*, 2001; *34*(18): 6373–6379.
24. Li, Y. J.; Dubin, P. L.; Dautzenberg, H.; Luck, U.; Hartmann, J.; Tuzar, Z. Dependence of Structure of Polyelectrolyte/Micelle Complexes upon Polyelectrolyte Chain-Length and Micelle Size. *Macromolecules*, 1995; *28*(20): 6795–6798.
25. Wang, Y. L.; Kimura, K.; Huang, Q. R.; Dubin, P. L.; Jaeger, W. Effects of Salt on Polyelectrolyte-Micelle Coacervation. *Macromolecules*, 1999; *32*(21): 7128–7134.
26. Evers, O. A.; Fleer, G. J.; Scheutjens, J. M. H. M.; Lyklema, J. Adsorption of Weak Polyelectrolytes from Aqueous Solution. *J. Colloid Interface Sci*, 1986; *111*(2): 446–454.
27. Vongoeler, F.; Muthukumar, M. Adsorption of Polyelectrolytes onto Curved Surfaces. *J. Chem. Phys*, 1994; *100*(10): 7796–7803.
28. Nguyen, T. T.; Shklovskii, B. I. Complexation of DNA with Positive Spheres: Phase Diagram of Charge Inversion and Reentrant Condensation. *J. Chem. Phys*, 2001; *115*(15): 7298–7308.
29. Zhang, R.; Shklovskii, B. T. Phase Diagram of Solution of Oppositely Charged Polyelectrolytes. *Physica A*, 2005; *352*(1): 216–238.
30. Menger, F. M.; Peresypkin, A. V. A combinatorially - derived structural phase diagram for 42 zwitterionic geminis. *J. Am. Chem. Soc*, 2001; *123*(23): 5614–5615.
31. Peresypkin, A. V.; Menger. F. M. Zwitterionic geminis. Coacervate formation from a single organic compound. *Org. Lett*, 1999; *1*(9): 1347–1350.
32. Bohidar, H. B. Coacervates: A novel state of matter. *J. Surf. Sci. Technol*, 2008; *24:* 105–124.
33. Michaeli, I.; Overbeek, J. T. G.; Voorn, M. J. Phase separation of polyelectrolyte solutions. *J. Polym. Sci*, 1957; *23*(123): 443–450.
34. Voorn M.J. Phase separation in polymer solutions. In: *Fortschritte Der Hochpolymeren-Forschung*. Advances in Polymer Science; Springer: Berlin, Heidelberg, 1959; vol 1/2, pp 192-233. https://doi.org/10.1007/BFb0050485.
35. Voorn, M. J. Complex coacervation. I. General theoretical considerations. *Rec. Trav. chim. Pays-Bas*, 1956; *75:* 317–330.
- Complex coacervation. II. Thermodynamic calculations on a specific model, with application to two-component systems. *Rec. Trav. chim. Pays-Bas*, 1956; *75:* 405–426.
- Complex coacervation. III. Thermodynamic calculations on three-component systems. *Rec. Trav. chim. Pays-Bas*, 1956; *75:* 427–446.
- Complex coacervation. IV. Thermodynamic calculations on four-component systems. *Rec. Trav. chim. Pays-Bas*, 1956; *75:* 925–937.
36. Veis, A.; Bodor, E.; Mussell, S. Molecular Weight Fractionation and the Self-Suppression of Complex Coacervation. *Biopolymers*,1967; *5*(1): 37-59.
37. Nakajima, A; Sato, H. Phase Relationships of an Equivalent Mixture of Sulfated Polyvinyl Alcohol and Aminoacetalyzed Polyvinyl Alcohol in Microsalt Aqueous-Solution. *Biopolymers*, 1972; *11*(7): 1345-1355.
38. Tainaka, K. I. Study of complex coacervation in low concentration by virial expansion method. I. Salt free systems. *J. Phys. Soc. Jpn*, 1979; *46*(6): 1899–1906.
39. Veis, A.; Aranyi, C. Phase separation in polyelectrolyte systems. I. Complex coacervates of gelatin. *J. Phys. Chem*, 1960; *64*(9): 1203-1210.
40. Lin, Y. H.; Song, J. H.; Forman-Kay, J. D.; Chan, H. S. Random-phase-approximation theory for sequence-dependent, biologically functional liquid-liquid phase separation of intrinsically disordered proteins. *J. Mol. Liq*, 2017; *228:* 176–193.
41. Das, S.; Eisen, A.; Lin, Y. H.; Chan, H. S. A lattice model of charge-pattern-dependent polyampholyte phase separation. *J. Phys. Chem. B*, 2018; *122*(21): 5418–5431.
42. Lin, Y. H.; Forman-Kay, J. D.; Chan, H. S. Sequence-specific polyampholyte phase separation in membraneless organelles. *Phys. Rev. Lett*, 2016; *117*(17): 178101, 1-6.
43. Biesheuvel, P. M.; Stuart, M. A. C. Electrostatic free energy of weakly charged macromolecules in solution and intermacromolecular complexes consisting

of oppositely charged polymers. *Langmuir*, 2004; *20*(7): 2785– 2791.
44. Fredrickson, G. H. *The Equilibrium Theory of Inhomogeneous Polymers;* Oxford Univ Press: New York, 2006.
45. Riggleman, R. A.; Kumar, R.; Fredrickson, G. H. Investigation of the interfacial tension of complex coacervates using field-theoretic simulations. *J. Chem. Phys*, 2012; *136*(2): 024903.
46. Oparin, A. I. *The origin of life*; Dover Publ: New York, 1953.
47. Koga, S.; Williams, D. S.; Perriman A. W.; Mann, S. *Nat. Chem*, 2011; *3*(9): 720–724.
48. Dora Tang, T. Y.; Rohaida Che Hak, C.; Thompson, A. J.; Kuimova, M. K.; Williams, D. S.; Perriman, A. W.; Mann, S. *Nat. Chem*, 2014; *6*(6): 527–533.
49. Aumiller, W. M Jr.; Keating, C. D. Phosphorylation-mediated RNA/peptide complex coacervation as a model for intracellular liquid organelles. *Nat Chem*, 2016; *8*(2): 129-37.
50. Yoshizawa, T.; Nozawa, R. S.; Jia, T. Z.; Saio, T.; Mori, E. Biological phase separation: Cell biology meets biophysics. *Biophys. Rev*, 2020; *12*: 519–539.
51. Wang, L.; Song, S.; van Hest, J.; Abdelmohsen, L. K. E. A.; Huang, X.; Sánchez, S. Biomimicry of Cellular Motility and Communication Based on Synthetic Soft-Architectures. *Small*, 2020; *16*(27): 1907680.
52. Oparin, A. I.; Gladilin, K. L. Evolution of self-assembly of probionts. *Biosystems*, 1980; *12*(3-4): 133–145.
53. Fox, S. W. The evolutionary significance of phase-separated microsystems. *Orig. Life*, 1976; *7*(1): 49–68.
54. Te Brinke, E.; Groen, J.; Herrmann, A.; Heus, H. A.; Rivas, G.; Spruijt, E.; Huck, W. T. S. Dissipative adaptation in driven self-assembly leading to self-dividing fibrils. *Nat. Nanotechnol*, 2018; *13*(9): 849–855.
55. Murray, D. T.; Kato, M.; Lin, Y.; Thurber, K. R.; Hung, I.; McKnight, S. L.; Tycko, R. *Cell*, 2017; *171*(3): 615–627.
56. Priftis, D.; Tirrell, M. Phase behaviour and complex coacervation of aqueous polypeptide solutions. *Soft Matter*, 2012; *8*(36): 9396–9405.
57. Sing, C. E.; Perry, S. L. Recent progress in the science of complex coacervation. *Soft Matter*, 2020; *16*(12): 2885–2914.
58. Deng, N.- N. Complex coacervates as artificial membraneless organelles and protocells. *Biomicrofluidics*, 2020; *14*(5): 051301 (1-6).
59. Alberti, S.; Gladfelter, A.; Mittag, T. Considerations and challenges in studying liquid-liquid phase separation and biomolecular condensates. *Cell*, 2019; *176*(3): 419–434.
60. Aguilera-Gomez, A.; Rabouille, C. Membrane-bound organelles versus membrane-less compartments and their control of anabolic pathways in Drosophila. *Dev. Biol*, 2017; *428*(2): 310–317.
61. Banani, S. F.; Lee, H. O.; Hyman, A. A.; Rosen, M. K. Biomolecular condensates: organizers of cellular biochemistry. *Nat. Rev. Mol. Cell Biol*, 2017; *18*(5): 285–298.
62. Gomes, E.; Shorter, J. The molecular language of membraneless organelles. *J. Biol. Chem*, 2019; *294*(18): 7115–7127.
63. Brangwynne, C. P.; Tompa, P.; Pappu, R. V. Polymer physics of intracellular phase transitions. *Nat. Phys*, 2015; *11:* 899–904.
64. Yewdall, N. A; André, A. A. M; Lu, T; Spruijt, E. Coacervates as models of membraneless organelles. *Curr. Opin. Colloid Interface Sci*, 2021; *52*: 101416 (1-14).
65. Lu, T.; Spruijt, E. Multiphase complex coacervate droplets. *J. Am. Chem. Soc*, 2020; *142*(6): 2905-2914.
66. Falahati, H.; Wieschaus, E. Independent active and thermodynamic processes govern the nucleolus assembly *in vivo*. *Proc. Natl. Acad. Sci. U.S.A*, 2017; *114*(6): 1335–1340.
67. Wajnerman, E. S.; Grinberg, W. J.; Tolstogusow, W. B. Investigation of the interaction of proteins with polysaccharides in the water medium. *Kolloid-Z. Poly*, 1972; *250*(10): 945–949.
68. Voorn, M. J. Complex Coacervation. *Ph. D Thesis.* University of Utrecht, Utrecht, The Netherlands, 1956.
69. Flory, P. J. *Principles of Polymer Chemistry*; Cornell University Press: Ithaca, NY, 1953.
70. Debye, P.; Hückel, E. Zur Theorie der Elektrolyte. *Phys. Z.* 1923, *24*, 185–206.
71. McQuarrie, D. A. *Statistical Mechanics*; University Science Books: Sausalito, California, 2000.
72. Tainaka, K. Calculation of Fourth and Fifth Virial Coefficients and Osmotic Pressure of Low Concentrated Polymer Solutions. *J. Phys. Soc. Jpn*, 1979; *47*(1): 282-285.
73. Spruijt, E.; Westphal, A. H.; Borst, J. W.; Cohen Stuart, M. A.; van der Gucht, J. Binodal Compositions of Polyelectrolyte Complexes. *Macromolecules*, 2010; *43*(15): 6476-6484.
74. Abbett, R. L.; Chen, Y.; Schlenoff, J. B. Self-Exchange of Polyelectrolyte in Multilayers: Diffusion as a Function of Salt Concentration and

Temperature. *Macromolecules*, 2021; *54*(20) : 9522-9531.
75. Grosberg, A. Y.; Nguyen, T. T.; Shklovskii, B. I. Colloquium: the physics of charge inversion in chemical and biological systems. *Rev. Mod. Phys*, 2002; *74*(2): 329–345.
76. Zhang, P.; Alsaifi, N. M.; Wu, J.; Wang, Z.-G. Polyelectrolyte Complex Coacervation: Effects of Concentration Asymmetry. *J. Chem. Phys*, 2018; *149*(16): 163303.
77. Lytle, T. K.; Chang, L. W.; Markiewicz, N.; Perry, S. L.; Sing, C. E. Designing Electrostatic Interactions via Polyelectrolyte Monomer Sequence. *ACS Cent Sci*, 2019; *5*(4): 709-718.
78. Priftis, D.; Xia, X.; Margossian, K. O.; Perry, S. L.; Leon, L.; Qin, J.; de Pablo, J. J.; Tirrell, M. Ternary, Tunable Polyelectrolyte Complex Fluids Driven by Complex Coacervation. *Macromolecules*, 2014; *47*(9): 3076-3085.
79. Overbeek, J. T. G.; Voorn, M. J. Phase Separation in Polyelectrolyte Solutions, Theory of Complex Coacervation. *J. Cell. Comp. Physiol*, 1957; *49*(S1): 7-26.
80. Srivastava, S.; Tirrell, M. V. In *Advances in Chemical Physics*; Rice, S. A. & Dinner, A. R. Eds.; John Wiley and Sons: Hoboken, NJ, 2016.
81. Sing, C. E. Development of the modern theory of polymeric complex coacervation, *Adv. Colloid Interface Sci*, 2017; *239:* 2–16.
82. Pothukuchi, R. P.; Prajapat, V. K.; Radhakrishna, M. Charge-Driven Self-Assembly of Polyelectrolyte-Grafted Nanoparticles in Solutions. *Langmuir*, 2021; *37*(41): 12007-12015.
83. Kim, S.; Lee, M.; Lee, W. B.; Choi, S.-H. Ionic-Group Dependence of Polyelectrolyte Coacervate Phase Behavior. *Macromolecules*, 2021; *54*(16): 7572-7581.
84. Zhang, P.; Shen, K.; Alsaifi, N. M.; Wang, Z.-G. Salt Partitioning in Complex Coacervation of Symmetric Polyelectrolytes. *Macromolecules*, 2018; *51*(15): 5586–5593.
85. de Vries, R.; Stuart, M. C. Theory and simulations of macroion complexation *Curr. Opin. Colloid Interface Sci*, 2006; *11*(5): 295–301.
86. van der Gucht, J.; Spruijt, E.; Lemmers, M.; Stuart, M. A. C. Polyelectrolyte complexes: Bulk phases and colloidal systems. *J. Colloid Interface Sci*, 2011; *361*(2): 407–422.
87. Qin, J.; Priftis, D.; Farina, R.; Perry, S. L.; Leon, L.; Whitmer, J.; Hoffmann, K.; Tirrell, M.; de Pablo, J. J. Interfacial Tension of Polyelectrolyte Complex Coacervate Phases. *ACS Macro Lett*, 2014; *3*(6): 565–568.
88. Perry, S. L.; Sing, C. E. PRISM-Based Theory of Complex Coacervation: Excluded Volume versus Chain Correlation. *Macromolecules*, 2015; *48*(14): 5040−5053.
89. Radhakrishna, M.; Basu, K.; Liu, Y.; Shamsi, R.; Perry, S. L.; Sing, C. E. Molecular Connectivity and Correlation Effects on Polymer Coacervation. *Macromolecules*, 2017; *50*(7): 3030-3037.
90. Huang, W.; Liu, D.; Zhu, L.; Yang, S. A Salt Controlled Scalable Approach for Formation of Polyelectrolyte Complex Fiber. *Chin. J. Chem*, 2020; *38*(5): 465-470.
91. Portnov, I. V.; Potemkin, I. I. Interpolyelectrolyte Complex Dissociation vs Polyelectrolyte Desorption from Oppositely Charged Surface upon Salt Addition. *J. Phys. Chem. B*, 2020; *124*(5): 914-920.
92. Zheng, B.; Avni, Y.; Andelman, D.; Podgornik, R. Phase Separation of Polyelectrolytes: The Effect of Charge Regulation. *J. Phys. Chem. B*, 2021; *125*(28): 7863-7870.
93. Li, L.; Srivastava, S.; Andreev, M.; Marciel, A. B.; de Pablo, J. J.; Tirrell, M. V. Phase Behavior and Salt Partitioning in Polyelectrolyte Complex Coacervates. *Macromolecules*, 2018; *51*(8): 2988–2995.
94. Liu, Y.; Momani, B.; Winter, H. H; Perry, S. Rheological characterization of liquid-to-solid transitions in bulk polyelectrolyte complexes. *Soft Matter*, 2017; *13*(40): 7332–7340.
95. Walter, H.; Brooks, D. E. Phase separation in cytoplasm, due to macromolecular crowding, is the basis for microcompartmentation. *FEBS Lett*, 1995; *361*(2–3): 135–139.
96. Priftis, D.; Laugel, N.; Tirrell, M. Thermodynamic Characterization of Polypeptide Complex Coacervation *Langmuir*, 2012; *28*(45): 15947–15957.
97. Fu, J.; Schlenoff, J. B. Driving Forces for Oppositely Charged Polyion Association in Aqueous Solutions: Enthalpic, Entropic, but Not Electrostatic. *J. Am. Chem. Soc*, 2016; *138*(3): 980– 990.
98. Zheng, J.; Gao, Q.; Ge, G.; Wu, J.; Tang, C.-h.; Zhao, M.; Sun, W. Sodium chloride-programmed phase transition of β-conglycinin/lysozyme electrostatic complexes from amorphous precipitates to complex coacervates. *Food Hydrocoll*, 2022; 124(A): 107247.
99. Katchalsky, A.; Alexandrowicz, Z.; Kedem, O. In *Chemical Physics of Ionic Solutions*; Conway, B. E., Barradas, R. G. Eds.; John

Wiley & Sons, Inc.: New York, 1966; p. 295.
100. Kayitmazer, A. B. Thermodynamics of complex coacervation. *Adv. Colloid Interface Sci*, 2017; *239:* 169– 177.
101. Rumyantsev, A. M.; Potemkin. I. I. Explicit description of complexation between oppositely charged polyelectrolytes as an advantage of the random phase approximation over the scaling approach. *Phys. Chem. Chem. Phys*, 2017; *19* (40), 27580-27592.
102. Ermoshkin, A. V.; Olvera de la Cruz, M. A modified random phase approximation of polyelectrolyte solutions. *Macromolecules*, 2003; *36*(20): 7824−7832.
103. Donley, J. P.; Heine, D. R.; Wu, D. T. Range-Optimized Theory of Polyelectrolyte Solutions: Basic Theory and Application to Rod Polymers. *Macromolecules*, 2005; *38*(3): 1007−1020.
104. Kudlay, A.; Olvera de la Cruz, M. Precipitation of oppositely charged polyelectrolytes in salt solutions. *J. Chem. Phys*, 2004; *120*(1): 404−412.
105. Djadoun, S.; Goldberg, R. N.; Morawetz, H. Ternary Systems Containing an Acidic Copolymer, a Basic Copolymer, and a Solvent. 1. Phase Equilibria *Macromolecules*, 1977; *10*(5): 1015–1020.
106. Jha, P. K.; Desai, P. S.; Li, J.; Larson, R. G. pH and Salt Effects on the Associative Phase Separation of Oppositely Charged Polyelectrolytes. *Polymers*, 2014; *6*(5): 1414−1436.
107. Voorn, M. J. Complex coacervation. V. Experiments on the distribution of salts. Comparison of theory and experiment. *Rec. Trav. Chim. Pays-Bas*, 1956; *75*(9): 1021–1030.
108. Veis, A.; Bodor, E. Structure and function of connective skeletal tissue. *Butterworth's*, 1965; 228–35.
109. Veis, A. A review of the early development of the thermodynamics of the complex coacervation phase separation. *Adv. Colloid and Interface Sci*, 2011; *167*(1-2): 2–11.
110. Cooper, C. L.; Dubin, P.L.; Kayitmazer, A.B.; Turksen, S. Polyelectrolyte-protein complexes. *Curr. Opin. Colloid Interface Sci*, 2005; *10*(1-2): 52–78.
111. Flanagan, S. E.; Malanowski, A. J.; Kizilay, E.; Seeman, D.; Dubin, P. L.; Donato-Capel, L.; Bovetto, L.; Schmitt, C. Complex equilibria, speciation, and heteroprotein coacervation of lactoferrin and β-lactoglobulin. *Langmuir*, 2015; *31*(5): 1776–1783.
112. Turgeon, S.L.; Beaulieu, M.; Schmitt, C.; Sanchez, C. Protein–polysaccharide interactions: Phase-ordering kinetics, thermodynamic and structural aspects. *Curr. Opin. Colloid Interface Sci*, 2003; *8*(4-5): 401–414.
113. Boral, S.; Bohidar, H. B. Effect of Ionic Strength on Surface- Selective Patch Binding-Induced Phase Separation and Coacervation in Similarly Charged Gelatin-Agar Molecular Systems. *J. Phys. Chem. B*, 2010; *114*(37): 12027–12035.
114. Wang, X.; Wang, Y. W.; Ruengruglikit, C.; Huang, Q. Effects of Salt Concentration on Formation and Dissociation of β-Lactoglobulin/ Pectin Complexes. *J. Agric. Food Chem*, 2007; *55*(25): 10432–10436.
115. Kumar, A.; Dubin, P. L.; Hernon, M. J.; Li, Y. J.; Jaeger, W. Temperature-Dependent Phase Behavior of Polyelectrolyte-Mixed Micelle Systems. *J. Phys. Chem. B*, 2007; *111*(29): 8468–8476.
116. Zhang R.; Shklovskii. B. I. Phase diagram of aggregation of oppositely charged colloids in salty water. *Phys. Rev. E - Statistical, Nonlinear, and Soft Matter Physics*, 2004; *69*(2): 021909 -1 - 021909 – 10.
117. Wang, Q.; Schlenoff, J. B. The Polyelectrolyte Complex/Coacervate Continuum. *Macromolecules*, 2014; *47*(9): 3108–3116.
118. Perry, S. L.; Li, Y.; Priftis, D.; Leon, L.; Tirrell, M. The effect of salt on the complex coacervation of vinyl polyelectrolytes. *Polymers* , 2014; *6*(6): 1756–1772.
119. Pacalin, N. M.; Leon L.; Tirrell, M. Directing the phase behavior of polyelectrolyte complexes using chiral patterned peptides. *Eur. Phys. J. Spec. Top*, 2016; *225*(8-9): 1805–1815.
120. Hoffmann, K. Q.; Perry, S. L.; Leon, L.; Priftis, D.; Tirrell M.; de Pablo, J. J. A molecular view of the role of chirality in charge-driven polypeptide complexation. *Soft Matter*, 2015; *11*: 1525–1538.
121. Wang, J.; Choi, J. M.; Holehouse, A. S.; Lee, H. O.; Zhang, X.; Jahnel, M.; Maharana, S.; Lemaitre, R.; Pozniakovsky, A.; Drechsel, D.; Poser, I.; Pappu, R. V.; Alberti, S.; Hyman, A. A. A Molecular Grammar Governing the Driving Forces for Phase Separation of Prion-like RNA Binding Proteins. *Cell*, 2018; *174*(3): 688-699.
122. Rubinstein, M.; Dobrynin, A. Solutions of associative polymers. *Trends Polym. Sci*, 1997; *5*(6): 181–186.
123. Semenov, A. N.; Rubinstein, M. Thermoreversible gelation in solutions of associative polymers: 1. Statics. *Macromolecules*, 1998; *31*(4): 1373–1385.

124. Carlsson, F.; Malmsten, M.; Linse, P. Protein-polyelectrolyte cluster formation and redissolution: A Monte Carlo study. *J. Am. Chem. Soc*, 2003; *125*(10): 3140-3149.
125. Schmitt, C.; Sanchez, C.; Despond, S.; Renard, D.; Thomas, F.; Hardy, J. Effect of protein aggregates on the complex coacervation between *β*-lactoglobulin and acacia gum at pH 4.2. *Food Hydrocolloids*, 2000; *14*(4): 403-413.
126. de Kruif, C. G.; Weinbreck, F.; de Vries, R. Complex coacervation of proteins and anionic polysaccharides. *Curr. Opin. Colloid Interface Sci*, 2004; *9*(5): 340– 349.
127. Gummel, J.; Cousin, F.; Bou, F. Counterions Release from Electrostatic Complexes of Polyelectrolytes and Proteins of Opposite Charge: A Direct Measurement. *J. Am. Chem. Soc*, 2007; *129*(18): 5806–5807.
128. Priftis, D.; Megley, K.; Laugel, N.; Tirrell, M. Complex coacervation of poly (ethylene-imine)/polypeptide aqueous solutions: Thermodynamic and rheological characterization. *J. Colloid Interface Sci*, 2013; *398:* 39–50.
129. Aberkane, L.; Jasniewski, J.; Gaiani, C.; Scher, J.; Sanchez, C. Thermodynamic Characterization of Acacia Gum-β-Lactoglobulin Complex Coacervation. *Langmuir*, 2010; *26*(15): 12523–12533.
130. Rathee, V. S.; Sidky, H.; Sikora, B. J.; Whitmer, J. K. Role of Associative Charging in the Entropy–Energy Balance of Polyelectrolyte Complexes. *J. Am. Chem. Soc*, 2018; *140*(45): 15319–15328.
131. Ou, Z.; Muthukumar, M. Entropy and enthalpy of polyelectrolyte complexation: Langevin dynamics simulations. *J. Chem. Phys*, 2006; *124*(15): 154902 (1-11).
132. Elder, R. M.; Emrick, T.; Jayaraman, A. Understanding the Effect of Polylysine Architecture on DNA Binding Using Molecular Dynamics Simulations. *Biomacromolecules*, 2011; *12*(11): 3870–3879.
133. Schmidt-Rohr, K. Expansion Work without the External Pressure, and Thermodynamics in Terms of Quasistatic Irreversible Processes. *J. Chem. Educ*, 2014; *91*(3): 402–409.
134. Record, M. T.; Anderson, C. F.; Lohman, T. M. Thermodynamic analysis of ion effects on the binding and conformational equilibria of proteins and nucleic acids: the roles of ion association or release, screening, and ion effects on water activity. *Q. Rev. Biophys*, 1978; *11*(2): 103–178.
135. Manning, G. S. Limiting Laws and Counterion Condensation in Polyelectrolyte Solutions I. Colligative Properties. *J. Chem. Phys*, 1969; *51*(3): 924–933.
136. Muthukumar, M. In *Molecular Basis of Polymer Networks*; Baumgärtner, A., Picot C. E., Eds.; Springer Proceedings in Physics, Springer: New York, 1989; Vol. 42, p 28.
137. Stapert, H. R.; Nishiyama, N.; Jiang, D. L.; Aida, T.; Kataoka, K. Polyion Complex Micelles Encapsulating Light-Harvesting Ionic Dendrimer Zinc Porphyrins. *Langmuir*, 2000; *16*(21): 8182−8188.
138. Sadman, K.; Wang, Q.; Chen, Y.; Keshavarz, B.; Jiang, Z.; Shull, K. R. Influence of Hydrophobicity on Polyelectrolyte Complexation. *Macromolecules*, 2017; *50*(23): 9417−9426.
139. Dubin, P. L.; Murrell, J. M. Size distribution of complexes formed between PDADMAC and BSA. *Macromolecules*, 1988; *21*(7): 2291- 2293.
140. Xia, J.; Dubin, P. L.; Kim, Y.; Muhoberac, B. B.; Klimkowski, V. J. Electrophoretic and quasi-elastic light scattering of soluble protein-polyelectrolyte complexes. *J. Phys. Chem*, 1993; *97*(17): 4528-4534.
141. Liu, Y.; Winter, H. H.; Perry, S. L. Linear viscoelasticity of complex coacervates. Adv. Colloid and Interface Sci, 2017; 239: 46-60.
142. Shamoun, R. F.; Reisch, A.; Schlenoff, J. B. Extruded Saloplastic Polyelectrolyte Complexes. *Adv. Funct. Mater*, 2012; *22*(9): 1923−1931.
143. Farhat, T. R.; Schlenoff, J. B. Doping-controlled ion diffusion in polyelectrolyte multilayers: mass transport in reluctant exchangers. *J. Am. Chem. Soc*, 2003; *125*(15): 4627−4636.
144. Schlenoff, J. B.; Rmaile, A. H.; Bucur, C. B. Hydration contributions to association in polyelectrolyte multilayers and complexes: visualizing hydrophobicity. *J. Am. Chem. Soc*, 2008; *130*(41): 13589−13597.
145. Jaber, J. A.; Schlenoff, J. B. Mechanical properties of reversibly cross-linked ultrathin polyelectrolyte complexes. *J. Am. Chem. Soc*, 2006; *128*(9): 2940−2947.
146. Dautzenberg, H.; Karibyants, N. Polyelectrolyte complex formation in highly aggregating systems. Effect of salt: response to subsequent addition of NaCl. *Macromol. Chem. Phys*, 1999; *200*(1): 118−125.
147. Dautzenberg, H.; Kriz, J. Response of polyelectrolyte complexes to subsequent addition of salts with different cations. *Langmuir*, 2003; *19*(13): 5204−5211.
148. Tainaka, K. I. Effect of Counterions on Complex Coacervation. *Biopolymers*, 1980; *19*(7): 1289-1298.
149. Burgess, D. J. Practical Analysis of Complex Coacervate Systems. *J. Colloid Interface Sci*, 1990; *140*(1): 227–238.

150. Biesheuvel, P. M.; Stuart, M. A. C. Cylindrical Cell Model for the Electrostatic Free Energy of Polyelectrolyte Complexes. *Langmuir*, 2004; *20*(11): 4764–4770.
151. Weinbreck, F.; de Vries, R.; Schrooyen, P.; de Kruif, C. G. Complex Coacervation of Whey Proteins and Gum Arabic. *Biomacromolecules*, 2003; *4*(2): 293−303.
152. Chollakup, R.; Smitthipong, W.; Eisenbach, C. D.; Tirrell, M. Phase Behavior and Coacervation of Aqueous Poly (acrylic acid)− Poly(allylamine) Solutions. *Macromolecules*, 2010; *43*(5): 2518−2528.
153. Veis, A. *Biological Poly Electrolytes;* Marcel Dekker: New York, 1970; Chap. 4.
154. Chollakup, R.; Beck, J. B.; Dirnberger, K.; Tirrell, M.; Eisenbach, C. D. Polyelectrolyte molecular weight and salt effects on the phase behavior and coacervation of aqueous solutions of poly(acrylic acid) sodium salt and poly(allylamine) hydrochloride. *Macromolecules*, 2013; *46*(6): 2376−2390.
155. Bungenberg de Jong, H. G. Morphology of coacervates. In *Colloid Science*; Kruyt, H. R., Ed.; Elsevier Publishing: Amsterdam, The Netherlands, 1949c; Vol. II, Chapter XI, pp 433-480.
156. Yamakawa, H. *Modern Theory of Polymer Solution;* Harper and Row: New York, 1971; Chap. 7.
157. Xia, J.; Dubin, P. L. In *Macromolecular Complexes in Chemistry and Biology*; Dubin, P. L., Bock, J., Davis, R., Schulz, D. N., Thies, C., Eds.; Springer-Verlag: Berlin, 1994; p 247.
158. Schmitt, C.; Sanchez, C.; Desobry-Banon, S.; Hardy, J. Structure and technofunctional properties of protein-polysaccharide complexes: a review. *Crit. Rev. Food Sci. Nutr*, 1998; *38*(8): 689-753.
159. Doublier, J. L.; Garnier, C.; Renard, D.; Sanchez, C. Protein–polysaccharide interactions. *Curr. Opin. Colloid Interface Sci*, 2000; *5*(3): 202-214.
160. Rumyantsev, A. M.; Zhulina, E. B.; Borisov, O. V. Complex Coacervate of Weakly Charged Polyelectrolytes: Diagram of States. *Macromolecules*, 2018; *51*(10): 3788−3801.
161. Sato, H.; Nakajima, A. Complex Coacervation in Sulfated Polyvinyl Alcohol-Aminoacetalyzed Polyvinyl Alcohol System - II. Formation of Coacervate Droplets. *Colloid Polym. Sci*, 1974; *252:* 944−948.
162. Sato, H.; Nakajima, A. Complex Coacervation in Sulfated Polyvinyl Alcohol-Aminoacetalyzed Polyvinyl Alcohol System - I. Conditions for Complex Coacervation. *Colloid Polym. Sci*, 1974; *252:* 294−297.
163. Friedowitz, S.; Salehi, A.; Larson, R. G.; Qin, J. Role of Electrostatic Correlations in Polyelectrolyte Charge Association. *J. Chem. Phys*, 2018; *149*(16): 163335.
164. Salehi, A.; Larson, R. G. A Molecular Thermodynamic Model of Complexation in Mixtures of Oppositely Charged Polyelectrolytes with Explicit Account of Charge Association/Dissociation. *Macromolecules*, 2016; *49*(24): 9706−9719.
165. Sun, J.; Perry, S. L.; Schiffman, J. D. Electrospinning Nanofibers from Chitosan/Hyaluronic Acid Complex Coacervates. *Biomacromolecules*, 2019; *20*(11): 4191−4198.
166. Tabandeh, S.; Leon, L. Engineering Peptide-Based Polyelectrolyte Complexes with Increased Hydrophobicity. *Molecules*, 2019; *24*(5): 868 (1 – 17).
167. Lou, J.; Friedowitz, S.; Qin, J.; Xia, Y. Tunable Coacervation of Well-Defined Homologous Polyanions and Polycations by Local Polarity. *ACS Cent. Sci*, 2019; *5*(3): 549−557.
168. Huang, J.; Morin, F. J.; Laaser, J. E. Charge-Density-Dominated Phase Behavior and Viscoelasticity of Polyelectrolyte Complex Coacervates. *Macromolecules*, 2019; *52*(13): 4957−4967.
169. Popov, Y. O.; Lee, J.; Fredrickson, G. H. Field-theoretic simulations of polyelectrolyte complexation. *J. Polym. Sci., Part B: Polym. Phys*, 2007; *45*(24): 3223–3230.
170. Lee, J.; Popov, Y. O.; Fredrickson, G. H. Complex coacervation: A field theoretic simulation study of polyelectrolyte complexation. *J. Chem. Phys*, 2008; *128*(22): 224908-1–224908-13.
171. Ali, S.; Bleuel, M.; Prabhu, V. M. Lower Critical Solution Temperature in Polyelectrolyte Complex Coacervates. *ACS MacroLett*, 2019; *8*(3): 289−293.
172. Adhikari, S.; Prabhu, V. M.; Muthukumar, M. Lower Critical Solution Temperature Behavior in Polyelectrolyte Complex Coacervates. *Macromolecules*, 2019; *52*(18): 6998−7004.
173. Pak, C. W.; Kosno, M.; Holehouse, A. S.; Padrick, S. B.; Mittal, A.; Ali, R. Sequence determinants of intracellular phase separation by complex coacervation of a disordered protein. *Mol. Cell*, 2016; *63*(1): 72–85.
174. Dignon, G. L.; Zheng, W.; Kim, Y. C.; Best, R. B.; Mittal, J. Sequence determinants of protein phase behavior from a coarse-grained model. *PLoS Comput. Biol*, 2018; *14*(1): e1005941 (1-23).
175. Langdon, E. M.; Qiu, Y.; Ghanbari Niaki, A.; McLaughlin, G. A.; Weidmann, C. A.;

Gerbich, T. M. mRNA structure determines specificity of a polyQ- driven phase separation. *Science*, 2018; *360*(6391): 922–927.
176. Shammas, S.L.; Knowles, T.P.; Baldwin, A.J.; Macphee, C.E.; Welland, M.E.; Dobson, C.M.; Devlin, G.L. Perturbation of the stability of amyloid fibrils through alteration of electrostatic interactions. *Biophys. J.*, 2011; *100*(11): 2783–2791.
177. Chang, L. W.; Lytle, T. K.; Radhakrishna, M.; Madinya, J. J.; Vélez, J.; Sing, C. E. Sequence and entropy-based control of complex coacervates. *Nat. Commun*, 2017; *8*(1): 1273 (1 – 8).
178. Delaney, K. T.; Fredrickson, G. H. Theory of polyelectrolyte complexation—Complex coacervates are self-coacervates. *J. Chem. Phys*, 2017; *146*(22): 224902.
179. Zhou, H.-X.; Nguemaha, V.; Mazarakos, K.; Qin, S. Why do disordered and structured proteins behave differently in phase separation? *Trends Biochem. Sci*, 2018; *43*(7): 499–516.
180. Flory, P. J. Statistical Thermodynamics of Mixtures of Rodlike Particles. 5. Mixtures with Random Coils. *Macromolecules*, 1978; *11*(6): 1138–1141.
181. Eisenbach, C. D.; Hofmann, J.; Goeldel, A.; Noolandi, J.; Shi, A. C. Miscibility of Rigid - Rod and Random - Coil Macromolecules Through Acid – Base Interactions. *Macromolecules*, 1999; *32*(5): 1463–1470.
182. Qin, J.; De Pablo, J. J. Criticality and Connectivity in Macromolecular Charge Complexation. *Macromolecules*, 2016; *49*(22): 8789–8800.
183. Shen, K.; Wang, Z. G. Electrostatic correlations and the polyelectrolyte self energy. *J. Chem. Phys*, 2017; *146*(8): 084901.
184. Castelnovo, M.; Joanny J. F. Complexation between oppositely charged polyelectrolytes: beyond the Random Phase Approximation. *Eur. Phys. J. E*, 2001; *6*(5): 377–86.
185. Borue, V. Y.; Erukhimovich, I. Y. A statistical theory of weakly charged polyelectrolytes: Fluctuations, equation of state, and microphase separation. *Macromolecules*, 1988; *21*(11): 3240–3249.
186. Borue, V. Y.; Erukhimovich, I. Y. A Statistical-Theory of Globular Polyelectrolyte Complexes. *Macromolecules*, 1990; *23*(15): 3625–3632.
187. Kudlay, A.; Ermoshkin, A. V.; Olvera de la Cruz, M. Complexation of Oppositely Charged Polyelectrolytes: Effect of Ion Pair Formation. *Macro-molecules*, 2004; *37*(24): 9231–9241.
188. Shusharina, N. P.; Zhulina, E. B.; Dobrynin, A. V.; Rubinstein, M. Scaling Theory of Diblock Polyampholyte Solutions. *Macromolecules*, 2005; *38*(21): 8870–8881.
189. Castelnovo, M.; Joanny, J. F. Phase Diagram of Diblock Polyampholyte Solutions. *Macromolecules*, 2002; *35*(11): 4531–4538.
190. Netz R. R.; Orland, H. Beyond Poisson–Boltzmann: Fluctuation effects and correlation functions. *Eur. Phys. J. E*, 2000; *1*(2): 203–214.
191. Solis, F. J.; de la Cruz, M. O. Collapse of flexible polyelectrolytes in multivalent salt solutions. *J. Chem. Phys*, 2000; *112*(4): 2030–2035.
192. Shklovskii, B. I. Wigner crystal model of counterion induced bundle formation of rod-like polyelectrolytes. *Phys. Rev. Lett*, 1999; *82*(16): 3268–3271.
193. de la Cruz, M. O.; Belloni, L.; Delsanti, M.; Dalbiez, J. P.; Spalla, O.; Drifford, M. Precipitation of highly-charged polyelectrolyte solutions in the presence of multivalent salts. *J. Chem. Phys*, 1995; *103*(13): 5781–5791.
194. Raspaud, E.; Olvera de la Cruz, M.; Sikorav, J. L.; Livolant, F. Precipitation of DNA by polyamines: a polyelectrolyte behavior. *Biophys. J*, 1998; *74*(1): 381–393.
195. Nyquist, R. M, Ha, B. Y, Liu, A. J. Counterion condensation in solutions of rigid polyelectrolytes. *Macromolecules*, 1999; *32*(10): 3481–3487.
196. Muthukumar M. Theory of counter-ion condensation on flexible polyelectrolytes: adsorption mechanism. *J. Chem. Phys*, 2004; *120*(19): 9343–9350.
197. Liu, S; Muthukumar, M. Langevin dynamics simulation of counterion distribution around isolated flexible polyelectrolyte chains. *J. Chem. Phys*, 2002; *116*(22): 9975-9982.
198. Muthukumar, M.; Hua, J.; Kundagrami, A. Charge regularization in phase separating polyelectrolyte solutions. *J. Chem. Phys*, 2010; *132*(8): 084901.
199. Audus, D. J.; Gopez, J. D.; Krogstad, D. V.; Lynd, N. A.; Kramer, E. J.; Hawker, C. J.; Fredrickson, G. H. Phase behavior of electrostatically complexed polyelectrolyte gels using an embedded fluctuation model. *Soft Matter*, 2015; *11*(6): 1214–1225.
200. Lytle T. K.; Radhakrishna, M.; Sing, C. E. High charge density coacervate assembly via hybrid Monte Carlo single chain in mean field theory. *Macromolecules*, 2016; *49*(24): 9693–9705.
201. Ong, G. M. C.; Sing, C. E. Mapping the phase behavior of coacervate-driven self-assembly in diblock copolyelectrolytes,”

Soft Matter, 2019; *15*(25): 5116–5127.
202. Lytle, T. K.; Sing, C. E. Transfer matrix theory of polymer complex coacervation. *Soft Matter*, 2017; *13*(39): 7001–7012.
203. Krogstad, D. V.; Lynd, N. A.; Miyajima, D.; Gopez, J.; Hawker, C. J.; Kramer, E. J.; Tirrell, M. V. Structural evolution of polyelectrolyte complexcore micelles and ordered-phase bulk materials. *Macromolecules*, 2014; *47*(22): 8026–8032.
204. Sing, C. E. Micro- to macro - phase separation transition in sequence-defined coacervates. *J. Chem. Phys*, 2020; *152*(2): 024902.
205. Decher, G. Layered nanoarchitectures via directed assembly of anionic and cationic molecules. In *Comprehensive supramolecular chemistry*, Sauvage, J. P., Hosseini, M. W., Eds.; Pergamon Press: Oxford, 1996; Vol. 9: Templating, self-assembly and self-organization, Chapter, 14: 507–528.
206. Yoo, D.; Shiratori, S. S.; Rubner, M. F. Controlling Bilayer Composition and Surface Wettability of Sequentially Adsorbed Multilayers of Weak Polyelectrolytes. *Macromolecules*, 1998; *31*(13): 4309–4318.
207. Shiratori, S. S.; Rubner, M. F. pH-Dependent Thickness Behavior of Sequentially Adsorbed Layers of Weak Polyelectrolytes. *Macromolecules*, 2000; *33*(11): 4213– 4219.
208. Decher, G. In *The Polymeric Materials Encyclopedia: Synthesis, Properties, and Applications*; Salamone, J. C., Ed.; CRC Press: Boca Raton, FL, 1996; 6: 4540.
209. Choi, J.; Rubner, M. F. Influence of the degree of ionization on weak polyelectrolyte multilayer assembly. *Macromolecules*, 2005; *38*(1): 116–124.
210. Sukhishvili, S. A.; Kharlampieva, E.; Izumrudov, V. Where Polyelectrolyte Multilayers and Polyelectrolyte Complexes Meet *Macromolecules*, 2006; *39*(26): 8873–8881.
211. Decher, G.; Hong, J. Buildup of ultrathin multilayer films by a self-assembly process, 1 consecutive adsorption of anionic and cationic bipolar amphiphiles on charged surfaces. *Makromol. Chem. Macromol. Symp*, 1991; *46(*1): 321–327.
212. Decher, G.; Hong, J. Buildup of Ultrathin Multilayer Films by a Self-Assembly Process: II. Consecutive Adsorption of Anionic and Cationic Bipolar Amphiphiles and Polyelectrolytes on Charged Surfaces. *Ber. Bunsen. Phys. Chem*, 1991; *95*(11): 1430–1434.
213. G. Decher, Fuzzy Nanoassemblies: Toward Layered Polymeric Multicomposites. *Science*, 1997; *277*(5330): 1232–1237.
214. Kovacevic, D.; van der Burgh, S.; de Keizer, A.; Cohen Stuart, M. A. Kinetics of Formation and Dissolution of Weak Polyelectrolyte Multilayers: Role of Salt and Free Polyions. *Langmuir*, 2002; *18*(14): 5607–5612.
215. Lindhoud, S.; Cohen Stuart, M. A. Relaxation Phenomena During Polyelectrolyte Complex Formation. In, *Polyelectrolyte Complexes in the Dispersed and Solid State I: Principles and Theory*, Müller, M., Ed., Springer Nature Switzerland AG: Switzerland, 2013; Vol. 255: Advances in Polymer Science, pp. 139-172.
216. Salehi, A.; Desai, P.; Li, J.; Steele, C. A.; Larson, R. G. Relationship between Polyelectrolyte Bulk Complexation and Kinetics of Their Layer-by-Layer Assembly. *Macromolecules*, 2015; *48*(2): 400–409.
217. Piacentini E. Coacervation. In: *Encyclopedia of Membranes*; Drioli, E., Giorno, L., Eds.; Springer: Berlin, Heidelberg, 2015. https://doi.org/10.1007/978-3-642-40872-4_2019-1.
218. Poon, W. C. K. The Physics of a Model Colloid-Polymer Mixture. *J. Phys.: Condens. Matter*, 2002; *14*(33): R859–R880.
219. Groenewold, J.; Kegel, W. K. Anomalously Large Equilibrium Clusters of Colloids. *J. Phys. Chem. B*, 2001; *105*(47): 11702–11709.
220. Lu, P. J.; Conrad, J. C.; Wyss, H. M.; Schofield, A. B.; Weitz, D. A. Fluids of Clusters in Attractive Colloids. *Phys. Rev. Lett*, 2006; *96*(2): 028306.
221. Sedgwick, H.; Egelhaaf, S. U.; Poon, W. C. K. Clusters and Gels in Systems of Sticky Particles. *J. Phys.: Condens. Matter*, 2004; *16*(42): S4913–S4922.
222. Stradner, A.; Sedgwick, H.; Cardinaux, F.; Poon, W. C. K.; Egelhaaf, S. U.; Schurtenberger, P. Equilibrium Cluster Formation in Concentrated Protein Solutions and Colloids. *Nature*, 2004; *432*(7016): 492–495.
223. Campbell, A. I.; Anderson, V. J.; vanDuijneveldt, J. S.; Bartlett, P. Dynamical Arrest in Attractive Colloids: The Effect of Long-Range Repulsion. *Phys. Rev. Lett*, 2005; *94*(20): 208301.
224. Gibson, H. M.; Wilding, N. B. Metastable Liquid-Liquid Coexistence and Density Anomalies in a Core-Softened Fluid. *Phys. Rev. E*, 2006; *73*(6): 061507.
225. Archer, A. J.; Wilding, N. B. Phase Behavior of a Fluid with Competing

Attractive and Repulsive Interactions. *Phys. Rev. E*, 2007; *76*(3): 031501.
226. Leisner, D.; Imae, T. Interpolyelectrolyte Complex and Coacervate Formation of Poly (glutamic acid) with a Dendrimer Studied by Light Scattering and SAXS. *J. Phys. Chem. B*, 2003; *107*(32): 8078–8087.
227. Schmidt, I.; Cousin, F.; Huchon, C.; Boue, F.; Axelos, M. A. V. Spatial Structure and Composition of Polysaccharide-Protein Complexes from Small Angle Neutron Scattering. *Biomacromolecules*, 2009; *10*(6): 1346–1357.
228. Cousin, F.; Gummel, J.; Clemens, D.; Grillo, I.; Boue, F. Multiple Scale Reorganization of Electrostatic Complexes of Poly-(styrenesulfonate) and Lysozyme. *Langmuir*, 2010; *26*(10): 7078–7085.
229. Gummel, J.; Boue, F.; Clemens, D.; Cousin, F. Finite Size and Inner Structure Controlled by Electrostatic Screening in Globular Complexes of Proteins and Polyelectrolytes. *Soft Matter*, 2008; *4*(8): 1653–1664.
230. Park, J. M.; Muhoberac, B. B.; Dubin, P. L.; Xia, J. Effects of protein charge heterogeneity in protein-polyelectrolyte complexation. *Macromolecules*, 1992; *25*(1): 290-295.
231. Mattison, K. W.; Brittain, I. J.; Dubin, P. L. Protein-Polyelectrolyte Phase Boundaries. *Biotechnol. Prog*, 1995; *11*(6): 632-637.
232. Mattison, K. W.; Dubin, P. L.; Brittain, I. J. Complex Formation between Bovine Serum Albumin and Strong Polyelectrolytes: Effect of Polymer Charge Density. *J. Phys. Chem. B*, 1998; *102*(19): 3830-3836.
233. Xia, J.; Dubin, P. L.; Dautzenberg H. Complexation of proteins with a strong polyanion in an aqueous salt-free system. *Langmuir*, 1993; *9*(8): 2015- 2019.
234. Girard, M.; Turgeon, S. L.; Gauthier, S. F. Quantification of the Interactions between β – Lactoglobulin and Pectin through Capillary Electrophoresis Analysis. *J. Agric. Food Chem*. 2003, *51* (20), 6043-6049.
235. Weinbreck, F.; Nieuwenhuijse, H.; Robijn, G. W.; de Kruif, C. G. Complex formation of whey proteins: Exocellular polysaccharide EPS B40. *Langmuir*, 2003; *19*(22): 9404-9410.
236. Girard, M.; Turgeon, L.; Gauthier, S. F. Interbiopolymer complexing between β-lactoglobulin and low- and high -methylated pectin measured by potentiometric titration and ultrafiltration. *Food Hydrocolloids*, 2002; *16*(6): 585-591.
237. Menger, F. M.; Seredyuk, V. A.; Caran K. L.; Apkarian, R. P. A Sponge Morphology in an Elementary Coacervate. *Langmuir*, 2000; *16*(24): 9113–9116.
238. Tribet, C.; Porcar, I.; Bonnefont, P. A.; Audebert, R. Association between hydrophobically modified polyanions and negatively charged bovine serum albumin. *J. Phys. Chem. B*, 1998; *102*(7): 1327-1333.
239. Tsuchida, E. Formation of Polyelectrolyte Complexes and Their Structures. *J. Mol. Sci.-Pure Appl. Chem*, 1994; *A31*(1): 1-15.
240. Kaibara, K.; Watanabe, T.; Miyakawa, K. Characterizations of critical processes in liquid–liquid phase separation of the elastomeric protein–water system: Microscopic observations and light scattering measurements. *Biopolymers*, 2000; *53*(5): 369-379.
241. Viehof, A.; Lamprecht, A. Oral Delivery of Low Molecular Weight Heparin by Polyaminomethacrylate Coacervates. *Pharm. Res*, 2013; *30*(8): 1990–1998.
242. Pergushov, D. V.; Muller, A. H. E.; Schacher, F. H. Micellar interpolyelectrolyte complexes. *Chem. Soc. Rev*, 2012; *41*(21): 6888−6901.
243. Pittella, F.; Kataoka, K. Polymeric Micelles for siDNA Delivery. In *Advances in Delivery Science and Technology*; Springer: Berlin, 2012.
244. Donati, I.; Feresini, M.; Travan, A.; Marsich, E.; Lapasin, R.; Paoletti, S. Polysaccharide-Based polyanion--polycation--polyanion Ternary Systems. A Preliminary Analysis of Interpolyelectrolyte Interactions in Dilute Solutions. *Biomacromolecules*, 2011; *12*(11*)*: 4044−4056.
245. Donati, I.; Borgogna, M.; Turello, E.; Cesaro, A.; Paoletti, S. Tuning Supramolecular Structuring at the Nanoscale Level: Non- stoichiometric Soluble Complexes in Dilute Mixed Solutions of Alginate and Lactose-Modified Chitosan (Chitlac). *Biomacromolecules*, 2007; *8*(5): 1471−1479.
246. Deng, X.; Cao, M.; Zhang, J.; Hu, K.; Yin, Z.; Zhou, Z.; Xiao, X.; Yang, Y.; Sheng, W.; Wu, Y.; Zeng, Y. Hyaluronic acid-chitosan nanoparticles for co- delivery of MiR-34a and doxorubicin in therapy against triple negative breast cancer. *Biomaterials*, 2014; *35*(14): 4333−4344.
247. de la Fuente, M.; Seijo, B.; Alonso, M. J. Novel hyaluronic acid- chitosan nanoparticles for ocular gene therapy. *Invest. Ophthalmol. Visual Sci*, 2008; *49*(5): 2016−2024.
248. Sacco, P.; Decleva, E.; Tentor, F.; Menegazzi, R.; Borgogna, M.; Paoletti, S.; Kristiansen, K. A.; Vårum, K. M.; Marsich,

E. Butyrate - Loaded Chitosan/Hyaluronan Nanoparticles: A Suitable Tool for Sustained Inhibition of ROS Release by Activated Neutrophils. *Macromol. Biosci*, 2017; *17*(11): 1700214.
249. Xu, A. Y.; Melton, L. D.; Ryan, T. M.; Mata, J. P.; Rekas, A.; Williams, M. A. K.; McGillivray, D. J. Effects of polysaccharide charge pattern on the microstructures of β-lactoglobulin-pectin complex coacervates, studied by SAXS and SANS, *Food Hydrocoll*, 2018; 77: 952-963.
250. Black, K. A.; Priftis, D.; Perry, S. L.; Yip, J.; Byun, W. Y.; Tirrell, M. Protein encapsulation via polypeptide complex coacervation. *ACS Macro Lett*, 2014; *3*(10): 1088−1091.
251. Zhou, L.; Shi, H.; Li, Z.; He, C. Recent Advances in Complex Coacervation Design from Macromolecular Assemblies and Emerging Applications. *Macromol. Rapid Commun*, 2020; *41*(21): 2000149.
252. Stewart, R. J, Wang, C. S. Adaptation of caddisfly larval silks to aquatic habitats by phosphorylation of h-fibroin serines. *Biomacromolecules*, 2010; *11*(4): 969–974.
253. Lawrence, P.G.; Lapitsky, Y. Ionically Cross-linked poly (allylamine) as a stimulus-responsive underwater adhesive: Ionic strength and pH effects. *Langmuir*, 2015; *31*(4): 1564–1574.
254. Narayanan, A.; Menefee, J. R.; Liu, Q.; Dhinojwala, A.; Joy, A. Lower Critical Solution Temperature-Driven Self-Coacervation of Nonionic Polyester Underwater Adhesives. *ACS Nano*, 2020, *14*(7): 8359-8367.
255. Xu, Y.; Mazzawi, M.; Chen, K.; Sun, L.; Dubin, P. L. Protein purification by polyelectrolyte coacervation: influence of protein charge anisotropy on selectivity. *Biomacromolecules*, 2011; *12*(5): 1512–1522.
256. Gan, Z.; Zhang, T.; Liu, Y.; Wu, D. Temperature-Triggered Enzyme Immobilization and Release Based on Cross-Linked Gelatin Nanoparticles. *PLoS One*, 2012; *7*(10): e47154 (1-10).
257. Gruber, J. V. Polyquaternium-10: Cornerstone of a Personal Care Revolution. *J. Cosmet. Sci*, 2009; *60*(3): 385–386.
258. Hernández-Fernández, M. Á.; García-Pinilla, S.; Ocampo-Salinas, O. I.; Gutiérrez-López, G. F.; Hernández-Sánchez, H.; Cornejo-Mazón, M.; de Jesús Perea-Flores, M.; Dávila-Ortiz, G. Microencapsulation of Vanilla Oleoresin (V. planifolia Andrews) by Complex Coacervation and Spray Drying: Physicochemical and Microstructural Characterization. *Foods*, 2020; *9*(10): 1375 (1- 17).
259. Lv, Y.; Yang, F.; Li, X. Y.; Zhang X. M.; and Abbas, S. Formation of heat-resistant nanocapsules of jasmine essential oil via gelatin/gum arabic based complex coacervation. *Food Hydrocoll*, 2014; *35:* 305–314.
260. Chen, M. J.; Liu, J. Y.; Liu, Y. J.; Guo, C.; Yang, Z. H.; Wu, H. Preparation and characterization of alginate–*N*-2-hydroxypropyl trimethyl ammonium chloride chitosan microcapsules loaded with patchouli oil. *RSC Adv*, 2015; *5*(19): 14522–14530.
261. Shao, H.; Bachus, K. N.; Stewart, R. J. A water-borne adhesive modeled after the sandcastle glue of P. californica. *Macromol. Biosci*, 2009; *9*(5): 464–471.
262. Schmitt, C.; Turgeon, S. L. Protein/ polysaccharide complexes and coacervates in food systems. *Adv. Colloid Interface Sci*, 2011; *167*(1-2): 63–70.
263. Yin, P. P.; Wu, G.; Dai, R. Y.; Qin, W. L.; Wang M.; Chen, H. Z. Fine encapsulation of dual-particle electronic ink by incorporating block copolymer for electrophoretic display application. *J. Colloid Interface Sci*, 2012; *388*(1): 67–73.
264. Stevens, M. J.; Steren, R. E.; Hlady,V.; Stewart, R. J. Multiscale Structure of the Underwater Adhesive of Phragmatopoma californica: A Nanostructured Latex with a Steep Microporosity Gradient. *Langmuir*, 2007; *23*(9): 5045–5049.
265. Nakashima, K. K.; Vibhute, M. A.; Spruijt, E. Biomolecular Chemistry in Liquid Phase Separated Compartments. *Front. Mol. Biosci*, 2019; *6*: 21 (1-9).
266. Blocher McTigue, W. C.; Perry, S. L. Design rules for encapsulating proteins into complex coacervates. *Soft Matter*, 2019; *15*(15): 3089–3103.
267. Williams, D. S.; Koga, S.; Hak, C. R. C.; Majrekar, A.; Patil, A.J.; Perriman, A. W.; Mann, S. Polymer/Nucleotide Droplets as Bio-Inspired Functional Micro-Compartments. *Soft Matter*, 2012; *8*(22): 6004−6014.
268. Tang, T.-Y. D.; Antognozzi, M.; Vicary, J. A.; Perriman, A. W.; Mann, S. Small-Molecule Uptake in Membrane-Free Peptide/Nucleotide Protocells. *Soft Matter*, 2013; *9*(31): 7647−7656.
269. Drobot, B.; Iglesias-Artola, J. M.; Le Vay, K.; Mayr, V.; Kar, M.; Kreysing, M.; Mutschler, H.; Tang, T.-Y. D. Compartmentalised RNA Catalysis in Membrane-Free Coacervate Protocells. *Nat. Commun*, 2018; *9*(1): 3643 (1-9).

270. Priftis, D.; Farina, R.; Tirrell, M. Interfacial Energy of Polypeptide Complex Coacervates Measured via Capillary Adhesion. *Langmuir*, 2012; *28*(23): 8721−8729.
271. Spruijt, E.; Sprakel, J.; Cohen Stuart, M. A.; van der Gucht, J. Interfacial tension between a complex coacervate phase and its coexisting aqueous phase. *Soft Matter*, 2010; *6*(1): 172−178.
272. Yeo, Y.; Bellas, E.; Firestone, W.; Langer, R.; Kohane, D. S. Complex Coacervates for Thermally Sensitive Controlled Release of Flavor Compounds. *J. Agric. Food Chem*, 2005; *53*(19): 7518-7525.
273. Wang, B.; Akanbi, T. O.; Agyei, D.; Holland, B. J.; Barrow, C. J. Coacervation Technique as an Encapsulation and Delivery Tool for Hydrophobic Biofunctional Compounds. In *Role of Materials Science in Food Bioengineering*, Grumezescu, A., Holban, A., Eds.; Elsevier Publishing: Amsterdam, The Netherlands, 2018; Chapter 7, pp 235-261.
274. Neitzel, A. E.; Fang, Y. N.; Yu, B.; Rumyantsev, A. M.; de Pablo, J. J.; and Tirrell, M. V. Polyelectrolyte Complex Coacervation across a Broad Range of Charge Densities. *Macromolecules*, 2021; *54*(14): 6878-6890.
275. Blocher McTigue, W. C.; Perry, S. L. Complex Coacervate-Based Materials for Biomedicine. *WIREs Nanomed Nanobiotechnol*, 2017; 9(4): e1442.
276. Chen, W. C. W.; Lee, B. G.; Park, D. W.; Kim, K.; Chu, H.; Kim, K.; Huard, J.; Wang, Y. Controlled dual delivery of fibroblast growth factor-2 and Interleukin-10 by heparin-based coacervate synergistically enhances ischemic heart repair. *Biomaterials*, 2015; *72*(c): 138–151.
277. Knaapila, M.; Costa, T.; Garamus, V. M.; Kraft, M.; Drechsler, M.; Scherf, U.; Burrows, H. D. Polyelectrolyte complexes of a cationic all conjugated fluorene–thiophene diblock copolymer with aqueous DNA. *J. Phys. Chem, B*, 2015; *119*(7): 3231–3241.
278. Winslow, B. D.; Shao, H.; Stewart, R. J.; Tresco, P. A. Biocompatibility of adhesive complex coacervates modeled after the sandcastle glue of Phragmatopoma californica for craniofacial reconstruction. *Biomaterials*, 2010; *31*(36): 9373–9381.
279. Winkler, S. M.; Harrison, M. R.; Messersmith, P. B. Biomaterials in fetal surgery. *Biomater. Sci.* 2019, *7* (8), 3092 – 3109.
280. Johnson, N. R.; Ambe, T.; Wang, Y. Lysine-based polycation: heparin coacervate for controlled protein delivery. *Acta Biomater*, 2014; *10*(1): 40–46.
281. Rauck, B. M.; Novosat, T. L.; Oudega, M.; Wang, Y. Biocompatibility of a coacervate-based controlled release system for protein delivery to the injured spinal cord. *Acta Biomater*, 2015; *11*(C): 204–211.
282. Wang, Z.; Huang, Y.; He, Y.; Khor, S.; Zhong, X.; Xiao, J.; Ye, Q.; Li, X. Myocardial protection by heparin-based coacervate of FGF10. *Bioact. Mater*, 2021; *6*(7): 1867-1877.
283. Li, H.; Van Herck, S.; Liu, Y.; Hao, Y.; Ding, X.; Nuhn, L.; Zhong, Z.; Combes, F.; Sanders, N. N.; Lienenklaus, S.; Koker, S. D.; David, S. A.; Wang, Y.; De Geest, B. G.; Zhang, Z. Imidazoquinoline-Conjugated Degradable Coacervate Conjugate for Local Cancer Immunotherapy. *ACS Biomater. Sci. Eng*, 2020; *6*(9): 4993-5000.
284. Zern, B. J.; Chu, H.; Wang, Y. Control Growth Factor Release Using a Self-Assembled [polycation:heparin] Complex. *PLoS One*, 2010; *5*(6): e11017 (1-7).
285. Wang, J.; Velders, A. H.; Gianolio, E.; Aime, S.; Vergeldt, F. J.; Van As, H.; Yan, Y.; Drechsler, M.; de Keizer, A.; Cohen Stuart, M. A.; van der Gucht, J. Controlled mixing of lanthanide (iii) ions in coacervate core micelles. *Chem. Commun*, 2013; *49*(36): 3736–3738.
286. Bourouina, N.; Cohen Stuart, M. A.; Kleijn, J. M. Complex coacervate core micelles as diffusional nanoprobes. *Soft Matter*, 2014; *10*(2): 320–331.
287. Bourouina, N.; de Kort, D. W.; Hoeben, F. J. M.; Janssen, H. M.; Van As, H.; Hohlbein, J.; van Duynhoven, J. P. M.; Kleijn, J. M. Complex coacervate core micelles with spectroscopic labels for diffusometric probing of biopolymer networks. *Langmuir*, 2015; *31*(46): 12635–12643.
288. do Amaral, P. H. R.; Andrade, P. L.; de Conto, L. C. Microencapsulation and Its Uses in Food Science and Technology: A Review. In *Microencapsulation - Processes, Technologies and Industrial Applications*, Salaün, F., Ed., IntechOpen: London, September 27th, 2019; DOI: 10.5772/intechopen.81997. (Available from: https://www.intechopen.com/chapters/67432).
289. Kolanowski, W.; Jaworska, D.; Weiâbrodt, J.; Kunz B. Sensory assessment of microencapsulated fish oil powder. *J. Am. Oil Chem.' Soc*, 2007; *84:* 37-45.
290. Comunian, T. A.; Thomazini, M.; Alves, A. J. G.; Matos Junior, F. E.; Carvalho Balieiro, J. C.; Favaro-Trindade, C. S.

Microencapsulation of ascorbic acid by complex coacervation: Protection and controlled release. *Food Res. Int,* 2013; *52*(1): 373-379.

291. Wu, J.; Ye, J.; Zhu, J.; Xiao, Z.; He, C.; Shi, H.; Wang, Y.; Lin, C.; Zhang, H.; Zhao, Y.; Fu, X.; Chen, H.; Li, X.; Li, L.; Zheng, J.; Xiao, J. Heparin-Based Coacervate of FGF2 Improves Dermal Regeneration by Asserting a Synergistic Role with Cell Proliferation and Endogenous Facilitated VEGF for Cutaneous Wound Healing. *Biomacromolecules*, 2016; *17*(6): 2168-2177.
292. McClements, D. J.; Decker, E. A.; Park, Y.; Weiss, J. Structural design principles for delivery of bioactive components in nutraceuticals and functional foods. *Crit. Rev. Food Sci. Nutr,* 2009; *49*(6): 577–606.
293. McClements, D. J.; Li, Y. Structured emulsion-based delivery systems: controlling the digestion and release of lipophilic food components. *Adv. Colloid Interface Sci*, 2010; *159*(2): 213–228.
294. Pippa, N.; Karayianni, M.; Pispas, S.; Demetzos, C. Complexation of Cationic-Neutral Block Polyelectrolyte with Insulin and in Vitro Release Studies. *Int. J. Pharm*, 2015; *491*(1): 136−143.
295. Altenburg, W. J.; Yewdall, N. A.; Vervoort, D. F. M.; vanStevendaal, M. H. M.; Mason, A. F.; van Hest, J. C. M. Programmed Spatial Organization of Biomacromolecules into Discrete, Coacervate - Based Protocells. *Nat. Commun*, 2020; *11*(1): 6282 (1-10).
296. Yewdall, N. A.; Buddingh, B. C.; Altenburg, W. J.; Timmermans, S. B. P. E.; Vervoort, D. F. M.; Abdelmohsen, L. K. E. A.; Mason, A. F.; van Hest, J. C. M. Physicochemical Characterization of Polymer-Stabilized Coacervate Protocells. *Chembiochem*, 2019; *20*(20): 2643−2652.
297. Schuster, B. S.; Reed, E. H.; Parthasarathy, R.; Jahnke, C. N.; Caldwell, R. M.; Bermudez, J. G.; Ramage, H.; Good, M. C.; Hammer, D. A. Controllable Protein Phase Separation and Modular Recruitment to Form Responsive Membraneless Organelles. *Nat. Commun*, 2018; *9*(1): 2985 (1-12).
298. Blocher McTigue, W. C.; Perry, S. L. Protein encapsulation using complex coacervates: what nature has to teach us. *Small*, 2020; *16*(27): 1907671.
299. Awada, H. K.; Long, D. W.; Wang, Z.; Hwang, M. P.; Kim, K.; Wang, Y. A Single Injection of Protein-Loaded Coacervate – Gel Significantly Improves Cardiac Function Post Infarction. *Biomaterials*, 2017; *125:* 65−80.
300. Nolles, A.; Westphal, A. H.; de Hoop, J. A.; Fokkink, R. G.; Kleijn, J. M.; van Berkel, W. J. H.; Borst, J. W.; Westphal, A. H. Encapsulation of GFP in complex coacervate core micelles. *Biomacromolecules*, 2015; *16*(5): 1542–1549.
301. Water, J. J.; Schack, M. M.; Velazquez-Campoy, A.; Maltesen, M. J.; van de Weert, M.; Jorgensen, L. Complex coacervates of hyaluronic acid and lysozyme: effect on protein structure and physical stability. *Eur. J. Pharm. Biopharm*, 2014; *88*(2): 325–331.
302. Kishimura, A.; Koide, A.; Osada, K.; Yamasaki, Y.; Kataoka, K. Encapsulation of myoglobin in PEGylated polyion complex vesicles made from a pair of oppositely charged block ionomers: a physiologically available oxygen carrier. *Angew. Chem. Int. Ed*, 2007; *46*(32): 6085–6088.
303. Vehlow, D.; Schmidt, R.; Gebert, A.; Siebert, M.; Lips, K.; Müller, M. Polyelectrolyte complex based interfacial drug delivery system with controlled loading and improved release performance for bone therapeutics. *Nanomaterials*, 2016; *6*(3): 53–21.
304. Anraku, Y.; Kishimura, A.; Oba, M.; Yamasaki, Y.; Kataoka, K. Spontaneous formation of nanosized unilamellar polyion complex vesicles with tunable size and properties. *J. Am. Chem. Soc*, 2010; *132*(5): 1631–1636.
305. Thomasin, C.; Nam-Tran, H.; Merkle, H. P.; Gander, B. Drug microencapsulation by PLA/PLGA coacervation in the light of thermodynamics. 1. Overview and theoretical considerations. *J. Pharm. Sci*, 1998; *87*(3): 259–268.
306. van Stevendaal, M. H. M. E.; Vasiukas, L.; Yewdall, N. A.; Mason, A. F.; van Hest, J. C. M. Engineering of Biocompatible Coacervate-Based Synthetic Cells. *ACS Appl. Mater. Interfaces*, 2021; *13*(7): 7879-7889.
307. Martin, N.; Li, M.; Mann, S. Selective uptake and refolding of globular proteins in coacervate microdroplets. *Langmuir*, 2016; *32*(23): 5881–5889.
308. Lindhoud, S.; de Vries, R.; Norde, W.; Cohen Stuart, M. A. Structure and Stability of Complex Coacervate Core Micelles with Lysozyme. *Biomacromolecules*, 2007; *8*(7): 2219−2227.
309. Nolles, A.; van Dongen, N. J. E.; Westphal, A. H.; Visser, A. J. W. G.; Kleijn, J. M.; van Berkel, W. J. H.; Borst, J. W. Encapsulation into Complex Coacervate Core Micelles Promotes EGFP Dimerization. *Phys. Chem. Chem. Phys*, 2017; *19*(18): 11380−11389.

310. Fathi, M.; Donsi, F.; McClements, D. J. Protein- based delivery systems for the nanoencapsulation of food ingredients. *Compr. Rev. Food Sci. Food Saf,* 2018; *17*(4): 920-936.
311. Moran, D. P. J.; Halstead, P. W.; Co, L. B. Food Product, U.S. Patent 4, 305, 964. December 15, 1981.
312. Kim, Y. H.; Lee, K.; Li, S. Nucleic Acids Based Polyelectrolyte Complexes: Their Complexation Mechanism, Morphology, and Stability. *Chem. Mater*, 2021; *33*(20): 7923-7943.
313. Oishi, M.; Nagasaki, Y.; Itaka, K.; Nishiyama, N.; Kataoka, K. Lactosylated Poly (Ethylene Glycol)- siRNA Conjugate Through Acid-Labile β-Thiopropionate Linkage to Construct pH-Sensitive Polyion Complex Micelles Achieving Enhanced Gene Silencing in Hepatoma Cells. *J. Am. Chem. Soc*, 2005; *127*(6): 1624−1625.
314. Johnson, N. R.; Wang, Y. Coacervate Delivery Systems for Proteins and Small Molecule Drugs. *Expert Opin. Drug Deliv*, 2014; *11*(12): 1829−1832.
315. Li, R.; Wu, J.; Lin, Z.; Nangle, M. R.; Li, Y.; Cai, P.; Liu, D.; Ye, L.; Xiao, Z.; He, C.; Ye, J.; Zhang, H.; Zhao, Y.; Wang, J.; Li, X.; He, Y.; Ye, Q.; Xiao, J. Single injection of a novel nerve growth factor coacervate improves structural and functional regeneration after sciatic nerve injury in adult rats. *Exp. Neurol*, 2017; *288:* 1-10.
316. Johnson, N. R.; Kruger, M.; Goetsch, K. P.; Zilla, P.; Bezuidenhout, D.; Wang, Y.; Davies, N. H. Coacervate Delivery of Growth Factors Combined with a Degradable Hydrogel Preserves Heart Function After Myocardial Infarction. *ACS Biomater. Sci. Eng*, 2015; *1*(9): 753−759.
317. Turovsky, T.; Khalfin, R.; Kababya, S.; Schmidt, A.; Barenholz,Y.; Danino, D. Celecoxib Encapsulation in β-Casein Micelles: Structure, Interactions, and Conformation. *Langmuir*, 2015; *31*(26): 7183−7192.
318. Rutz, J. K.; Borges, C. D.; Zambiazi, R. C.; Crizel-Cardozo, M. M.; Kuck, L. S.; Noreña, C. P. Z. Microencapsulation of Palm Oil by Complex Coacervation for Application in Food Systems. *Food Chem*, 2017; *220:* 59−66.
319. Muhoza, B.; Xia, S.; Wang, X.; Zhang, X.; Li, Y.; Zhang, S. Microencapsulation of essential oils by complex coacervation method: preparation, thermal stability, release properties and applications. *Crit. Rev. Food Sci. Nutr*, 2020; 1-20.
320. Zhao, M.; Zacharia, N. S. Sequestration of Methylene Blue Into Polyelectrolyte Complex Coacervates. *Macromol. Rapid Commun*, 2016; *37*(15): 1249−1255.
321. Zhao, M.; Eghtesadi, S. A.; Dawadi, M. B.; Wang, C.; Huang, S.; Seymore, A. E.; Vogt, B. D.; Modarelli, D. A.; Liu, T.; Zacharia, N. S. Partitioning of Small Molecules in Hydrogen-Bonding Complex Coacervates of Poly(Acrylic Acid) and Poly(Ethylene Glycol) or Pluronic Block Copolymer. *Macromolecules*, 2017; *50*(10): 3818−3830.
322. Obermeyer, A. C.; Mills, C. E.; Dong, X.-H.; Flores, R. J.; Olsen, B. D. Complex coacervation of supercharged proteins with polyelectrolytes. *Soft Matter*, 2016; *12*(15): 3570–3581.
323. Kapelner, R. A.; Obermeyer, A.C. Ionic polypeptide tags for protein phase separation. *Chem. Sci*, 2019; *10*(9): 2700–2707.
324. Lindhoud, S.; Claessens, M. M. A. E. Accumulation of small protein molecules in a macroscopic complex coacervate. *Soft Matter*, 2015; *12*(2): 408–413.
325. Sarmento, B.; Ribeiro, A; Veiga, F.; Sampaio, P.; Neufeld, R.; Ferreira, D. Alginate/chitosan nanoparticles are effective for oral insulin delivery. *Pharm. Res*, 2007; *24*(12); 2198−2206.
326. Sakiyama-Elbert, S. E.; Hubbell, J. A. Controlled release of nerve growth factor from a heparin-containing fibrin-based cell ingrowth matrix. *J. Control. Release*, 2000; *69*(1): 149–158.
327. Malmo, J.; Sørgård, H.; Vårum, K. M.; Strand, S. P. siRNA delivery with chitosan nanoparticles: Molecular properties favoring efficient gene silencing. *J. Control. Release*, 2012; *158*(2): 261−268.
328. Malmo, J.; Vårum, K. M.; Strand, S. P. Effect of Chitosan Chain Architecture on Gene Delivery: Comparison of Self-Branched and Linear Chitosans. *Biomacromolecules*, 2011; *12*(3): 721−729.
329. Strand, S. P.; Lelu, S.; Reitan, N. K.; de Lange Davies, C.; Artursson, P.; Vårum, K. M. Molecular design of chitosan gene delivery systems with an optimized balance between polyplex stability and polyplex unpacking. *Biomaterials*, 2010; *31*(5): 975−987.
330. Li, Y.; Humphries, B.; Wang, Z.; Lang, S.; Huang, X.; Xiao, H.; Jiang, Y.; Yang, C. Complex Coacervation-Integrated Hybrid Nanoparticles Increasing Plasmid DNA Delivery Efficiency in Vivo. *ACS Appl. Mater. Interfaces*, 2016; *8*(45): 30735−30746.
331. Li, M. F.; Chen, L.; Xu, M. Z.; Zhang, J. L.; Wang, Q.; Zeng, Q. Z.; Wei, X. C.; Yuan, Y. The formation of zein-chitosan complex

coacervated particles: Relationship to encapsulation and controlled release properties. *Int. J. Biol. Macromol*, 2018; *116:* 1232−1239.
332. Ren, X.; Hou, T.; Liang, Q.; Zhang, X.; Hu, D.; Xu, B.; Chen, X.; Chalamaiah, M.; Ma, H. Effects of frequency ultrasound on the properties of zein-chitosan complex coacervation for resveratrol encapsulation. *Food Chem*, 2019; *279:* 223−230.
333. Li, X.; Erni, P.; van der Gucht, J.; de Vries, R. Encapsulation using plant proteins: Thermodynamics and kinetics of wetting for simple zein coacervates. *ACS Appl. Mater. Interfaces*, 2020; *12*(13): 15802−15809.
334. Lee, A. L. Z.; Voo, Z. X.; Chin, W.; Ono, R. J.; Yang, C.; Gao, S.; Hedrick, J. L.; Yang, Y. Y. Injectable coacervate hydrogel for delivery of anticancer drug-loaded nanoparticles in vivo. *ACS Appl. Mater. Interfaces*, 2018; *10*(16): 13274−13282.
335. Huei, G. O. S.; Muniyandy, S.; Sathasivam, T.; Veeramachineni, A. K.; Janarthanan, P. Iron cross-linked carboxymethyl cellulose−gelatin complex coacervate beads for sustained drug delivery. *Chem. Pap*, 2016; *70*(2): 243-252.
336. Chenglong, W.; Shuhan, X.; Jiayi, Y.; Wencai, G.; Guoxiong, X.; Hongjing, D. Dextran-based coacervate nanodroplets as potential gene carriers for efficient cancer therapy. *Carbohydr. Polym*, 2020; *231:* 115687.
337. Barthold, S.; Kletting, S.; Taffner, J.; de Souza Carvalho-Wodarz, C.; Lepeltier, E.; Loretz, B.; Lehr, C. M. Preparation of nanosized coacervates of positive and negative starch derivatives intended for pulmonary delivery of proteins. *J. Mater. Chem. B*, 2016; *4*(13): 2377−2386.
338. Alsharabasy, A. M.; Moghannem, S. A.; El-Mazny, W. N. Physical preparation of alginate/chitosan polyelectrolyte complexes for biomedical applications. *J. Biomater. Appl*, 2016: *30*(7): 1071–1079.
339. Johnson, N. R.; Wang, Y. Controlled delivery of heparin-binding EGF-like growth factor yields fast and comprehensive wound healing. *J. Controlled Release*, 2013; *166*(2): 124–129.
340. Chu, H.; Gao, J.; Chen, C.-W.; Huard, J.; Wang, Y. Injectable fibroblast growth factor-2 coacervate for persistent angiogenesis. *Proc. Natl. Acad. Sci. U. S. A*, 2011; *108*(33): 13444–13449.
341. Chu, H.; Chen, C.-W.; Huard, J.; Wang, Y. The effect of a heparin-based coacervate of fibroblast growth factor-2 on scarring in the infarcted myocardium. *Biomaterials*, 2013; *34*(6): 1747–1756.
342. Lee, K.-W.; Johnson, N. R.; Gao, J.; Wang, Y. Human progenitor cell recruitment via SDF-1α coacervate-laden PGS vascular grafts. *Biomaterials*, 2013; *34*(38): 9877–9885.
343. Li, H.; Johnson, N. R.; Usas, A.; Lu, A.; Poddar, M.; Wang, Y.; Huard, J. Sustained release of bone morphogenetic protein 2 via coacervate improves the osteogenic potential of muscle-derived stem cells. *Stem Cells Transl. Med*, 2013; *2*(9): 667–677.
344. Chu, H.; Johnson, N. R.; Mason, N. S.; Wang, Y. A [polycation:heparin] complex releases growth factors with enhanced bioactivity. *J. Controlled Release*, 2011; *150*(2): 157–163.
345. Moore, K. W.; de Waal Malefyt, R.; Coffman, R. L.; OGarra, A. Interleukin-10 and the interleukin-10 receptor. *Annu. Rev. Immunol*, 2001; *19*(1): 683–765.
346. Lim, Z. W.; Ping, Y.; Miserez, A. Glucose responsive peptide coacervates with high encapsulation efficiency for controlled release of insulin. *Bioconjugate Chem*, 2018; *29*(7): 2176−2180.
347. Sato, T.; Mello, D.; Vasconcelos, L.; Valente, A. J. M.; Borges, A. Chitosan based coacervate polymers for propolis encapsulation: Release and cytotoxicity studies. *Int. J. Mol. Sci*, 2020; *21*(12): 4561.
348. Truong-Le, V. L.; August, J. T.; Leong, K. W. Controlled gene delivery by DNA-gelatin nanospheres. *Hum. Gene. Ther*, 1998; *9:* 1707–1717.
349. Truong-Le, V. L.; Walsh, S. M.; Schweibert, E.; Mao, H.-Q.; Guggino, W. B.; August, J. T.; Leong, K. W. Gene transfer by DNA–gelatin nanospheres. *Arch. Biochem. Biophys*, 1999; *361*(1): 47–56.
350. Leong, K. W.; Mao, H. Q.; Truong-Le, V. L.; Roy, K.; Walsh, S. M.; August, J. T. DNA-polycation nanospheres as non-viral gene delivery vehicles. *J. Controlled Release*, 1998; *53*(1-3): 183–193.
351. Ozbas-Turan, S.; Aral, C.; Kabasakal, L.; Keyer-Uysal, M.; Akbuga, J. Co-encapsulation of two plasmids in chitosan microspheres as a non-viral gene delivery vehicle. *J. Pharm. Pharm. Sci*, 2003; *6*(1): 27–32.
352. Voets, I. K.; de Keizer, A.; Cohen Stuart, M. A. Complex coacervate core micelles. *Adv. Colloid Interface Sci*, 2009; *147-148* (C), 300–318.
353. Kuo, C.-H.; Leon, L.; Chung, E. J.; Huang, R.-T.; Sontag, T. J.; Reardon, C. A.; Getz, G. S.; Tirrell, M.; Fang, Y. Inhibition of atherosclerosis-promoting microRNAs via targeted polyelectrolyte complex micelles. *J. Mater. Chem. B*, 2014; *2:* 8142–8153.

354. Katayose, S.; Kataoka, K. Remarkable increase in nuclease resistance of plasmid DNA through supramolecular assembly with poly(ethylene glycol). *J. Pharm. Sci*, 1998; *87:* 160–163.
355. Katayose, S.; Kataoka, K. Water-soluble polyion complex associates of DNA and aoly(ethylene glycol)−aoly(L-lysine) Block copolymer. *Bioconjugate Chem*, 1997; *8*(5): 702–707.
356. Peng, H. T.; Shek, P. N. Novel wound sealants: biomaterials and applications. *Expert Rev. Med. Devices*, 2014; *7*(5): 639–659.
357. Wolfert, M. A.; Schacht, E. H.; Toncheva, V.; Ulbrich, K.; Nazarova, O.; Seymour, L. W. Characterization of vectors for gene therapy formed by self-assembly of DNA with synthetic block co-polymers. *Hum. Gene. Ther*, 1996; *7*(17): 2123–2133.
358. Tangsangasaksri, M.; Takemoto, H.; Naito, M.; Maeda, Y.; Sueyoshi, D.; Kim, H. J.; Miura, Y.; Ahn, J.; Azuma, R.; Nishiyama, N.; Miyata, K.; Kataoka, K. siRNA-loaded polyion complex micelle decorated with charge- conversional polymer tuned to undergo stepwise response to intra-tumoral and intra-endosomal pHs for exerting enhanced RNAi efficacy. *Biomacromolecules*, 2016; *17*(1): 246–255.
359. Ghobadi, A. F.; Letteri, R.; Parelkar, S. S.; Zhao, Y.; Chan-Seng, D.; Emrick, T.; Jayaraman, A. Dispersing zwitterions into comb polymers for nonviral transfection: Experiments and molecular simulation. *Biomacromolecules*, 2016; *17*(2): 546–557.
360. Li, S.; Huang, L. Nonviral gene therapy: promises and challenges. *Gene Ther*, 2000; *7*(1): 31–34.
361. Chesnoy, S.; Huang, L. Structure and function of lipid-DNA complexes for gene delivery. *Annu. Rev. Biophys. Biomol. Struct*, 2000; *29:* 27–47.
362. Martin, B.; Sainlos, M.; Aissaoui, A.; Oudrhiri, N.; Hauchecorne, M.; Vigneron, J.; Lehn, J.; Lehn, P. The design of cationic lipids for gene delivery. *Curr. Pharm. Des*, 2005; *11*(3): 375–394.
363. Ainalem, M.-L.; Nylander, T. DNA condensation using cationic dendrimers—morphology and supramolecular structure of formed aggregates. *Soft Matter*, 2011; *7*(10): 4577–4594.
364. Cai, J.; Yue, Y.; Rui, D.; Zhang, Y.; Liu, S.; Wu, C. Effect of chain length on cytotoxicity and endocytosis of cationic polymers. *Macromolecules*, 2011; *44*(7): 2050–2057.
365. Wu, B.-C.; Degner, B.; McClements, D. J. Soft matter strategies for controlling food texture: Formation of hydrogel particles by biopolymer complex coacervation. *J. Phys.: Condens. Matter*, 2014; *26*(46): 464104–464112.
366. Madene, A.; Jacquot, M.; Scher, J.; Desobry, S. Flavour encapsulation and controlled release - a review. *Int. J. Food Sci. Technol*, 2006; *41*(1): 1–21.
367. Augustin, M. A.; Hemar, Y. Nano- and micro-structured assemblies for encapsulation of food ingredients. *Chem. Soc. Rev*, 2009; *38*(4): 902–912.
368. Mazza, P. P. A.; Martini, F.; Sala, B.; Magi, M.; Colombini, M.P.; Giachi, G.; Landucci, F.; Lemorini, C.; Modugno, F.; Ribechini, E. A new Palaeolithic discovery: tar-hafted stone tools in a European Mid-Pleistocene bone-bearing bed. *J. Archaeol. Sci*, 2006; *33*(9): 1310−1318.
369. Bhagat, V.; Becker, M. L. Degradable Adhesives for Surgery and Tissue Engineering. *Biomacromolecules*, 2017; *18*(10): 3009−3039.
370. Rahimnejad, M.; Zhong, W. Mussel-inspired hydrogel tissue adhesives for wound closure. *RSC Adv*, 2017; *7*(75): 47380−47396.
371. Weiser, T. G.; Haynes, A. B.; Molina, G.; Lipsitz, S. R.; Esquivel, M. M.; Uribe-Leitz, T.; Fu, R.; Azad, T.; Chao, T. E.; Berry, W. R.; Gawande, A. A. Estimate of the global volume of surgery in 2012: An assessment supporting improved health outcomes. *Lancet*, 2015; *385*(Suppl 2): S11.
372. Weiser, T. G.; Regenbogen, S. E.; Thompson, K. D.; Haynes, A.B.; Lipsitz, S. R.; Berry, W. R.; Gawande, A. A. An estimation of the global volume of surgery: A modelling strategy based on available data. *Lancet*, 2008; *372*(9633): 139−144.
373. Bouten, P. J. M.; Zonjee, M.; Bender, J.; Yauw, S. T. K.; vanGoor, H.; van Hest, J. C. M.; Hoogenboom, R. The chemistry of tissue adhesive materials. *Prog. Polym. Sci*, 2014; *39*(7): 1375−1405.
374. Bochyńska, A. I.; Hannink, G.; Verhoeven, R.; Grijpma, D. W.; Buma, P. The effect of tissue surface modification with collagenase and addition of TGF-β3 on the healing potential of meniscal tears repaired with tissue glues in vitro. *J. Mater. Sci. Mater. Med*, 2017; *28*(1): 22.
375. Lauto, A.; Mawad, D.; Foster, L. J. R. Adhesive biomaterials for tissue reconstruction. *J. Chem. Technol. Biotechnol*, 2008; *83*(4): 464−472.
376. Stewart, R. J.; Wang, C. S.; Shao, H. Complex coacervates as a foundation for synthetic underwater adhesives. *Adv. Colloid Interface Sci*, 2011; *167*(1-2): 85-93.

377. Shao, H.; Stewart, R. J. Biomimetic underwater adhesives with environmentally triggered setting mechanisms. *Adv. Mater*, 2010; *22*(6): 729-733.
378. Filippov, A. D.; Sprakel, J.; Kamperman, M. Complex coacervation and metal–ligand bonding as synergistic design elements for aqueous viscoelastic materials. *Soft Matter*, 2021; *17*(12): 3294 - 3305.
379. Sun, T. L.; Kurokawa, T.; Kuroda, S.; Ihsan, A.B.; Akasaki, T.; Sato, K.; Haque, M. A.; Nakajima, T.; Gong, J. P. Physical hydrogels composed of polyampholytes demonstrate high toughness and viscoelasticity. *Nat. Mater*. 2013; *12*(10): 932–937.
380. Wei, W.; Ma, Y. Z.; Yao, X. D.; Zhou, W. Y.; Wang, X. Z.; Li, C. L.; Lin, J. X.; He, Q. L.; Leptihn, S.; Ouyang, H. W. Advanced hydrogels for the repair of cartilage defects and regeneration. *Bioact. Mater*, 2021; *6* (4), 998-1011.
381. Hwang, D. S.; Zeng, H.; Srivastava, A.; Krogstad, D. V.; Tirrell, M.; Israelachvili, J. N.; Waite, J. H. Viscosity and interfacial properties in a mussel-inspired adhesive coacervate. *Soft Matter*, 2010; *6*(14): 3232 – 3236.
382. Elisseeff, J.; McIntosh, W.; Fu, K.; Blunk, B. T.; Langer, R. Controlled-release of IGF-I and TGF-beta1 in a photopolymerizing hydrogel for cartilage tissue engineering. *J. Orthop. Res*, 2001; *19*(6): 1098–1104.
383. Waite, J. H.; Andersen, N. H.; Jewhurst, S.; Sun. C. Mussel Adhesion: Finding the Tricks Worth Mimicking. *J. Adhes*, 2005; *81*(3-4): 297-317.
384. Walker, G. The histology, histochemistry and ultrastructure of the cement apparatus of three adult sessile barnacles, *Elminius modestus*, *Balanus balanoides* and *Balanus hameri*. *Mar. Biol*, 1970; *7*: 239–248.
385. Stewart, R. J.; Weaver, J. C.; Morse, D. E.; Waite, J. H. The tube cement of Phragmatopoma californica: a solid foam. *J. Exp. Biol*, 2004; *207*(Pt 26): 4727-4734.
386. Dompé, M.; Vahdati, M.; van Ligten, F.; Cedano-Serrano, F. J.; Hourdet, D.; Creton, C.; Zanetti, M.; Bracco, P.; van der Gucht, J.; Kodger, T.; Kamperman, M. Enhancement of the Adhesive Properties by Optimizing the Water Content in PNIPAM-Functionalized Complex Coacervates. *ACS Appl. Polym. Mater*, 2020; *2*(4): 1722-1730.
387. Hwang, D. S.; Zeng, H.; Lu, Q.; Israelachvili, J.; Waite, J. H. Adhesion mechanism in a DOPA-deficient foot protein from green mussels. *Soft Matter*, 2012; *8*(20): 5640–5648.
388. Wei, W.; Tan, Y.; Rodriguez, N. R. M.; Yu, J.; Israelachvili, J. N.; Waite, J. H. A mussel-derived one component adhesive coacervate. *Acta Biomater*, 2014; *10*(4): 1663–1670.
389. Zhang, L.; Lipik, V.; Miserez, A. Complex coacervates ofoppositely charged co-polypeptides inspired by the sandcastle wormglue. *J. Mater. Chem. B*, 2016; *4*(8): 1544−1556.
390. Stewart, R. J.; Wang, C. S.; Song, I. T.; Jones, J. P. The role of coacervation and phase transitions in the sandcastle worm adhesive system. *Adv. Colloid Interface Sci*, 2017; *239;* 88 - 96.
391. Kaur, S.; Weerasekare, G. M.; Stewart, R. J. Multiphase Adhesive Coacervates Inspired by the Sandcastle Worm. *ACS Appl. Mater. Interfaces*, 2011; *3*(4): 941−944.
392. Jones, J. P.; Sima, M.; O'Hara, R. G.; Stewart, R. J. Water-Borne Endovascular Embolics Inspired by the Undersea Adhesive of Marine Sandcastle Worms. *Adv. Healthc. Mater*, 2016; 5(7): 795-801.
393. Ahn, B. K.; Das, S.; Linstadt, R.; Kaufman, Y.; Martinez-Rodriguez, N. R.; Mirshafian, R.; Kesselman, E.; Talmon, Y.; Lipshutz, B. H.; Israelachvili, J. N.; Waite, J. H. High-performance mussel-inspired adhesives of reduced complexity. *Nat. Commun*, 2015; *6*: 8663 (1-7).
394. Seo, S.; Das, S.; Zalicki, P. J.; Mirshafian, R.; Eisenbach, C. D.; Israelachvili, J. N.; Waite, J. H.; Ahn, B. K. Microphase Behavior and Enhanced Wet-Cohesion of Synthetic Copolyampholytes Inspired by a Mussel Foot Protein. *J. Am. Chem. Soc*, 2015; *137*(29): 9214−9217.
395. Zhao, Q.; Lee, D. W.; Ahn, B. K.; Seo, S.; Kaufman, Y.; Israelachvili, J. N.; Waite, J. H. Underwater contact adhesion and microarchitecture in polyelectrolyte complexes actuated by solvent exchange. *Nat. Mater*, 2016; *15*(4): 407 – 412.
396. Zhang, C.; Huang, J.; Zhang, J.; Liu, S.; Cui, M.; An, B.; Wang, X.; Pu, J.; Zhao, T.; Fan, C.; Lu, T. K.; Zhong, C. Engineered *Bacillus subtilis* biofilms as living glues. *Mater. Today*, 2019; *28:* 40−48.
397. Kelmansky, R.; McAlvin, B. J.; Nyska, A.; Dohlman, J. C.; Chiang, H. H.; Hashimoto, M.; Kohane, D. S.; Mizrahi, B. Strong tissue glue with tunable elasticity. *Acta Biomater*, 2017; *53:* 93−99.
398. Feldstein, M. M. Molecular Nature of Pressure-Sensitive Adhesion. In *Fundamentals of Pressure Sensitivity*; Benedek, I., Feldstein, M. M., Eds., Taylor & Francis Group, LLC: Boca Raton, FL, 2008.

399. Chalykh, A. A.; Chalykh, A. E.; Novikov, M. B.; Feldstein, M. M. Pressure-sensitive adhesion in the blends of poly (N-vinylpyrrolidone) and poly(ethylene glycol) of disparate chain lengths. *J. Adhes*, 2002; *78*(8): 667−694.
400. Roos, A.; Creton, C.; Novikov, M. B.; Feldstein, M. M. Viscoelasticity and tack of poly (vinyl pyrrolidone)-poly (ethyleneglycol) blends. *J. Polym. Sci., Part B: Polym. Phys*, 2002; *40*(20): 2395−2409.
401. Kim, H. J.; Yang, B.; Park, T. Y.; Lim, S.; Cha, H. J. Complex coacervates based on recombinant mussel adhesive proteins: their and applications, *Soft Matter*, 2017; *13*(42): 7704-7716.
402. Lim, S.; Choi, Y. S.; Kang, D. G.; Song, Y. H.; Cha, H. J. The adhesive properties of coacervated recombinant hybrid mussel adhesive proteins. *Biomaterials*, 2010; *31*(13): 3715−3722.
403. Kim, B. J.; Oh, D. X.; Kim, S.; Seo, J. H.; Hwang, D. S.; Masic, A.; Han, D. K.; Cha, H. J. Mussel-mimetic protein-based adhesive hydrogel. *Biomacromolecules*, 2014; *15*(5): 1579−1585.
404. Yang, B.; Ayyadurai, N.; Yun, H.; Choi, Y. S.; Hwang, B. H.; Huang, J.; Lu, Q.; Zeng, H.; Cha, H. J. In vivo residue-specific dopa-incorporated engineered mussel bioglue with enhanced adhesion and water resistance. *Angew. Chem*, 2014; *126*(49): 13578−13582.
405. Jeon, E. Y.; Hwang, B. H.; Yang, Y. J.; Kim, B. J.; Choi, B.-H.; Jung, G. Y.; Cha, H. J. Rapidly light-activated surgical protein glue inspired by mussel adhesion and insect structural crosslinking. *Biomaterials*, 2015; *67:* 11−19.
406. Zhong, C.; Gurry, T.; Cheng, A. A.; Downey, J.; Deng, Z.; Stultz, C. M.; Lu, T. K. Strong underwater adhesives made by self- assembling multi-protein nanofibres. *Nat. Nanotechnol*, 2014; *9*(10): 858− 866.
407. Stewart, R. J., Adhesive complex coacervates produced from electrostatically associated block copolymers and methods for making and using the same. International Publication Number: WO 2011/106595 A1, Office Code: CA 2788998, 2011-09-01.
408. Wang, W.; Xu, Y.; Li, A.; Li, T.; Liu, M.; Klitzing, von, R.; Ober, C. K.; Kayitmazer, A. B.; Li, L.; Guo, X. Zinc induced polyelectrolyte coacervate bioadhesive and its transition to a self-healing hydrogel. *RSC Adv*, 2015; *5*(82): 66871–66878.
409. Lam, J.; Clark, E. C.; Fong, E. L. S.; Lee, E. J.; Lu, S.; Tabata, Y.; Mikos, A. G. Evaluation of cell-laden polyelectrolyte hydrogels incorporating poly(l-Lysine) for applications in cartilage tissue engineering. *Biomaterials*, 2016; *83*(c): 332–346.
410. Wang, D.-A.; Varghese, S.; Sharma, B.; Strehin, I.; Fermanian, S.; Gorham, J.; Fairbrother, D. H.; Cascio, B.; Elisseeff, J. H. Multifunctional chondroitin sulphate for cartilage tissue–biomaterial integration. *Nat. Mater*, 2007; *6*(5): 385–392.
411. Favi, P. M.; Yi, S.; Lenaghan, S. C.; Xia, L.; Zhang, M. Inspiration from the natural world: from bio-adhesives to bio-inspired adhesives. *J. Adhes. Sci. Technol*, 2013; *28*(3-4): 290–319.
412. Cai, H.; Gabryelczyk, B.; Manimekalai, M. S. S.; Grüber, G.; Salentinig, S.; Miserez, A. Self-coacervation of modular squid beak proteins – a comparative study. *Soft Matter*, 2017; *13*(42): 7740-7752.
413. Sun, J.; Xiao, L.; Li, B.; Zhao, K.; Wang, Z.; Zhou, Y.; Ma, C.; Li, J.; Zhang, H.; Herrmann, A.; Liu, K. Genetically Engineered Polypeptide Adhesive Coacervates for Surgical Applications. *Angew. Chem. Int. Ed*, 2021; *60(44):* 23687 – 23694.
414. Kim, H. J.; Hwang, B. H.; Lim, S.; Choi, B.-H.; Kang, S. H.; Cha, H. J. Mussel adhesion-employed water-immiscible fluid bioadhesive for urinary fistula sealing. *Biomaterials*, 2015; *72:* 104–111.
415. Papanna, R.; Mann, L. K.; Tseng, S. C. G.; Stewart, R. J.; Kaur, S. S.; Swindle, M. M.; Kyriakides, T. R.; Tatevian, N.; Moise, K. J., Jr. Cryopreserved human amniotic membrane and a bioinspired underwater adhesive to seal and promote healing of iatrogenic fetal membrane defect sites. *Placenta*, 2015; *36*(8): 888–894.
416. Papanna, R.; Moise, K. J., Jr; Mann, L. K.; Fletcher, S.; Schniederjan, R.; Bhattacharjee, M. B.; Stewart, R. J.; Kaur, S.; Prabhu, S. P.; Tseng, S. C. G. Cryopreserved human umbilical cord patch for in-uterospina bifida repair. *Ultrasound Obstet. Gynecol*, 2016; *47*(2): 168–176.
417. Hwang, D. S.; Waite, J. H.; Tirrell, M. Promotion of osteoblast proliferation on complex coacervation-based hyaluronic acid–recombinant mussel adhesive protein coatings on titanium. *Biomaterials*, 2010; *31*(6): 1080–1084.
418. Mann, L. K.; Papanna, R.; Moise, K. J., Jr; Byrd, R. H.; Popek, E. J.; Kaur, S.; Tseng, S. C. G.; Stewart, R. J. Fetal membrane patch and biomimetic adhesive coacervates as a sealant for fetoscopic defects. *Acta Biomater*, 2012; *8*(6): 2160–2165.
419. Lee, H.; Scherer, N.F.; Messersmith, P.B. Single-molecule mechanics of mussel adhesion. *Proc. Natl. Acad. Sci. U. S. A*,

2006; *103*(35): 12999–13003.
420. Zhou, J.; Defante, A. P.; Lin, F.; Xu, Y.; Yu, J.; Gao, Y.; Childers, E.; Dhinojwala, A.; Becker, M. L. Adhesion properties of catechol-based biodegradable amino acid-based poly(ester urea) copolymers inspired from mussel proteins. Biomacromolecules, 2015; *16*(1): 266−274.
421. Jo, S. H.; Sohn, J. S. Biomimetic adhesive materials containing cyanoacryl group for medical application. *Molecules (Basel, Switzerland),* 2014; *19*(10): 16779–16793.
422. Oparin, A. I. *The Origin of Life*; The Macmillan Company: London, 1938.
423. Frankel, E. A.; Bevilacqua, P. C.; Keating, C. D. Polyamine/Nucleotide coacervates provide strong compartmentalization of Mg^{2+}, nucleotides, and RNA. *Langmuir*, 2016; *32*(8): 2041–2049.
424. Yin, Y.; Niu, L.; Zhu, X.; Zhao, M.; Zhang, Z.; Mann, S.; Liang, D. Non-equilibrium behaviour in coacervate-based protocells under electric-field-induced excitation. *Nat. Commun*, 2016; *7:* 10658 (1-7).
425. Monnard, P.-A.; Walde, P. Current ideas about prebiological compartmentalization. *Life*, 2015; *5*(2): 1239–1263.
426. Mann, S. The origins of life: old problems, new chemistries. *Angew. Chem. Int. Ed*, 2012; *52*(1): 155–162.
427. Keating, C. D. Aqueous phase separation as a possible route to compartmentalization of biological molecules. *Acc. Chem. Res*, 2012; *45*(12): 2114–2124.
428. Dominak, L. M.; Gundermann, E. L.; Keating, C. D. Microcompartmentation in artificial cells: pH- induced conformational changes alter protein localization. *Langmuir*, 2010; *26*(8): 5697 – 5705.
429. Long, M. S.; Jones, C. D.; Helfrich, M. R.; Mangeney-Slavin, L. K.; Keating, C. D. Dynamic microcompartmentation in synthetic cells. *Proc. Natl. Acad. Sci. U. S. A*, 2005; *102*(17): 5920–5925.
430. Kolb, V. M.; Swanson, M.; Menger, F. M. Coacervates and their Prebiotic Potential. In *Instruments, Methods, and Missions for Astrobiology XV*; Hoover, R. B., Levin, G. V., Rozanov, A. Y. Eds.; *Proc. of SPIE*, 2012; 8521: 85210E (1-8).
431. Menger, F. M.; Sykes, B. M. Anatomy of a Coacervate. *Langmuir*, 1998; *14*(15): 4131–4137.
432. Devi, N.; Sarmah, M.; Khatun, B.; Maji, T. K. Encapsulation of active ingredients in polysaccharide- protein complex coacervates. *Adv. Colloid Interface Sci*, 2017; *239:* 136-145.
433. Koppers, M., Özkan, N., & Farías, G. G. Complex Interactions Between Membrane-Bound Organelles, Biomolecular Condensates and the Cytoskeleton. *Front. Cell Dev. Biol*, 2020; *8:* 618733 (1-22).
434. Decker, C. J.; Parker, R. P-bodies and stress granules: possible roles in the control of translation and mRNA degradation. *Cold Spring Harb. Perspect. Biol*, 2012; *4*(9): a012286.
435. Mao, Y. S. Zhang B, Spector D. L. Biogenesis and function of nuclear bodies. *Trends Genet*, 2011; *27*(8): 295–306.
436. Oparin, A. I. Coacervate drops as models of prebiological systems. In *Prebiotic and Biochemical Evolution*; Kimball, A. P., Oro, J., Eds., North-Holland Publishing Co.: Amsterdam, 1971; pp. 1–7.
437. Jia, T. Z.; Chandru, K.; Hongo, Y.; Afrin, R.; Usui, T.; Myojo, K.; Cleaves, H. J 2nd. Membraneless polyester microdroplets as primordial compartments at the origins of life. *Proc. Natl. Acad. Sci. U. S. A*, 2019; *116*(32): 15830–15835.
438. Longo, L. M.; Despotović, D.; Weil-Ktorza, O.; Walker, M. J.; Jabłońska, J.; Fridmann-Sirkis, Y.; Varani, G.; Metanis, N.; Tawfik, D. S. Primordial emergence of a nucleic acid binding protein via phase separation and statistical ornithine to arginine conversion. *Proc. Natl. Acad. Sci. U. S. A*, 2020; *117*(27): 15731-15739.
439. Weber, S. C.; Brangwynne, C. P. Inverse size scaling of the nucleolus by a concentration-dependent phase transition. *Curr. Biol*, 2015; *25*(5): 641–646.
440. Nott, T. J.; Petsalaki, E.; Farber, P.; Jervis, D.; Fussner, E.; Plochowietz, A.; Craggs, T. D.; Bazett-Jones, D. P.; Pawson, T.; Forman-Kay, J. D.; Baldwin, A. J. Phase Transition of a Disordered Nuage Protein Generates Environmentally Responsive Membraneless Organelles. *Mol. Cell*, 2015; *57*(5): 936−947.
441. Saha, S.; Weber, C. A.; Nousch, M.; Adame-Arana, O.; Hoege, C.; Hein, M. Y.; Osborne-Nishimura, E.; Mahamid, J.; Jahnel, M.; Jawerth, L.; Pozniakovski, A.; Eckmann, C. R.; Jülicher, F.; Hyman, A. A. Polar Positioning of Phase-Separated Liquid Compartments in Cells Regulated by an mRNA Competition Mechanism. *Cell*, 2016; *166*(6): 1572−1584.
442. Brangwynne, C. P.; Eckmann, C. R.; Courson, D. S.; Rybarska, A.; Hoege, C.; Gharakhani, J.; Jülicher, F.; Hyman, A. A. Germline P Granules Are Liquid Droplets That Localize by Controlled Dissolution / Condensation. *Science*, 2009; *324*(5935): 1729−1732.

443. Hyman, A. A.; Weber, C. A.; Jülicher, F. Liquid-Liquid Phase Separation in Biology. *Annu. Rev. Cell Dev. Biol*, 2014; *30*(1): 39−58.
444. Li, P.; Banjade, S.; Cheng, H. C.; Kim, S.; Chen, B.; Guo, L.; Llaguno, M.; Hollingsworth, J. V.; King, D. S.; Banani, S. F.; Russo, P.S.; Jiang, Q. X.; Nixon, B. T.; Rosen, M. K. Phase Transitions in the Assembly of Multivalent Signalling Proteins. *Nature*, 2012; *483*(7389): 336−340.
445. Spector, D. L. Nuclear domains. *J. Cell Sci*, 2001; *114* (Pt 16): 2891–2893.
446. Hubstenberger, A.; Noble, S. L.; Cameron, C.; Evans, T. C. Translation repressors, an RNA helicase, and developmental cues control RNP phase transitions during early development. *Dev. Cell*, 2013; *27*(2): 161–173.
447. Berry, J.; Weber, S. C.; Vaidya, N.; Haataja, M.; Brangwynne, C. P. RNA transcription modulates phase transition-driven nuclear body assembly. *Proc. Natl. Acad. Sci. U. S. A*, 2015; *112*(38): E5237−E5245.
448. Zhou, M.; Li, W.; Li, J.; Xie, L.; Wu, R.; Wang, L.; Fu, S.; Su, W.; Hu, J.; Wang, J.; Li, P. Phase-separated condensate-aided enrichment of biomolecular interactions for high-throughput drug screening in test tubes. *Biol. Chem*, 2020; *295*(33): 11420–11434.
449. Wippich, F.; Bodenmiller, B.; Trajkovska, M. G.; Wanka, S.; Aebersold, R.; Pelkmans, L. Dual Specificity Kinase DYRK3 Couples Stress Granule Condensation/Dissolution to mTORC1 Signaling. *Cell*, 2013; *152*(4): 791−805.
450. Zeng, M.; Shang, Y.; Araki, Y.; Guo, T.; Huganir, R. L.; Zhang, M. Phase transition in postsynaptic densities underlies formation of synaptic complexes and synaptic plasticity. *Cell*, 2016; *166*(5): 1163–1175. e12.
451. Lin, Y.; Protter, D. S. W.; Rosen, M. K.; Parker, R. Formation and Maturation of Phase-Separated Liquid Droplets by RNA-Binding Proteins. *Mol. Cell*, 2015; *60*(2): 208−219.
452. Han, T. W.; Kato, M.; Xie, S.; Wu, L. C.; Mirzaei, H.; Pei, J.; Chen, M.; Xie, Y.; Allen, J.; Xiao, G.; McKnight, S. L. Cell-free formation of RNA granules: bound RNAs identify features and components of cellular assemblies, *Cell*, 2012; *149*(4): 768-779.
453. Zhang, H. Y.; Elbaum-Garfinkle, S.; Langdon, E. M.; Taylor, N.; Occhipinti, P.; Bridges, A. A.; Brangwynne, C. P.; Gladfelter, A. S. RNA Controls PolyQ Protein Phase Transitions. *Mol. Cell*, 2015; *60*(2): 220−230.
454. Mitrea, D. M.; Kriwacki, R. W. Phase separation in biology; functional organization of a higher order. *Cell Commun. Signal*, 2016; *14*(1): 1–20.
455. Hyman, A. A, Brangwynne, C. P. Beyond stereospecificity: liquids and mesoscale organization of cytoplasm. *Dev. Cell*, 2011; *21*(1): 14–16.
456. Mason, A. F.; van Hest, J. C. M. Multifaceted Cell Mimicry in Coacervate-Based Synthetic Cells. *Emerg. Top. Life Sci*, 2019; *3*(5): 567−571.
457. Deshpande, S.; Brandenburg, F.; Lau, A.; Last, M. G. F.; Spoelstra, W. K.; Reese, L.; Wunnava, S.; Dogterom, M.; Dekker, C. Spatiotemporal Control of Coacervate Formation within Liposomes. *Nat. Commun*, 2019; *10*(1): 1800 (1-11).
458. Deng, N.; Huck, W. T. S. Microfluidic Formation of Monodisperse Coacervate Organelles in Liposomes. *Angew. Chem. Int. Ed. Engl*, 2017; *56*(33): 9736−9740.
459. Yewdall, N. A.; Mason, A. F.; van Hest, J. C. M. The Hallmarks of Living Systems: Towards Creating Artificial Cells. *Interface Focus*, 2018; *8*(5): 20180023.
460. Buddingh', B. C.; van Hest, J. C. M. Artificial Cells: Synthetic Compartments with Life-like Functionality and Adaptivity. *Acc. Chem. Res*, 2017; *50*(4): 769−777.
461. Narayanaswamy, R.; Levy, M.; Tsechansky, M.; Stovall, G. M.; O'Connell, J. D.; Mirrielees, J.; Ellington, A. D.; Marcotte, E. M. Widespread reorganization of metabolic enzymes into reversible assemblies upon nutrient starvation. *Proc. Natl. Acad. Sci. U S A*, 2009; *106*(25): 10147–10152.
462. Eulalio, A.; Behm-Ansmant, I.; Izaurralde, E. P bodies: at the crossroads of post-transcriptional pathways. *Nat. Rev. Mol. Cell Biol*, 2007; *8*(1): 9–22.
463. Brangwynne, C. P.; Mitchison, T. J.; Hyman, A. A. Active liquid-like behavior of nucleoli determines their size and shape in Xenopus laevis oocytes. *Proc. Natl. Acad. Sci. U S A*, 2011; *108*(11): 4334–4339.
464. Feng, Z.; Jia, B.; Zhang, M. Liquid–Liquid Phase Separation in Biology: Specific Stoichiometric Molecular Interactions vs Promiscuous Interactions Mediated by Disordered Sequences. *Biochemistry*, 2021; *60*(31): 2397-2406.
465. Stoeger, T.; Battich, N.; Pelkmans, L. Passive noise filtering by cellular compartmentalization. *Cell*, 2016; *164*(6): 1151–1161.
466. Patel, A.; Lee, H. O.; Jawerth, L.; Maharana, S.; Jahnel, M.; Hein, M. Y.; Stoynov, S.;

Mahamid, J.; Saha, S.; Franzmann, T. M.; Pozniakovski, A; Poser, I.; Maghelli, N.; Royer, L. A.; Weigert, M.; Myers, E. W.; Grill, S.; Drechsel, D.; Hyman, A. A.; Alberti, S. A liquid-to-solid phase transition of the ALS protein FUS accelerated by disease mutation. *Cell*, 2015; *162*(5): 1066–1077.

467. Kawamura, A.; Harada, A.; Kono, K.; Kataoka, K. Self-assembled nano-bioreactor from block ionomers with elevated and stabilized enzymatic function. *Bioconjugate Chem*, 2007; *18*(5): 1555– 1559.
468. Kataoka, K.; Harada, A. Pronounced activity of enzymes through the incorporation into the core of polyion complex micelles made from charged block copolymers. *J. Control. Release*, 2001; *72*(1-3): 85– 91.
469. Anraku, Y.; Kishimura, A.; Kamiya, M.; Tanaka, S.; Nomoto, T.; Toh, K.; Matsumoto, Y.; Fukushima, S.; Sueyoshi, D.; Kano, M. R.; Urano Y, Nishiyama N, Kataoka K. Systemically injectable enzyme-loaded polyion complex vesicles as in vivo nanoreactors functioning in tumors. *Angew. Chem. Int. Ed. Engl*, 2016; 55(2): 560 - 565.
470. Lv, K.; Perriman, A. W.; Mann, S. Photocatalytic multiphase micro-droplet reactors based on complex coacervation. *Chem. Commun. (Camb)*, 2015; *51*(41): 8600–8602.
471. Shin, Y.; Brangwynne, C. P. Liquid Phase Condensation in Cell Physiology and Disease. *Science*, 2017; *357*(6357), eaaf4382.
472. Holehouse, A. S.; Pappu, R. V. Functional Implications of Intracellular Phase Transitions. *Biochemistry*, 2018; *57*(17), 2415−2423.
473. Li, Y. R.; King, O. D.; Shorter, J.; Gitler, A. D. Stress Granules as Crucibles of ALS Pathogenesis. *J. Cell Biol*, 2013; *201*(3): 361−372.
474. Aguzzi, A.; Altmeyer, M. Phase Separation: Linking Cellular Compartmentalization to Disease. *Trends Cell Biol*, 2016; *26*(7): 547−558.
475. Strom, A. R.; Emelyanov, A. V.; Mir, M.; Fyodorov, D. V.; Darzacq, X.; Karpen, G. H. Phase Separation Drives Heterochromatin Domain Formation. *Nature*, 2017; *547*(7662): 241−245.
476. Abbondanzieri, E. A.; Meyer, A. S. More than Just a Phase: The Search for Membraneless Organelles in the Bacterial Cytoplasm. *Curr. Genet*, 2019; *65*(3): 691−694.
477. Ulianov, S.V.; Velichko, A. K.; Magnitov, M. D.; Luzhin, A. V.; Golov, A. K.; Ovsyannikova, N.; Kireev, I. I.; Gavrikov, A. S.; Mishin, A. S.; Garaev, A. K.; Tyakht, A. V.; Gavrilov, A. A.; Kantidze, O. L.; Razin, S. V. Suppression of liquid–liquid phase separation by 1,6-hexanediol partially compromises the 3D genome organization in living cells. *Nucleic Acids Res*, 2021; *49*(18): 10524–10541.
478. Altmeyer, M.; Neelsen, K. J.; Teloni, F.; Pozdnyakova, I.; Pellegrino, S.; Grøfte, M.; Rask, M. B. D.; Streicher, W.; Jungmichel, S.; Nielsen, M. L.; Lukas, J. Liquid Demixing of Intrinsically Disordered Proteins Is Seeded by Poly(ADP-Ribose). *Nat. Commun*, 2015; *6:* 8088 (1-12).
479. Nott, T. J.; Craggs, T. D.; Baldwin, A. J. Membraneless Organelles Can Melt Nucleic Acid Duplexes and Act as Biomolecular Filters. *Nat. Chem*, 2016; *8*(6): 569−575.
480. Molliex, A.; Temirov, J.; Lee, J.; Coughlin, M.; Kanagaraj, A. P.; Kim, H. J.; Mittag, T.; Taylor, J. P. Phase Separation by Low Complexity Domains Promotes Stress Granule Assembly and Drives Pathological Fibrillization. *Cell*, 2015; *163*(1): 123−133.
481. Cho, W. K.; Spille, J. H.; Hecht, M.; Lee, C.; Li, C.; Grube, V.; Cisse, I. I. Mediator and RNA Polymerase II Clusters Associate in Transcription-Dependent Condensates. *Science*, 2018; *361*(6400): 412−415.
482. Chong, S.; Dugast-Darzacq, C.; Liu, Z.; Dong, P.; Dailey, G. M.; Cattoglio, C.; Heckert, A.; Banala, S.; Lavis, L.; Darzacq, X.; Tjian, R. Imaging Dynamic and Selective Low-Complexity Domain Interactions That Control Gene Transcription. *Science*, 2018; *361*(6400): eaar2555 (1-9).
483. Sabari, B. R.; Dall'Agnese.; Boija, A.; Klein, I. A.; Coffey, E. L.; Shrinivas, K.; Abraham, B. J.; Hannett, N. M.; Zamudio, A. V.; Manteiga, J. C.; Li, C. H.; Guo, Y. E.; Day, D. S.; Schuijers, J.; Vasile, E.; Malik, S.; Hnisz, D.; Ihn Lee, T.; Cisse, I. I.; Roeder, R. G. Coactivator Condensation at Super-Enhancers Links Phase Separation and Gene Control. *Science*, 2018; *361*(6400): eaar3958 (1-11).
484. Sokolova, E.; Spruijt, E.; Hansen, M. M. K.; Dubuc, E.; Groen, J.; Chokkalingam, V.; Piruska, A.; Heus, H. A.; Huck, W. T. S. Enhanced Transcription Rates in Membrane-Free Protocells Formed by Coacervation of Cell Lysate. *Proc. Natl. Acad. Sci. U. S. A*, 2013; *110*(29): 11692−11697.
485. Freeman Rosenzweig E. S.; Xu B.; Kuhn Cuellar L.; Martinez-Sanchez A.; Schaffer M.; Strauss M.; Cartwright H. N.; Ronceray P.; Plitzko J. M.; Förster F.; Wingreen N. S.; Engel B. D.; Mackinder L. C. M.; Jonikas M. C. The Eukaryotic CO_2-Concentrating

Organelle Is Liquid-Like and Exhibits Dynamic Reorganization. *Cell*, 2017; *171*(1): 148–162.
486. Ewers, H.; Römer, W.; Smith, A. E.; Bacia, K.; Dmitrieff, S.; Chai, W.; Mancini, R.; Kartenbeck, J.; Chambon, V.; Berland, L.; Oppenheim, A.; Schwarzmann, G.; Feizi, T.; Schwille, P.; Sens, P.; Helenius, A.; Johannes, L. GM1 structure determines SV40-induced membrane invagination and infection. *Nat. Cell Biol*, 2010; *12*(1): 11-18, sup pp 1-12.
487. Chong, P. A.; Forman-Kay, J. D. Liquid−Liquid Phase Separation in Cellular Signaling Systems. *Curr. Opin. Struct. Biol*, 2016; *41*: 180−186.
488. Beutel, O.; Maraspini, R.; Pombo-García, K.; Martin-Lemaitre, C.; Honigmann, A. Phase Separation of Zonula Occludens Proteins Drives Formation of Tight Junctions. *Cell*, 2019; *179*(4): 923−936, e11.
489. Bergeron-Sandoval, L.-P.; Kumar, S.; Heris, H. K.; Chang, C.; Cornell, C. E.; Keller, S. L.; François, P.; Hendricks, A. G.; Ehrlicher, A. J.; Pappu, R. V.; Michnick, S. W. Proteins with prion-like domains can form viscoelastic condensates that enable membrane remodeling and endocytosis. *bioRxiv*, 2021; 145664(1 – 29), DOI: https://doi.org/10.1101/145664 (accessed 2021-11-28).
490. Sheth, U.; Pitt, J.; Dennis, S.; Priess, J. R. Perinuclear PGranules Are the Principal Sites of MRNA Export in Adult C. Elegans Germ Cells. *Development*, 2010; *137*(8): 1305−1314.
491. Huang, W. Y. C.; Alvarez, S.; Kondo, Y.; Kwang Lee, Y.; Chung,J. K.; Monatrice Lam, H. Y.; Biswas, K. H.; Kuriyan, J.; Groves, J. T. A Molecular Assembly Phase Transition and Kinetic Proofreading Modulate Ras Activation by SOS. *Science*, 2019; *363*(6431): 1098−1103.
492. Case, L. B.; Zhang, X.; Ditlev, J. A.; Rosen, M. K. Stoichiometry Controls Activity of Phase-Separated Clusters of Actin Signaling Proteins. *Science*, 2019; *363*(6431): 1093−1097.
493. Su, X.; Ditlev, J. A.; Hui, E.; Xing, W.; Banjade, S.; Okrut, J.; King, D. S.; Taunton, J.; Rosen, M. K.; Vale, R. D. Phase Separation of Signaling Molecules Promotes T Cell Receptor Signal Transduction. *Science*, 2016; *352*(6285): 595−599.
494. Ditlev, J. A.; Vega, A. R.; Köster, D. V.; Su, X.; Tani, T.;Lakoduk, A. M.; Vale, R. D.; Mayor, S.; Jaqaman, K.; Rosen, M. K. A Composition-Dependent Molecular Clutch between T Cell Signaling Condensates and Actin. *eLife*, 2019; *8*: e42695.
495. Bergeron-Sandoval, L. -P.; Michnick, S. W. Mechanics, Structure and Function of Biopolymer Condensates. *J. Mol. Biol*, 2018; *430*(23): 4754−4761.
496. Faltova, L.; Küffner, A. M.; Hondele, M.; Weis, K.; Arosio, P. Multi-functional protein materials and microreactors using low complexity domains as molecular adhesives. *ACS Nano*, 2018; *12*(10): 9991–9999.
497. Küffner, A. M.; Prodan, M.; Zuccarini, R.; Capasso Palmiero, U.; Faltova, L.; Arosio, P. Acceleration of an enzymatic reaction in liquid phase separated compartments based on intrinsically disordered protein domains. *ChemSystems Chem*, 2020; *2*(4): e2000001 (1-7).
498. Dzuricky, M.; Rogers, B. A.; Shahid, A.; Cremer, P. S.; Chilkoti, A. Denovo engineering of intracellular condensates using artificial disordered proteins. *Nat. Chem*, 2020; *12*(9): 814–825.
499. Zwicker, D.; Seyboldt, R.; Weber, C. A.; Hyman, A. A.; Jülicher, F. Growth and division of active droplets provides a model for protocells. *Nature Phys*, 2017; *13*(4): 408–413.
500. Feric, M.; Vaidya, N.; Harmon, T. S.; Mitrea, D. M.; Zhu, L.; Richardson, T. M.; Kriwacki, R. W.; Pappu, R. V.; Brangwynne, C. P. Coexisting liquid phases underlie nucleolar subcompartments. *Cell*, 2016; *165*(7): 1686–1697.
501. Sawyer, I. A.; Sturgill, D.; Dundr, M. Membraneless nuclear organelles and the search for phases within phases. *Wiley Interdiscip. Rev. RNA*, 2019; 10(2): e1514.
502. Spoelstra, W. K.; van der Sluis, E. O.; Dogterom, M.; Reese, L. Nonspherical coacervate shapes in an Enzyme-driven active system. *Langmuir*, 2020; *36*(8): 1956–1964.
503. Donau, C.; Spath, F.; Sosson, M.; Kriebisch, B. A. K.; Schnitter, F.; Tena-Solsona, M.; Kang, H. S.; Salibi, E.; Sattler, M.; Mutschler, H.; Boekhoven, J. Active coacervate droplets as a model for membraneless organelles and protocells. *Nat. Commun*, 2020; *11*(1): 5167 (1-10).
504. Hone, J. H. E.; Howe, A. M.; Cosgrove, T. A Small-Angle Neutron Scattering Study of the Structure of Gelatin/Polyelectrolyte Complexes. *Macromolecules*, 2000; *33*(4): 1206-1212.
505. Weinbreck, F.; Wientjes, R. H. W.; Nieuwenhuijse, H.; Robijn, G. W.; de Kruif, C. G. Rheological properties of whey protein/gum Arabic coacervates. *J. Rheol*, 2004; *48*(6): 1215−1228.
506. Wang, X.; Lee, J.; Wang, Y.-W.; Huang, Q.

Composition and Rheological Properties of β-Lactoglobulin/Pectin Coacervates: Effects of Salt Concentration and Initial Protein/Polysaccharide Ratio. *Biomacromolecules*, 2007; *8*(3): 992−997.
507. Cirulis, J. T.; Keeley, F. W.; James, D. F. Viscoelastic properties and gelation of an elastin-like polypeptide. *J. Rheol.(N. Y. N. Y.)*, 2009; *53(*5): 1215−1228.
508. Nikolaeva, O.; Budtova, T.; Brestkin, Y.; Zoolshoev, Z.; Frenkel, S. J. Rheological properties of an interpolymer complex formed between poly(acrylic acid) and methyl cellulose. *Appl. Polym. Sci*, 1999; *72(*12): 1523−1528.
509. Spruijt, E.; Cohen Stuart, M. A.; van der Gucht, J. Linear Viscoelasticity of Polyelectrolyte Complex Coacervates. *Macromolecules*, 2013; *46*(4): 1633−1641.
510. Tiwari, A.; Bindal, S.; Bohidar, H. B. Kinetics of Protein−Protein Complex Coacervation and Biphasic Release of Salbutamol Sulfate from Coacervate Matrix. *Biomacromolecules*, 2009; *10*(1): 184–189.
511. Lvov, Y.; Decher, G.; Moehwald, H. Assembly, structural characterization, and thermal behavior of layer-by-layer deposited ultrathin films of poly(vinyl sulfate) and poly(allylamine). *Langmuir*, 1993; *9*(2): 481-486.
512. Wang, B.; Jin, T.; Xu, Q.; Liu, H.; Ye, Z.; Chen, H. Direct loading and tunable release of antibiotics from polyelectrolyte multilayers to reduce bacterial adhesion and biofilm formation. *Bioconjugate Chem*, 2016; *27(*5): 1305–1313.
513. Rydzek, G.; Pakdel, A.; Witecka, A.; Shri, D. N. A.; Gaudière, F.; Nicolosi, V.; Mokarian-Tabari, P.; Schaaf, P.; Boulmedais, F.; Ariga, K. pH-Responsive Saloplastics Based on Weak Polyelectrolytes: From Molecular Processes to Material Scale Properties. *Macromolecules*, 2018; *51(*12): 4424-4434.
514. Shamoun, R. F.; Hariri, H. H.; Ghostine, R. A.; Schlenoff, J. B. Thermal Transformations in Extruded Saloplastic Polyelectrolyte Complexes. *Macromolecules*, 2012; *45(*24): 9759−9767.
515. Porcel, C. H.; Schlenoff, J. B. Compact polyelectrolyte complexes: "saloplastic" candidates for biomaterials. *Biomacromolecules*, 2009; *10*(11): 2968-2975.
516. Hariri, H. H.; Schlenoff, J. B. Saloplastic Macroporous Polyelectrolyte Complexes: Cartilage Mimics. *Macromolecules*, 2010; *43*(20): 8656-8663.
517. Gabryelczyk, B., Cai, H., Shi, X.; Sun, Y.; Swinkels, P. J. M.; Salentinig, S.; Pervushin, K.; Miserez, A. Hydrogen bond guidance and aromatic stacking drive liquid-liquid phase separation of intrinsically disordered histidine-rich peptides. *Nat. Commun*, 2019; *10(*1): 5465(1-12).
518. Phoeung, T.; Spanedda, M. V.; Roger, E.; Heurtault, B.; Foumel, S.; Reisch, A.; Mutschler, A.; Perrin-Schmitt, F.; Hemmerle, J.; Collin, D.; Rawiso, M.; Boulmedais, F.; Schaaf, P.; Lavalle, P.; Frisch, B., Alginate/Chitosan Compact Polyelectrolyte Complexes: A Cell and Bacterial Repellent Material. *Chem. Mater*, 2017; *29*(24): 10418-10425.
519. Kelly, K. D.; Schlenoff, J. B. Spin-Coated Polyelectrolyte Coacervate Films. *ACS Appl. Mater. Interfaces*, 2015; *7*(25): 13980-13986.
520. Kurtz, I. S.; Sui, S.; Hao, X.; Huang, M.; Perry, S. L.; Schiffman, J. D. Bacteria-Resistant, Transparent, Free-Standing Films Prepared from Complex Coacervates. *ACS Appl. Bio Mater*, 2019; *2*(9): 3926-3933.
521. Zhu, F.; Cheng, L.; Yin, J.; Wu, Z. L.; Qian, J.; Fu, J.; Zheng, Q. 3D Printing of Ultratough Polyion Complex Hydrogels. *ACS Appl. Mater. Interfaces*, 2016; *8*(45): 31304–31310.
522. Meng, X.; Perry, S. L.; Schiffman, J. D Complex Coacervation: Chemically Stable Fibers Electrospun from Aqueous Polyelectrolyte Solutions. *ACS Macro Lett*, 2017; *6*(5): 505-511.
523. Meng, X.; Schiffman, J. D.; Perry, S. L. Electrospinning Cargo-Containing Polyelectrolyte Complex Fibers: Correlating Molecular Interactions to Complex Coacervate Phase Behavior and Fiber Formation. *Macromolecules*, 2018; *51*(21): 8821–8832.
524. Qazvini, N. T.; Bolisetty, S.; Adamcik, J.; Mezzenga, R. Self-Healing Fish Gelatin/Sodium Montmorillonite Biohybrid Coacervates: Structural and Rheological Characterization. *Biomacromolecules*, 2012; *13(*7): 2136–2147.
525. Elbaum-Garfinkle, S.; Kim, Y.; Szczepaniak, K.; Chen, C. C.; Eckmann, C. R.; Myong, S.; Brangwynne, C. P. The disordered P granule protein LAF-1 drives phase separation into droplets with tunable viscosity and dynamics. *Proc. Natl. Acad. Sci. U. S. A.*, 2015; *112*(23): 7189-7194.
526. Benedek, G. B. Cataract as a protein condensation disease: the Proctor Lecture. *Invest. Ophthalmol. Vis. Sci*, 1997; *38*(10): 1911–1921.
527. Lee, K. H.; Zhang, P.; Kim, H. J.; Mitrea, D. M.; Sarkar, M.; Freibaum, B. D.; Cika, J.;

Coughlin, M.; Messing, J.; Molliex, A.; Maxwell, B. A.; Kim, N. C.; Temirov, J.; Moore, J.; Kolaitis, R. M.; Shaw, T. I.; Bai, B.; Peng, J.; Kriwacki, R. W.; Taylor, J. P. C9orf72 Dipeptide Repeats Impair the Assembly, Dynamics, and Function of Membrane-Less Organelles. *Cell*, 2016; *167*(3): 774-788.e17.

528. Lee, E. B.; Lee, V. M.; Trojanowski, J. Q. Gains or losses: molecular mechanisms of TDP43-mediated neurodegeneration. *Nat. Rev. Neurosci*, 2011; *13(*1): 38–50.
529. Harrison, A. F.; Shorter, J. RNA-binding proteins with prion-like domains in health and disease. *Biochem. J*, 2017; *474*(8): 1417–1438.
530. Courchaine, E. M.; Lu, A.; Neugebauer, K. M. Droplet organelles? *EMBO J.*, 2016; *35(*15): 1603–1612.
531. Scoca, V.; Nunzio, F. D. Membraneless organelles restructured and built by pandemic viruses: HIV-1 and SARS-CoV-2. *J. Mol. Cell Biol*, 2021; *13(*4): 259–268.
532. Luo, Y.; Na, Z.; Slavoff, S. A. P-bodies: composition, properties, and functions. *Biochemistry*, 2018; *57*(17): 2424–2431.
533. Protter, D. S. W.; Parker, R. Principles and properties of stress granules. *Trends Cell Biol*, 2016; *26*(9): 668–679.
534. Wolozin, B.; Ivanov, P. Stress granules and neurodegeneration. *Nat. Rev. Neurosci*, 2019; *20*(11): 649–666.
535. Feng, Z.; Chen, X.; Wu, X.; Zhang, M. Formation of biological condensates via phase separation: characteristics, analytical methods, and physiological implications. *J. Biol. Chem*, 2019; *294(*40): 14823–14835.
536. Mateju, D.; Franzmann, T. M.; Patel, A.; Kopach, A.; Boczek, E. E.; Maharana, S.; Lee, H. O.; Carra, S.; Hyman, A. A.; Alberti, S. An aberrant phase transition of stress granules triggered by misfolded protein and prevented by chaperone function. *EMBO J*, 2017; *36(*12): 1669–1687.
537. Bolognesi, B.; Gotor, N. L.; Dhar, R.; Cirillo, D.; Baldrighi, M.; Tartaglia, G. G.; Lehner, B. A concentration-dependent liquid phase separation can cause toxicity upon increased protein expression. *Cell Rep*, 2016; *16*(1): 222–231.
538. Asakawa, K.; Handa, H.; Kawakami, K. Optogenetic modulation of TDP-43 oligomerization accelerates ALS-related pathologies in the spinal motor neurons. *Nat. Commun*, 2020; *11(*1): 1004(1-16).
539. Mann, J. R.; Gleixner, A. M.; Mauna, J. C.; Gomes, E.; DeChellis-Marks, M. R.; Needham, P. G.; Copley, K. E.; Hurtle, B.; Portz, B.; Pyles, N. J.; Guo, L.; Calder, C. B.; Wills, Z. P.; Pandey, U. B.; Kofler, J. K.; Brodsky, J. L.; Thathiah, A.; Shorter, J.; Donnelly, C. J. RNA Binding Antagonizes Neurotoxic Phase Transitions of TDP-43. *Neuron*, 2019; *102*(2): 321-338.e8.
540. Watanabe, S.; Inami, H.; Oiwa, K.; Murata, Y.; Sakai, S.; Komine, O.; Sobue, A.; Iguchi, Y.; Masahisa Katsuno, M.; Yamanaka, K. Aggresome formation and liquid–liquid phase separation independently induce cytoplasmic aggregation of TAR DNA-binding protein 43. *Cell Death Dis*, 2020; *11(*10): 909(1-15).
541. DeJesus-Hernandez, M.; Mackenzie, I. R.; Boeve, B. F.; Boxer, A. L.; Baker, M.; Rutherford, N. J.; Nicholson, A. M.; Finch, N. A.; Flynn, H.; Adamson, J.; Kouri, N.; Wojtas, A.; Sengdy, P.; Hsiung, G. Y.; Karydas, A.; Seeley, W. W.; Josephs, K. A.; Coppola, G.; Geschwind, D. H.; Wszolek, Z. K.; Feldman, H.; Knopman, D. S.; Petersen, R. C.; Miller, B. L.; Dickson, D. W.; Boylan, K. B.; Graff-Radford, N. R.; Rademakers, R. Expanded GGGGCC hexanucleotide repeat in noncoding region of C9ORF72 causes chromosome 9p-linked FTD and ALS. *Neuron*, 2011; *72*(2): 245-56.
542. Renton, A. E.; Majounie, E.; Waite, A.; Simón-Sánchez, J.; Rollinson, S.; Gibbs, J. R.; Schymick, J. C.; Laaksovirta, H.; van Swieten, J. C.; Myllykangas, L.; Kalimo, H.; Paetau, A.; Abramzon, Y.; Remes, A. M.; Kaganovich, A.; Scholz, S. W.; Duckworth, J.; Ding, J.; Harmer, D. W.; Hernandez, D. G.; Johnson, J. O.; Mok, K.; Ryten, M.; Trabzuni, D.; Guerreiro, R. J.; Orrell, R. W.; Neal, J.; Murray, A.; Pearson, J.; Jansen, I. E.; Sondervan, D.; Seelaar, H.; Blake, D.; Young, K.; Halliwell, N.; Callister, J. B.; Toulson, G.; Richardson, A.; Gerhard, A.; Snowden, J.; Mann, D.; Neary, D.; Nalls, M. A.; Peuralinna, T.; Jansson, L.; Isoviita, V. M.; Kaivorinne, A. L.; Hölttä-Vuori, M.; Ikonen, E.; Sulkava, R.; Benatar, M.; Wuu, J.; Chiò, A.; Restagno, G.; Borghero, G.; Sabatelli, M; ITALSGEN Consortium.; Heckerman, D.; Rogaeva, E.; Zinman, L.; Rothstein, J. D.; Sendtner, M.; Drepper, C.; Eichler, E. E.; Alkan, C.; Abdullaev, Z.; Pack, S. D.; Dutra, A.; Pak, E.; Hardy, J.; Singleton, A.; Williams, N. M.; Heutink, P.; Pickering-Brown, S.; Morris, H. R.; Tienari, P. J.; Traynor, B. J. A hexanucleotide repeat expansion in C9ORF72 is the cause of chromosome 9p21-linked ALS-FTD. *Neuron*, 2011; *72*(2): 257-268.
543. Xiao, S.; MacNair, L.; McGoldrick, P.; McKeever, P. M.; McLean, J. R.; Zhang, M.; Keith, J.; Zinman, L.; Rogaeve, E.;

Robertson, J. Isoform-specific antibodies reveal distinct subcellular localizations of C9orf72 in amyotrophic lateral sclerosis. *Ann. Neurol*, 2015; *78*(4): 568–583.
544. Sivadasan, R.; Hornburg, D.; Drepper, C.; Frank, N.; Jablonka, S.; Hansel, A.; Lojewski, X.; Sterneckert, J.; Hermann, A.; Shaw, P. J.; Ince, P. G.; Mann, M.; Meissner, F.; Sendtner, M. C9orf72 interaction with cofilin modulates actin dynamics in motor neurons. *Nat. Neurosci*, 2016; *19(*12): 1610–1618.
545. Farg, M. A.; Sundaramoorthy, V.; Sultana, J. M.; Yang, S.; Atkinson, R. A. K.; Levina, V., M. A.; Gleeson, P. A.; Blair, I. P.; Soo, K. S.; King, A. E.; Atkin, J. D. C9ORF72, implicated in amytrophic lateral sclerosis and frontotemporal dementia, regulates endosomal trafficking. *Hum. Mol. Genet*, 2014; *23(*13): 3579–3595.
546. Sellier, C.; Campanari, M.-L.; Julie Corbier, C.; Gaucherot, A.; Kolb-Cheynel, I.; Oulad-Abdelghani, M.; Ruffenach, F.; Page, A.; Ciura, S.; Kabashi, E.; Berguerand, N. C. Loss of C9orf72 impairs autophagy and synergizes with polyQ Ataxin-2 to induce motor neuron dysfunction and cell death. *EMBO J*, 2016; *35*(12): 1276–1297.
547. Webster, C. P.; Smith, E. F.; Bauer, C. S.; Moller, A.; Hautbergue, G. M.; Ferraiuolo, L.; Myszczynska, M. A.; Higginbottom, A.; Walsh, M. J.; Whitworth, A. J.; Kasper, B. K.; Meyer, K.; Shaw, P. J.; Grierson, A. J.; J De Vos, K.(). The C9orf72 protein interacts with Rab1a and the ULK1 complex to regulate initiation of autophagy. *EMBO J*, 2016; *35(*15): 1656–1676.
548. O'Rourke, J. G.; Bogdanik, L.; Muhammad, A. K. M. G.; Gendron, T. F.; Kim, K. J.; Austin, A.; Cady, J.; Liu, E. Y.; Zarrow, J.; Grant, S.; Ho, R.; Bell, S.; Carmona, S.; Simpkinson, M.; Lall, D.; Wu, K.; Daughrity, L.; Dickson, D. W.; Harms, M. B.; Petrucelli, L.; Lee, E. B.; Lutz, C. M.; Baloh, R. H. C9orf72 BAC transgenic mice display typical pathologic features of ALS/FTD. *Neuron*, 2015; *88*(5): 892–901.
549. Atanasio, A.; Decman, V.; White, D.; Ramos, M.; Ikiz, B.; Lee, H. C.; Siao, C.-J.; Brydges, S.; LaRosa, E.; Bai, Y.; Fury, W.; Burfeind, P.; Zamfirova, R.; Warshaw, G.; Orengo, J.; Oyejide, A.; Fralish, M.; Auerbach, W.; Poueymirou, W.; Freudenberg, J.; Gong, G.; Zambrowicz, B.; Valenzuela, Yancopoulos, G.; Murphy, A.; Thurston, G.; Lai, K-M. V. C9orf72 ablation causes immune dysregulation characterized by leukocyte expansion, autoantibody production, and glomerulonephropathy in mice. *Sci. Rep*, 2016; *6:* 23204(1-14).
550. Burberry, A.; Suzuki, N.; Wang, J-Y.; Moccia, R.; Mordes, D. A.; Stewart, M. H.; Suzuki-Uematsu, S.; Ghosh, S.; Singh, A.; Merkle, F. T.; Koszka, K.; Li, Q-Z.; Zon, L.; Rossi, D. J.; Trowbridge, J. J.; Notarangelo, L. D.; Eggan, K. Loss-of-function mutations in the C9ORF72 mouse ortholog cause fatal autoimmune disease. *Sci. Transl. Med*, 2016; *8*(374): ra93.
551. Jiang, J.; Zhu, Q.; Gendron, T. F.; Saberi, S.; McAlonis-Downes, M.; Seelman, A.; Stauffer, J. E.; Jafar-Nejad, P.; Drenner, K.; Schulte, D.; Chun, S.; Sun, S.; Ling, S. C.; Myers, B.; Engelhardt, J.; Katz, M.; Baughn, M.; Platoshyn, O.; Marsala, M.; Watt, A.; Heyser, C. J.; Ard, M. C.; De Muynck, L.; Daughrity, L. M.; Swing, D. A.; Tessarollo, L.; Jung, C. J.; Delpoux, A.; Utzschneider, D. T.; Hedrick, S. M.; de Jong, P. J.; Edbauer, D.; Van Damme, P.; Petrucelli, L.; Shaw, C. E.; Bennett C. F.; Da Cruz, S.; Ravits, J.; Rigo, F.; Cleveland, D. W.; Lagier-Tourenne, C. Gain of Toxicity from ALS/FTD-Linked Repeat Expansions in C9ORF72 Is Alleviated by Antisense Oligonucleotides Targeting GGGGCC-Containing RNAs. *Neuron*, 2016; *90(*3): 535-550.
552. Sudria-Lopez, E.; Koppers, M.; de Wit, M.; van der Meer, C.; Westeneng, H. J.; Zundel, C. A.; Youssef, S. A.; Harkema, L.; de Bruin, A.; Veldink, J. H.; van den Berg, L. H.; Pasterkamp, R. J. Full ablation of C9orf72 in mice causes immune system-related pathology and neoplastic events but no motor neuron defects. *Acta Neuropathol*, 2016; *132*(1): 145-147.
553. Sullivan, P. M.; Zhou, X.; Robins, A. M.; Paushter, D. H.; Kim, D.; Smolka, M. B.; Hu, F. The ALS/FTLD associated protein C9orf72 associates with SMCR8 and WDR41 to regulate the autophagy-lysosome pathway. *Acta Neuropathol. Commun*, 2016; *4*(1): 51(1-16).
554. Solomon, D. A.; Smikle, R.; Reid, M. J.; Mizielinska, S. Altered Phase Separation and Cellular Impact in C9orf72-Linked ALS/FTD. *Front. Cell. Neurosci*, 2021; *15*, 664151(1-24).
555. Korgstad, D. V.; Lynd, N. A.; Choi, S-H.; Spruell, J. M.; Hawker, C. J.; Kramer, E.J.; Tirrell, M. V. Effects of polymer and salt concentration on the structure and properties of triblock copolymer coacervate hydrogels. *Macromolecules*, 2013; *46(*4): 1512–1518.
556. Macosko, C. W. *Rheology: Principles, Measurements, and Applications;* VCH Publishers, Inc.: University of Minnesota, Minneapolis, 1994.
557. Fuller, G. G. *Optical Rheometry of Complex*

Fluids. Oxford University Press: New York, 1995.
558. Spruijt, E.; Sprakel, J.; Lemmers, M.; Stuart, M. A. C.; van der Gucht, J. Relaxation Dynamics at Different Time Scales in Electrostatic Complexes: Time-Salt Superposition. *Phys. Rev. Lett*, 2010; *105(*20): 208301(1-4).
559. Fan, Y.; Tang, S.; Thomas, E. L.; Olsen, B. D. Responsive block copolymer photonics triggered by protein-polyelectrolyte coacervation. *ACS Nano*, 2014; *8(*11): 11467–73.
560. Krogstad, D. V, Choi, S-H, Lynd, N. A.; Audus, D. J.; Perry, S. L.; Gopez, J. D.; Hawker, C. J.; Kramer, E. J.; Tirrell, M. V. Small angle neutron scattering study of complex coacervate micelles and hydrogels formed from ionic diblock and triblock copolymers. *J. Phys. Chem. B,* 2014; *118*(45): 13011–13018.
561. Ortony, J. H.; Choi, S-H.; Spruell, J. M.; Hunt, J. N.; Lynd, N. A.; Krogstad, D. V.; Urban, V. S.; Hawker, C. J.; Kramer, E. J.; Han, S. Fluidity and water in nanoscale domains define coacervate hydrogels. *Chem. Sci*, 2014; *5(*1): 58–67.
562. Radhakrishna, M.; Sing, C. E. Charge correlations for precise, Coulombically driven self assembly. *Macromol. Chem. Phys*, 2016; *217*(2): 126–136.
563. Schaaf, P.; Schlenoff, J. B. Saloplastics: processing compact polyelectrolyte complexes. *Adv. Mater*, 2015; 27(15): 2420-2432.
564. Yildirim, E.; Zhang, Y.; Lutkenhaus, J. L.; Sammalkorpi, M. Thermal transitions in poly-electrolyte assemblies occur via a dehydration mechanism; 2015. *ACS Macro Lett*, 2015; *4*(9): 1017-1021.
565. Wang, Z.-G. Fluctuation in electrolyte solutions: the self energy. *Phys. Rev. E*, 2010; *81*(2): 021501(1–12).
566. Lim, S.; Moon, D.; Kim, H. J, Seo, J. H.; Kang, I. S.; Cha, H. J. Interfacial tension of complex coacervated mussel adhesive protein according to the hofmeister series. *Langmuir*, 2014; *30*(4): 1108–1115.
567. Simon, J. R.; Carroll, N. J.; Rubinstein, M.; Chilkoti, A.; López, G. P. Programming molecular self-assembly of intrinsically disordered proteins containing sequences of low complexity. *Nat. Chem*, 2017; *9(*6): 509–515.
568. Harmon, T. S.; Holehouse, A. S.; Pappu, R. V. To Mix, or To Demix, That Is the Question. *Biophys J*, 2017; *112*(4): 565-567.
569. Mace, C. R.; Akbulut, O.; Kumar, A. A.; Shapiro, N. D.; Derda, R.; Patton, M. R.; Whitesides, G. M. Aqueous multiphase systems of polymers and surfactants provide self-assembling step-gradients in density. *J. Am. Chem. Soc*, 2012; *134*(22): 9094–9097.
570. Torre, P.; Keating, C. D.; Mansy, S. S. Multiphase water-in-oil emulsion droplets for cell-free transcription–translation. *Langmuir*, 2014; *30(*20): 5695–5699.
571. Mason, A. F.; Buddingh', B. C.; Williams, D. S.; van Hest, J. C. M. Hierarchical self-assembly of a copolymer-stabilized coacervate protocell. *J. Am. Chem. Soc*, 2017; *139(*48): 17309–17312.
572. Zwicker, D.; Hyman, A. A.; Jülicher, F. Suppression of Ostwald ripening in active emulsions. *Phys. Rev, E* 2015, *92(*1): 012317(1-13).

Prof. (Dr.) Partha Sarathi Roy is M.Tech. Pharmaceutical Chemistry from Vellore Institute of Technology (VIT-Deemed University), Vellore, PhD from Department of Pharmaceutical Technology, Jadavpur University, Kolkata. He has undergone Post Doctoral training in University of the Pacific, Stockton, California and University of Missouri-Kansas City, USA. His research interests include polymer chemistry, surface chemistry, material science and polymer engineering for site - specific targeted drug delivery. He has several international publications from American Chemical Society, Washington and other reputed international journals. He is the recipient of several research fellowships from central government agencies, e.g., UGC-JRF in Engineering (Pharmacy), UGC Major Research Project Fellow, UGC-RUSA-PDF as well as scholarships/salary as a postdoctoral research assistant in the United States. With 17 years of teaching experience he is presently working as a Professor in Medicinal Chemistry in Bharat Institute of Engineering and Technology, Hyderabad.